

University of Pretoria etd – Meintjes, S W v d M (2004)

**COMPARATIVE STUDY INTO OCCUPANT SUPPORT CONCEPTS WITH RESPECT TO  
CRASH RESPONSE**

**SCHALK WILLEM VAN DER MERWE MEINTJES**

**A dissertation submitted in partial fulfilment of the requirements for the degree of**

**MASTER OF ENGINEERING (AERONAUTICAL ENGINEERING)**

**In the**

**FACULTY OF ENGINEERING**

**UNIVERSITY OF PRETORIA**

**October 2003**

## **Comparative Study into Occupant Support Concepts with Respect to Crash Response**

**By:** S W vd M Meintjes

**Supervisor:** Prof N J Theron

**Co-Supervisor:** Mr R J Huyssen

**Department:** Mechanical and Aeronautical Engineering

**University:** University of Pretoria

**Degree:** Master of Engineering (Aeronautical Engineering)

### ***ABSTRACT***

*It is argued that together with improved protection structures and energy dissipation systems, a favourable pilot position with sufficient support and restraint could reduce fatalities in aviation accidents. In this document the crash response of three different pilot positions are compared to justify the proposal of supporting a pilot in the rather unusual prone position.*

*The normal seated and supine pilot positions have already been adopted and implemented in various aircraft. The occupant's response to specified crash scenarios in these two positions was compared to that of a pilot in the prone position. To obtain the best prone pilot support configuration, different concepts were considered during the analysis. A dynamic event simulation program called ADAMS was used to perform the analysis and existing injury criteria and a study of common causes of aviation fatalities and human body tolerance limits were used to compare the results.*

*Additionally, methods to improve survivability of a pilot in the prone position during likely accidents were investigated with ADAMS. Concepts for the Exulans fuselage layout and energy absorption systems were proposed and recommendations for the pilot support system were derived from the results.*

## Comparative Study into Occupant Support Concepts with Respect to Crash Response

**Deur:** S W vd M Meintjes

**Studieleier:** Prof N J Theron

**Mede studieleier:** Mnr R J Huysen

**Departement:** Meganiese en Lugvaartkundige Ingenieurswese

**Universiteit:** Universiteit van Pretoria

**Graad:** Magister (Lugvaartkundige Ingenieurswese)

### ***SAMEVATTING***

*Dit word geargumenteer dat lewensverlies tydens lugvaartongelukke verminder kan word deur 'n geskikte liggaamsposisie met voldoende ondersteuning en beperking in kombinasie met verbeterde strukture en energie absorberende materiale en meganismes, te implimenteer. Met hierdie dokument word die impakreaksie van drie verskillende liggaamsposisies vergelyk, om sodoende die voorstel om die vlieënier in die ietwat ongewone vooroorlêhouding te ondersteun, te staaf.*

*Die regop sittende en agteroor sittende vlieëniers posisies is alreeds aanvaar en kom algemeen in verskeie vliegtuie voor. Die vlieënier se reaksie op verskillende impak situasies in hierdie twee posisies was vergelyk met die van 'n vlieënier in die vooroorlêhouding. Om te verseker dat die beste vooroorlêhouding konsep gebruik word, was verskeie konfigurasies van hierdie posisie oorweeg tydens die analiese. Die rekenaar program genaamd "ADAMS", wat die dinamika van enige meganiese stelsel simuleer, was gebruik om die analieses mee te doen. Bestaande beseringskriteria en 'n studie van algemene oorsake van lewensverlies tydens lugvaart ongelukke en liggaamsimpaktoleransielimiete was gebruik om die resultate te vergelyk.*

*Addisioneel was metodes om die oorleefbaarheid van 'n vlieënier in die vooroorlêhouding tydens waarskynlike vliegtuigongelukke te verbeter ook ondersoek met "ADAMS". Konsepte vir die uitleg van Exulans II se rompstruktuur en energieabsorberendesisteme asook aanbevelings vir die vlieënier se ondersteuningsstelsel, was afgelei vanuit die resultate.*

## ACKNOWLEDGEMENTS

I wish to express my gratitude to the following organisations and persons who made this dissertation possible:

- a) Armscor and Land Mobility Technologies for the provision of data during the course of the study.
- b) The following persons are gratefully acknowledged for their assistance during the course of the study:
  - i) Robert Cathro
  - ii) Andy Hodgson
  - iii) Elton Murison
  - iv) Jaco Nolte
  - v) Klaus Schwerdtfeger
  - vi) Clinton Stone
- c) Professor N J Theron my supervisor, and Mr R J Huysen, my co-supervisor for their guidance and support.
- d) My parents for their encouragement and support during the study.
- e) My God for granting me the ability and opportunity to complete this study.

## TABLE OF CONTENTS

|                                                   |    |
|---------------------------------------------------|----|
| LIST OF TABLES                                    | vi |
| LIST OF FIGURES                                   | vi |
| NOMENCLATURE                                      | x  |
| <br>                                              |    |
| CHAPTER 1: INTRODUCTION                           | 1  |
| 1.1 Project Background                            | 2  |
| 1.2 Thesis Overview                               | 2  |
| 1.3 Document Layout                               | 3  |
| <br>                                              |    |
| CHAPTER 2: LITERATURE SURVEY                      | 4  |
| 2.1 Introduction                                  | 5  |
| 2.2 Causes of Aviation Fatalities                 | 6  |
| 2.3 Human Impact Tolerance Limits                 | 7  |
| 2.4 Crash Survivability                           | 11 |
| 2.5 Crash Survival Design Considerations          | 12 |
| 2.6 Impact Injury Criteria                        | 15 |
| 2.7 Crash Pulse Shapes                            | 20 |
| 2.8 Dynamic Crashworthiness Testing               | 23 |
| 2.9 Pilot Support Positions                       | 25 |
| 2.10 Summary                                      | 35 |
| <br>                                              |    |
| CHAPTER 3: PROPOSED CONCEPTS                      | 37 |
| 3.1 Thesis Specifications                         | 38 |
| 3.2 Proposed Pilot support Position               | 39 |
| 3.3 Reasons Leading to the Pilot Support Proposal | 41 |
| 3.4 CREEP Concept Design Proposals                | 43 |
| 3.4.1 Container Concept                           | 43 |
| 3.4.2 Restraint Concept                           | 44 |
| 3.4.3 Energy Absorption Concept                   | 45 |
| 3.4.4 Environment Considerations                  | 46 |
| 3.4.5 Post-Crash Factors                          | 46 |
| 3.5 Conclusion                                    | 47 |

|            |                                                |     |
|------------|------------------------------------------------|-----|
| CHAPTER 4: | DYNAMIC ANALYSIS                               | 48  |
| 4.1        | The Approach                                   | 49  |
| 4.2        | The Analysis Tools                             | 49  |
| 4.3        | Meet The Pilots                                | 50  |
| 4.4        | Validation and Verification                    | 52  |
| 4.5        | Sled Impact Tests                              | 59  |
|            | 4.5.1 Normal Seated Position                   | 64  |
|            | 4.5.2 Prone Pilot Position                     | 65  |
|            | 4.5.3 Supine Seated Position                   | 67  |
|            | 4.5.4 Sled Test Results                        | 67  |
|            | 4.5.5 Conclusion                               | 74  |
| 4.6        | Fuselage Crash Tests                           | 75  |
|            | 4.6.1 Crash Scenarios                          | 75  |
|            | 4.6.2 The Analysis                             | 77  |
|            | 4.6.3 Crash Test Results                       | 81  |
|            | 4.6.4 Conclusion                               | 82  |
| CHAPTER 5: | FINAL CONCLUSION AND RECOMMENDATIONS           | 83  |
| REFERENCES |                                                | 87  |
| APPENDIX A | THE HYBRID III CRASH TEST DUMMY                | 91  |
| APPENDIX B | SHOULDER HARNESS AND SAFETY BELT INSTALLATIONS | 97  |
| APPENDIX C | JOINT AVIATION REGULATIONS SELECTIONS          | 108 |
| APPENDIX D | ADAMS AND FIGURE HUMAN MODELLER                | 117 |
| APPENDIX E | ADDITIONAL RESULTS                             | 123 |
| APPENDIX F | COMPACT DISC                                   | 133 |

## LIST OF TABLES

|     |                                                           |     |
|-----|-----------------------------------------------------------|-----|
| 2.1 | Accelerations known to cause bone fracture and concussion | 10  |
| 2.2 | Critical intercepts for neck injury criteria              | 18  |
| 4.1 | Validation injury criteria comparison                     | 56  |
| 4.2 | Sled test injury criteria results                         | 74  |
| 4.3 | Fuselage crash tests injury criteria results              | 82  |
| A1  | Comparison of weight                                      | 94  |
| A2  | Segmented weights                                         | 94  |
| A3  | Dimensions                                                | 94  |
| A4  | Instrumentation                                           | 95  |
| E1  | Calculation of neck injury criteria                       | 131 |
| E2  | Injury criteria results                                   | 132 |
| E3  | Impact force on mandible of prone positioned pilot        | 132 |

## LIST OF FIGURES

|      |                                                                                |    |
|------|--------------------------------------------------------------------------------|----|
| 2.1  | Energy absorbing crew seat used in the V-22 aircraft                           | 5  |
| 2.2  | Typical impact acceleration pulse shape                                        | 8  |
| 2.3  | Aircraft axis convention                                                       | 9  |
| 2.4  | Acceleration axes for imaginary eyeball terminology                            | 9  |
| 2.5  | Acceptable range of neck loading modes for the Hybrid III mid-sized male       | 18 |
| 2.6  | Rectangular acceleration pulse shape                                           | 21 |
| 2.7  | Increasing acceleration pulse shape                                            | 21 |
| 2.8  | Decreasing acceleration pulse shape                                            | 22 |
| 2.9  | Increasing decreasing acceleration pulse shape                                 | 22 |
| 2.10 | FAR 23.562 dynamic Test 1                                                      | 24 |
| 2.11 | FAR 23.562 dynamic Test 2                                                      | 24 |
| 2.12 | Aviator in the normal seated position                                          | 26 |
| 2.13 | Three-point restraint                                                          | 26 |
| 2.14 | Four and five-point restraint                                                  | 27 |
| 2.15 | Historic flight by Orville Wright on 17 December 1903, note the prone position | 28 |
| 2.16 | Hang glider with pilot in prone position                                       | 29 |
| 2.17 | The Berlin B-9 prone pilot aircraft                                            | 29 |
| 2.18 | The Horten Ho IV flying wing with the pilot in the prone position              | 30 |

## University of Pretoria etd – Meintjes, S W v d M (2004)

|      |                                                                          |    |
|------|--------------------------------------------------------------------------|----|
| 2.19 | A close-up of the Ho IV showing the prone pilot position                 | 30 |
| 2.20 | The MasterBlaster aerobatics aircraft concept with prone pilot           | 31 |
| 2.21 | Exulans II glider with prone pilot                                       | 31 |
| 2.22 | The rider of a super bike in the riding position                         | 32 |
| 2.23 | Gloster Meteor F8 prone pilot experimental aircraft                      | 33 |
| 2.24 | The supine position used in sailplanes                                   | 34 |
| 2.25 | Recommended lap and shoulder belt attachment point in supine position    | 35 |
|      |                                                                          |    |
| 3.1  | Prone pilot position ergonomical investigation                           | 40 |
| 3.2  | Steel frame mock-up                                                      | 40 |
| 3.3  | Direction of impact load on prone pilot during likely crash scenario     | 41 |
| 3.4  | High angle of attack landing executed in different pilot positions       | 42 |
| 3.5  | Exulans II container concept                                             | 43 |
| 3.6  | Pilot wearing the custom manufactured harness                            | 44 |
| 3.7  | Collapsible landing skid mechanism                                       | 45 |
|      |                                                                          |    |
| 4.1  | The normal seated pilot in the normal seated position                    | 51 |
| 4.2  | The prone pilot in the prone position                                    | 51 |
| 4.3  | The supine seated pilot in the supine position                           | 51 |
| 4.4  | Vertical impact experiment with Hybrid III ATD                           | 52 |
| 4.5  | ADAMS model of vertical impact experiment                                | 53 |
| 4.6  | Lumbar spine force comparison                                            | 54 |
| 4.7  | Head acceleration magnitude comparison                                   | 54 |
| 4.8  | Lumbar spine force peak comparison                                       | 55 |
| 4.9  | Head acceleration magnitude peak comparison                              | 55 |
| 4.10 | Static seat characterisation experimental test set-up                    | 56 |
| 4.11 | Artificial buttock with typical seat cushion                             | 57 |
| 4.12 | Seat stiffness data obtained from static test                            | 57 |
| 4.13 | ADAMS model of seat characterisation experiment                          | 58 |
| 4.14 | Experimental and ADAMS seat stiffness data                               | 58 |
| 4.15 | Test 1 model with translation constraints and applied crash pulse vector | 59 |
| 4.16 | Test 2 model with translation constraints and applied crash pulse vector | 60 |
| 4.17 | Webbing stiffness curves                                                 | 61 |
| 4.18 | Modelling belt slack and belt pretension with the ADAMS spline function  | 61 |
| 4.19 | Pulse shape calculation for Test 1                                       | 62 |
| 4.20 | Pulse shape calculation for Test 2                                       | 63 |
| 4.21 | Test sled with normal seated configuration                               | 64 |



## University of Pretoria etd – Meintjes, S W v d M (2004)

|      |                                                                                                                              |     |
|------|------------------------------------------------------------------------------------------------------------------------------|-----|
| 4.22 | Test sled with prone restraint concept 1                                                                                     | 65  |
| 4.23 | Test sled with prone restraint concept 2                                                                                     | 66  |
| 4.24 | Test sled with prone restraint concept 3                                                                                     | 66  |
| 4.25 | Test sled with supine seated configuration                                                                                   | 67  |
| 4.26 | Dynamic Test 1: lumbar spine force results calculated by ADAMS<br>with grey acceleration pulse scaled to right vertical axis | 68  |
| 4.27 | Dynamic Test 1: head acceleration magnitude results calculated by ADAMS<br>with grey acceleration pulse shape on scale       | 69  |
| 4.28 | Dynamic Test 1: flailing envelopes calculated by ADAMS                                                                       | 70  |
| 4.29 | Dynamic Test 2: lumbar spine force results calculated by ADAMS<br>with grey acceleration pulse scaled to right vertical axis | 72  |
| 4.30 | Dynamic Test 2: head acceleration magnitude results calculated by ADAMS<br>with grey acceleration pulse on scale             | 72  |
| 4.31 | Dynamic Test 2: flailing envelopes calculated by ADAMS                                                                       | 73  |
| 4.32 | Fuselage crash test cage with pilots in different positions                                                                  | 78  |
| 4.33 | Airframe impact attitude of Crash Scenario 1                                                                                 | 79  |
| 4.34 | Airframe impact attitude of Crash Scenario 2                                                                                 | 80  |
| 4.35 | Airframe impact attitude of Crash Scenario 3                                                                                 | 80  |
| A1   | The Hybrid III crash test dummy family                                                                                       | 91  |
| A2   | Hybrid III neck sensors                                                                                                      | 92  |
| A3   | Steel ribs with measuring equipment in upper torso                                                                           | 93  |
| A4   | ATD axes definition                                                                                                          | 96  |
| B1   | Single strap 3-point restraint                                                                                               | 98  |
| B2   | Dual strap 4-point restraint                                                                                                 | 98  |
| B3   | Dual strap 5-point restraint                                                                                                 | 98  |
| B4   | Acceptable lap belt attachment angles                                                                                        | 101 |
| B5   | Incorrect shallow and steep belt angles                                                                                      | 102 |
| B6   | Correct and incorrect single diagonal shoulder harness attachment                                                            | 102 |
| B7   | Incorrect upper shoulder harness attachments                                                                                 | 103 |
| B8   | Typical concepts for dual shoulder harness installations                                                                     | 104 |
| B9   | Incorrect and correct shoulder harness safety belt installations                                                             | 104 |
| B10  | Installation of the negative-G strap                                                                                         | 104 |
| B11  | Acceptable range of upper attachment points                                                                                  | 105 |
| B12  | Compression of spine due to incorrect shoulder strap installation                                                            | 106 |
| B13  | Spinal compression due to resultant restraint force                                                                          | 106 |

## University of Pretoria etd – Meintjes, S W v d M (2004)

|     |                                                                        |     |
|-----|------------------------------------------------------------------------|-----|
| C1  | Lap and shoulder belt attachment points in supine position             | 109 |
| D1  | ADAMS Impact function force exponent ranges                            | 119 |
| D2  | ADAMS Impact function penetration depth and damping step function      | 119 |
| D3  | Human models displayed as ellipsoids, skeletal or a skin clothed model | 120 |
| D4  | Typical active simulation with FIGURE                                  | 121 |
| E1  | Validation seat rig input displacement                                 | 123 |
| E2  | Test 1 prone concepts lumbar load comparison                           | 124 |
| E3  | Test 1 prone concepts head acceleration comparison                     | 124 |
| E4  | Test 2 prone concepts lumbar load comparison                           | 125 |
| E5  | Test 2 prone concepts head acceleration comparison                     | 125 |
| E6  | Test 1 neck axial loads and bending moments                            | 126 |
| E7  | Test 2 neck axial loads and bending moments                            | 127 |
| E8  | Crash 1 neck axial loads and bending moments                           | 128 |
| E9  | Crash 2 neck axial loads and bending moments                           | 129 |
| E10 | Crash 3 neck axial loads and bending moments                           | 130 |

## NOMENCLATURE

### *Symbols*

|            |                                                     |
|------------|-----------------------------------------------------|
| $g$        | Gravitational Acceleration ( $9.81\text{m/s}^2$ )   |
| $G_m$      | Maximum acceleration as a multiple of $g$           |
| $G_x$      | Acceleration in x direction as a multiple of $g$    |
| $G_y$      | Acceleration in y direction as a multiple of $g$    |
| $G_z$      | Acceleration in z direction as a multiple of $g$    |
| $t$        | Time (seconds)                                      |
| $t_m$      | Time at maximum acceleration or rise time (seconds) |
| $V_0$      | Initial Velocity (m/s)                              |
| $V_f$      | Final Velocity (m/s)                                |
| $\Delta V$ | Velocity Change (m/s)                               |

### *Abbreviations*

|       |                                                  |
|-------|--------------------------------------------------|
| ADAMS | Automatic Dynamic Analysis of Mechanical Systems |
| ATD   | Anthropomorphic Test Dummy                       |
| CAD   | Computer Aided Drawing                           |
| CFIT  | Controlled Flight Into Terrain                   |
| CFR   | Code of Federal Regulations                      |
| CG    | Centre of Gravity                                |
| DRI   | Dynamic Response Index                           |
| FAA   | Federal Aviation Administration                  |
| FAR   | Federal Aviation Regulations                     |
| FMVSS | Federal Motor Vehicle Safety Standard            |
| HANS  | Head and Neck Support                            |
| HIC   | Head Index Criteria                              |
| JAR   | Joint Aviation Regulations                       |
| LLC   | Lumbar Load Criteria                             |
| LMT   | Land Mobility Technologies                       |
| NHTSA | National Highway Traffic Safety Administration   |
| TSO   | Technical Standard Order                         |
| 3D    | Three Dimensional                                |

## CHAPTER 1: INTRODUCTION

### Preview

1. In this chapter the reader is introduced to the Exulans project and some background on the thesis are provided.
2. The motivation behind the thesis and the actions to be expected during the course of this document is summarised in the thesis overview.
3. The chapter is concluded with an overview of the layout of this document.

## **1.1 Project Background**

The Department of Mechanical and Aeronautical Engineering at the University of Pretoria has undertaken a project in which a new aircraft is being developed. In this project various shortcomings of current aviation practice are being investigated. One of the shortcomings relates to occupant protection during survivable mishaps and it is argued that many aviation fatalities could be avoided through better design. This thesis forms a central part in the ambition of improving occupant protection in light aircraft and also proposes a pilot protection system for the Exulans glider.

Exulans is a high performance ultra-light glider under development at the University of Pretoria. It is unique in the fact that it has no tail and that it utilises the concept of variable outer wing sweep to perform certain aerodynamical tasks. The tailless gull-wing configuration was copied from the Albatross and initial tests with the first prototype indicated that this configuration proved to possess great potential for tailless flight and short field take-off and landing.

In the Exulans project the challenge of pilot protection is addressed from two sides, the aerodynamic side and the structural/systems side. The challenge of this thesis, however, was to look at pilot protection from a structural and ergonomical point of view during a crash or bad landing. Pilot protection during an impact event is essentially an energy management task that requires the absorption or deflection of crash energy away from the occupant.

## **1.2 Thesis Overview**

Generally speaking, aviation is considered dangerous because of the huge amount of energy involved in flight. The challenge of pilot protection, however, arises in the management of the energy at the end of the flight. The potential energy component of an aircraft is dissipated into the atmosphere during the descent and in special cases a portion of the kinetic energy can also be dissipated prior to the landing.

The tailless aerodynamic layout of Exulans allows the execution of a high angle of attack or “flared” landing. During this action the angle of attack of the glider is suddenly increased to allow the wing to act as a massive airbrake. This action releases some of the kinetic energy into the atmosphere but still leaves the glider with enough energy that could injure or kill the pilot during a mishap.

It was suspected that higher crash survivability could be obtained with a pilot supported in the prone position. This suspicion and several other reasons led to the suggestion of supporting the pilot in the prone position within the Exulans cockpit. To verify this suggestion, the crash survivability in this position was investigated by comparing the crash response of a pilot supported in the prone position with those supported in conventional flying positions. The positions selected for the comparison were the normal seated position adopted by most powered aircraft and the supine seated position found in many sailplane designs.

The three positions were subjected to common crash scenarios using a mechanical system simulation software package called ADAMS. This program simulates dynamic events by setting up and solving the equations of motion for the system and is also equipped with a virtual Hybrid III crash dummy to simulate human response to impact. By using impact injury criteria and investigating frequent aviation fatalities and human body tolerance limits the results of the three different positions were compared to each other.

### **1.3 Document Layout**

In this document Chapter 1 serves as an introduction and also contains some background to the thesis. The summary of the literature study is contained in Chapter 2 and is followed by Chapter 3, which states the thesis specifications and concept proposals. The technical detail and results of the dynamic analysis are contained in Chapter 4. The final conclusions and recommendations are made in Chapter 5 and a list of references is included at the end of the report.

Information on the Hybrid III crash test dummy used to evaluate human response to impact was included in Appendix A while guidelines and recommendations on restraining aircraft occupants were submitted as Appendix B. Some of the relevant Joint Aviation Regulations were summarised in Appendix C and the capabilities of ADAMS and FIGURE Human Modeller are described in Appendix D. Appendix E contains additional results of the dynamic analysis and a layout of the contents of the compact disk is included as Appendix F.

## CHAPTER 2: LITERATURE SURVEY

### Preview

1. To familiarise ourselves with historical studies on the topic of occupant protection in aircraft a literature study was launched.
2. This chapter summarises the results of the literature survey. Topics that were investigated during this phase include:
  - Similar studies on the topic of occupant protection in aircraft
  - The major causes of aviation fatalities
  - Human impact tolerance limits
  - Crash survivability and crash survival design considerations
  - The criteria for impact injury
  - Crash pulse shapes
  - The requirements for dynamic crashworthiness testing
  - Different pilot support positions
3. A summary and some remarks on the literature study conclude this chapter.

## 2.1 Introduction

Amongst several studies on the topic of occupant protection during aircraft accidents, Winkelman & Laananen (1996) reported that the U.S Army conducted crash testing and accident analyses, which led to the establishment of crashworthy requirements for Army rotorcraft and small fixed wing aircraft. The U.S Military's SH-60 B Sea Hawk, UH-60 A Black Hawk and AH-64 A Apache helicopters have been designed in accordance with the crashworthy requirements and have been equipped with energy-absorbing crew seats.

According to Labun & Rapaport (1994) the energy-absorbing crew seat design featured a moveable seat bucket attached to the aircraft structure through an energy absorber (Figure 2.1), which displace or "stroke" towards the helicopter floor to absorb some of the energy during a high impact event. Much of the work in the past was however, predominantly focused on protection of normal seated pilots where the main objective of the EA seat was to prevent spinal injury to the aviator in this position. (Rapaport, Yeiser & Oslon 1995; Richards & Podop 1997).

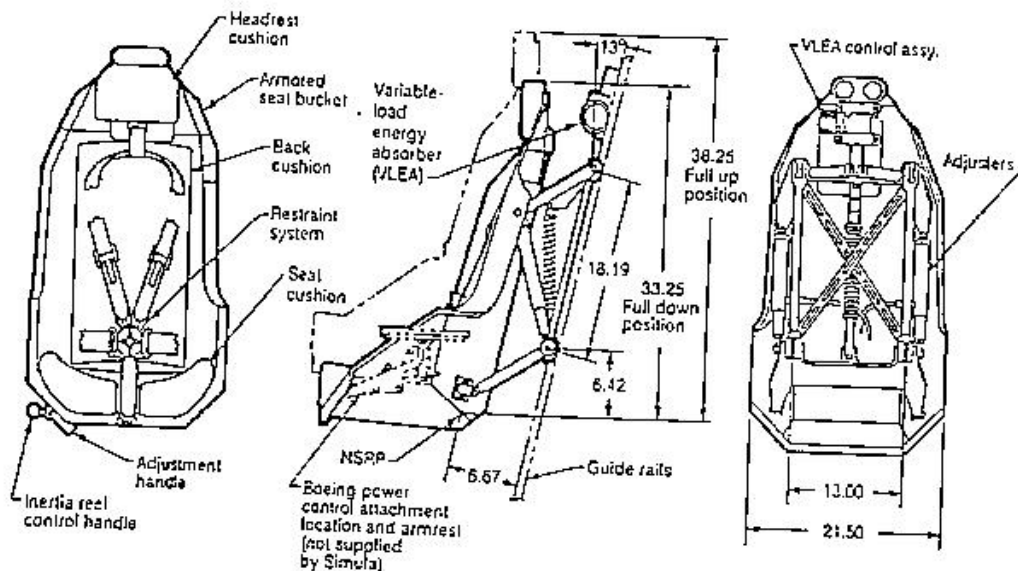


Figure 2.1: Energy absorbing crew seat used in the V-22 aircraft (Rapaport, Yeiser & Oslon 1995)



## **2.2 Causes of Aviation Fatalities**

The major causes of aviation fatalities are classified into four categories. According to The Naval Flight Surgeon's Pocket Reference to Aircraft Mishap Investigation (1995), the four major injury types associated with aviation accidents include the following:

### **Thermal**

Thermal injury is the cause of 50% of all aviation fatalities and involves burning and smoke inhalation.

### **Intrusive**

Intrusive injuries occur when the living or occupiable space is lost due to penetration of the container. Cases that have occurred are decapitation by electrical wires or fences, body penetrations by sticks, push rods, fractured structural pieces etc. These type of injury leads to excessive bleeding and/or organ damage.

### **Impact**

Impact injury involves impact of the body into an object or visa versa or impact into the belts of the restraint system. Reported cases include impact into the control stick and restraint system causing organ damage and/or lacerations. Head injury, responsible for a third of all aviation fatalities, often occur due to head impact into the instrument panel and can lead to concussion or skull fracture (The Naval Flight Surgeon's Pocket Reference to Aircraft Mishap Investigation 1995) Dynamic overshoot can occur when the head gains a greater relative velocity than the surrounding cabin and would result in an impact force exceeding that of the actual crash force.

It could further be argued that head injury or any other injury for that matter, sustained during the dynamic portion of the crash, would contribute to thermal aviation fatalities. An occupant surviving the impact could die due to thermal injury if he was left unconscious in the burning wreckage due to a head injury sustained during the crash.

## Decelerative

The organs of the human body are very sensitive to high accelerations. The following injuries have occurred as a result of high deceleration.

- Fracture dislocation of the neck (C1 on C2) 20 – 40g
- Concussion 60g over 0.02 seconds  
100g over 0.005 seconds
- Aorta transection 80 – 100g
- Pelvic fracture 100 – 200g
- Vertebral body transection 200 – 300g
- Total body fragmentation 350g

### **2.3 Human Impact Tolerance Limits**

The name Colonel John Paul Stapp is synonymous with body tolerance limit studies. According to the History of Research in Space Biology and Biodynamics (1985) and Cavanaugh (2000), Col. Stapp conducted rocket sled acceleration tests in the 1950's, which provided most of the data on human tolerance to high magnitude deceleration. High magnitude deceleration is classified as deceleration exceeding 10g and lasts for less than one second. According to the Advisory Circular (1985), further body tolerance limits resulted from tests with voluntary human subjects who were exposed to increasingly severe impacts whilst being held by a specific seat and restraint system. The level of the impacts was increased until a subject felt that further tests would be unbearable.

With modern technology, the use of the Anthropomorphic Test Dummy (ATD) and computer simulation programs became more appropriate in determining the response of humans to high magnitude decelerations. The ATD is a dummy used in place of a human to evaluate crash impact protection systems by simulating human response in dynamic events. It was designed to resemble the mass and dimensions and the kinematic behaviour of the prominent joints and ligaments in the human body. More information on the Hybrid III ATD is contained in Appendix A.

The Naval Flight Surgeon's Pocket Reference to Aircraft Mishap Investigation (1995) states that human tolerance to acceleration is a function of the following aspect (see also Figure 2.2).

- The acceleration pulse shape and the initial acceleration slope (rate of onset in g/second)
- The acceleration direction with respect to the body
- The acceleration duration or the time interval from initial impact velocity to zero velocity
- The acceleration magnitude (peak g)
- The type of seat and restraint
- The physical characteristics of the aviator
- Secondary impact of body into subjects
- The distribution of force over the body

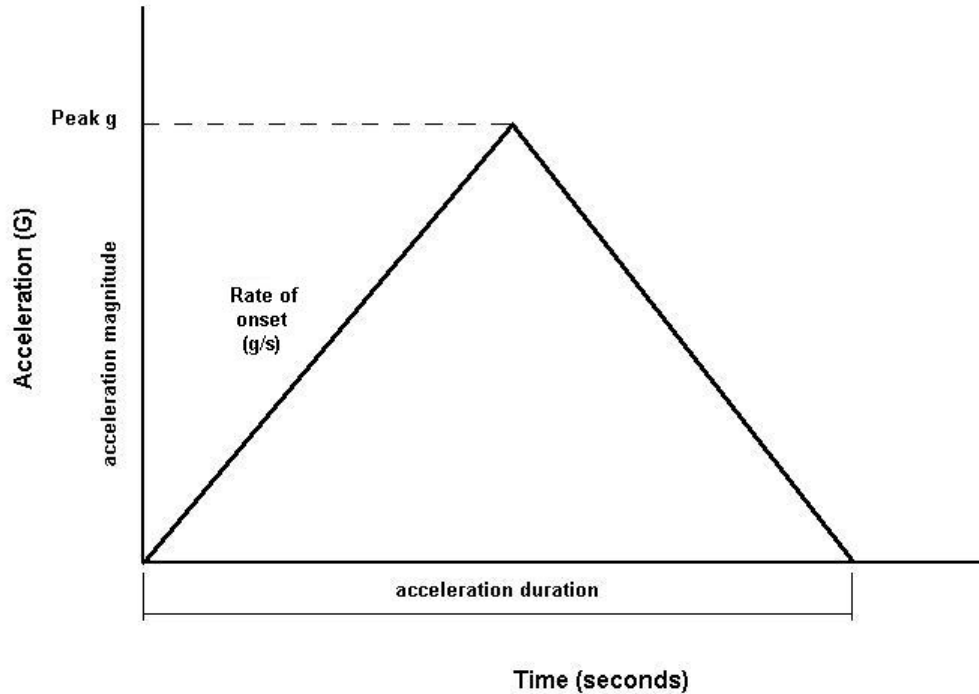


**Figure 2.2: Typical impact acceleration pulse shape**

It is difficult or rather impossible to isolate each of these factors, but it is known that the longer the duration, the greater the magnitude, or the higher the rate of onset, the less likely a person is to survive.

The crash forces and accelerations experienced by the airframe and occupants in an accident is a three dimensional event along the three axes. Normally the aircraft's axes are referred to as X, forward and parallel to the fuselage, Y to the right and parallel to the wing and Z downwards as shown in Figure 2.3.

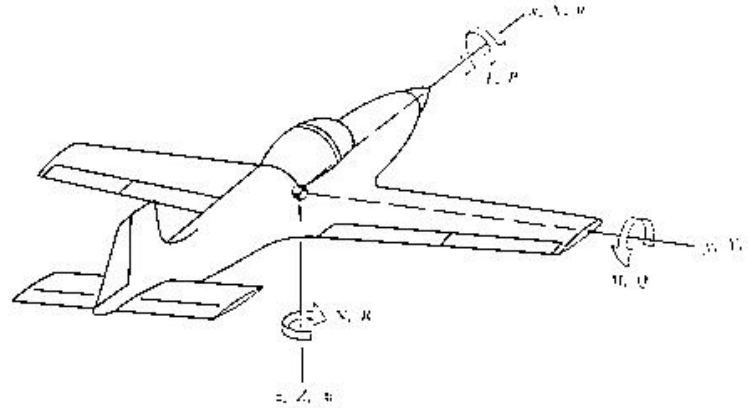


Figure 2.3: Aircraft axis convention (McCormick 1979: 478)

The co-ordinate system used to describe forces and accelerations on the occupant will however differ from the above in the sense that positive Z will be upward and positive Y will be to the left as indicated in Figure 2.4. As described by Wood & Sweginnes (1996), a discussion of accelerations acting on the human body in these three directions can get confusing, therefore an imaginary eyeball movement terminology has been adopted. The terminology states that a chest to back acceleration ( $-G_x$ ) e.g. aircraft carrier landing will cause an eyeballs-out scenario. An ejection seat will cause an eyeballs-down acceleration ( $+G_z$ ) while sideways acceleration will cause eyeballs-left or eyeballs-right scenarios as indicated in Figure 2.4.

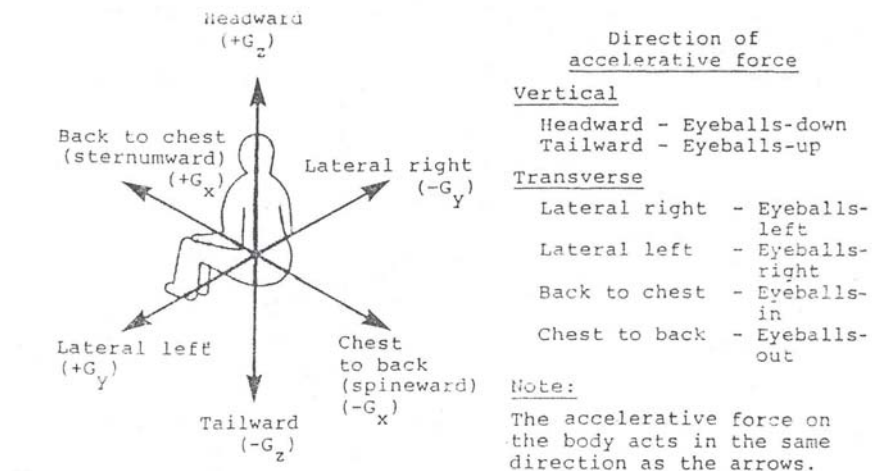


Figure 2.4: Acceleration axes for imaginary eyeball terminology (Wood & Sweginnes 1996)

University of Pretoria etd – Meintjes, S W v d M (2004)

The following limits are realistic for a properly restraint occupant for duration and rate of onset found in most survivable mishaps (The Naval Flight Surgeon’s Pocket Reference to Aircraft Mishap Investigation 1995)

- +G<sub>z</sub> (eyeballs-down)            25g over 0.1 seconds
- -G<sub>z</sub> (eyeballs-up)                15g over 0.1 seconds
- +G<sub>x</sub> (eyeballs-in)                45g over 0.1 seconds
- -G<sub>x</sub> (eyeballs-out)                45g over 0.1 seconds
- +G<sub>y</sub> (eyeballs-right)            11.5g - 20g over 0.1 seconds
- -G<sub>y</sub> (eyeballs-left)              11.5g - 20g over 0.1 seconds

The accelerations known to cause bone fracture or concussion are listed in Table 2.1

**Table 2.1: Accelerations known to cause bone fracture and concussion (Naval Aerospace Medical Institute 1991)**

| <b>Regional Impact Accelerations Known to Cause Bone Fracture or Concussion</b>                                                  |       |           |
|----------------------------------------------------------------------------------------------------------------------------------|-------|-----------|
| Body Area                                                                                                                        | Force | Duration  |
| Head (frontal bone, 2" diam. application)                                                                                        | 180 G | 0.002 sec |
|                                                                                                                                  | 57 G  | .02 sec   |
| Nose                                                                                                                             | 30 G  | *         |
| Maxilla                                                                                                                          | 50 G  | *         |
| Teeth                                                                                                                            | 100 G | *         |
| Mandible                                                                                                                         | 40 G  | *         |
| Brain (concussion)                                                                                                               | 60 G  | .02 sec   |
|                                                                                                                                  | 100 G | .005 sec  |
|                                                                                                                                  | 180 G | .002 sec  |
| *Duration figures not available.<br>(from Crash Survival Investigator's School, Arizona State University, Tempe, Arizona, 1986). |       |           |

According to The Naval Flight Surgeon’s Pocket Reference to Aircraft Mishap Investigation (1995) and History of Research in Space Biology and Biodynamics (1985), the most severe measured impact survived by a human volunteer was the accidental exposure of Captain Eli L. Beeding to an eyeballs-in acceleration (+G<sub>x</sub>) of 83g over 0.04 seconds at a rate of onset of 3800g/sec on 16 May 1958. Captain Beeding went into a state of shock but recovered after ten minutes with no permanent ill condition.

## **2.4 Crash Survivability**

Hugh De Haven, who is referred to as the “Father of Crash Survivability” in The Naval Flight Surgeon’s Pocket Reference to Aircraft Mishap Investigation (1995), established the Aviation Safety and Research Facility at Cornell University in the early nineteen hundreds. He analysed over 5000 aircraft accidents and in a report published in 1939 he recommended the following:

- Head injuries should be prevented by the use of helmets
- Seat belts should be worn at a 45° angle
- A 40G cockpit should be provided for the occupants

According to De Haven a survivable crash is one in which:

- Crash forces do not exceed human tolerances
- Habitable space is maintained
- The occupants do not burn up

It should be realised that many aircraft crashes are not potentially survivable, with enough speed at impact and a high enough impact angle it is unrealistic to expect survival. On the other hand, there are still too many survivable accidents in which the occupants sustain serious injury or die.

Although aircraft structures are designed to fly and not crash, Crash Survivability should be considered throughout the design of the aircraft fuselage. A publication by Davidson (1994), suggested that crash survivability is also dependent on how the aircraft crash, implying that a pilot can improve his odds by following several rules during a crash event.

### **Rule 1**

When preparing for an emergency landing try to maintain the best glide speed until flaring just before impact. Many injuries are the result of getting the aeroplane too slow while it is still too far from the ground. Pilots often decrease the forward airspeed of the aircraft too soon by pulling up the nose. Although the forward airspeed of the aircraft might cause the trees to rush past at a horrifying rate it is normally the vertical velocity that causes the most damage during an accident.

### **Rule 2**

Use the airframe to absorb as much crash energy as possible. If the pilot thinks in terms of letting the airframe absorb the initial impact, reducing the energy level before it reaches the occupants an EA scenario for that particular situation might be orchestrated by the pilot. For example, the pilot might use the wings as energy absorbers. Tearing the wings off by landing between two trees or by sticking the wing into the

ground at the last second will absorb some of the energy by crushing the wing. Don't hit a large immovable object head on!

#### Rule 3

Plan your actions ahead of the crash. Should the engine stall at 50 feet (16m) off the end of the runway, the emergency plan should already be in place and be activated by instinct. It has been experienced that the brain becomes the least useful organ in the body when panic hits.

## **2.5 Crash Survival Design Considerations**

When designing an aircraft fuselage for maximum survivability, five design factors should be considered (The Naval Flight Surgeon's Pocket Reference to Aircraft Mishap Investigation 1995; Wood & Sweginnes 1996). These five design considerations have the acronym **CREEP** and control the survivability of occupants during a crash.

**C**ontainer

**R**estraint

**E**nergy Absorption

**E**nvironment

**P**ost Crash Factors

The first four of the CREEP factors relate to the dynamic portion of the crash while the fifth factor controls injury not directly related to the dynamics of the crash. The following paragraphs will describe the five design factors.

### **Container**

A "living space" or protective shell around the occupants must be provided. This protective shell is referred to as the container. The container is created by the main structural components of the fuselage. If the container should collapse during the dynamic portion of the crash, survivability will fall drastically. De Haven (The Naval Flight Surgeon's Pocket Reference to Aircraft Mishap Investigation 1995) and Wood & Sweginnes (1996) recommended a cockpit designed to withstand a 40g load as desirable. In the evaluation of the crashworthiness of an aircraft structure specific attention should be directed to the anticipated dynamic response under most probable conditions of impact angle and aircraft attitude.

## University of Pretoria etd – Meintjes, S W v d M (2004)

According to the Naval Flight Surgeon's Pocket Reference to Aircraft Mishap Investigation (1995), the preferred container should have the following structural properties

- Crushable structures between the outer skin and occupant's compartment including a multiple keel belly over the forward 20% of the nose
- Enough structural stiffness to prevent crushing of occupants by wings, transmissions and rotors and to avoid inward buckling during impact. A floor-seat tie-down that would stay intact even after the fuselage has fractured
- Sufficient structural continuity to maintain a protective shell in cartwheel or rollovers and especially during water impacts
- The use of ductile material at deformation points and sufficient provision at known fracture sites

The following aspects have caused failure of the container in past accidents:

- Forward movement of the container into the stationary engine in single engine aircraft
- The downward displacement of engines and transmissions in helicopters
- The downward collapse of the container onto lower structures e.g. landing gear
- Insufficient rollover protection for low and mid-winged small aircraft

According to the Naval Flight Surgeon's Pocket Reference to Aircraft Mishap Investigation (1995), statistics indicate that serious injury in general aviation accidents is most frequently sustained at the head. More specifically, one out of every three aviation fatalities is due to head injury and therefore this topic deserves more attention. A helmet can be considered as a container inside a container protecting the occupant's head. A good helmet should possess the following design qualities:

- Circumferential anchorage to the neck remaining in place for up to 400lbf (1780N). of deceleration force
- The external shell must be fracture and tear resistant with a crushable liner that limits peak impact decelerations to 150g
- The helmet must have a maximum weight of 2lbs (910g) with the CG close to the heads CG, a shatterproof visor and minimum external projections

### Restraint

Occupants must be protected from being thrown against the sides of the container or having objects such as cargo or equipment thrown at them. Any failure in the restraint system also referred to as the "Tie-Down Chain" will decrease chances of survival. Further more, the restraint system must not contribute to injury in an attempt to prevent unwanted movement.



It was previously mentioned that serious injury in general aviation accidents is most frequently sustained at the head. This can mainly be attributed to the lack of adequate torso restraint, which causes the head to impact objects in its path with a high velocity, also known as dynamic overshoot of the head. This is especially true for aviators sitting in the cockpit facing the instrument panel (see Figure 2.5). The shoulders provide a sufficient attachment point for torso restraint but shoulder straps should be designed to remain in the correct position during the impact. Special attention should also be given to the angle and position of attachment of the shoulder belts to the structure. Incorrect belt angles between the shoulder and trailing length of the shoulder strap could result in spinal injury due to the compressive load introduced by the shoulder strap angle.

The pelvic joint is the portion of the body best able to withstand high g loads therefore the lap belt is used to prevent forward movement. Lap belts providing restraint above the pelvic joint will put excessive loads onto the stomach and other internal organs while loose belts are likely to allow “submarining”. This phenomenon occurs when the occupant slides under the belt causing additional injury to the lower abdominal in the process of being squeezed through the gap between lap belt and seat. Lap belt tie-down or crotch straps are used to prevent “submarining” by resisting the upward movement of lap belt. Wood & Sweginnes (1996) states that webbing with a large width is desirable to decrease injury due to the restraint system. Lap belts with a minimum width of 64 mm and 100 mm in the centre abdominal area and 50 mm for shoulder straps are recommended for forward facing seats. A detailed discussion on restraining occupants in aircraft is provided in Appendix B.

## Energy Absorption

Even if an adequate living space has been maintained and the occupants have been restrained sufficiently, the forces acting on the airframe and occupants during a crash can be high enough to cause serious or fatal injury. Energy absorbing materials and mechanisms must be used in the construction of the airframe to attenuate crash forces to tolerable levels. Farley (1983) showed that the specific energy absorption value of 100kJ/kg obtained for a graphite/epoxy tube could exceed that of an aluminium tube (80kJ/kg) of the same dimensions. Elastic structures with energy storing properties can cause dynamic overshoot, which produce delayed amplified decelerations of the occupant. On the other hand, materials that deform at relative high loads absorbing energy as they are crushed can attenuate crash forces significantly.

In U.S military helicopters energy absorption during a crash is accomplished primarily through three mechanisms, stroking of the seats, stroking of the landing gear and crushing of the fuselage sub-floor structure. Energy absorbing crew seats, which absorb energy as they gradually “stroke” over a large distance, have been designed and successfully implemented into these helicopters. The design challenge is thus to provide energy-absorbing mechanisms that will “stroke” through a distance or energy absorption through the structure.

## Environment

Although it is possible to design a restraint system good enough to restrain the torso, it is impractical to secure the head and limbs, which are used to perform normal flying tasks. According to Wood & Sweginnes (1996), the volume through which unrestrained portions of the body are able to move is described as the flail volume. A “clean” environment should be provided in this flailing volume, this should involve the elimination of any sharp or potentially harmful objects inside the occupants flailing envelope. Padding should be provided at potential impact surfaces and where a lethal object could not be moved from the flailing envelope. Attention should be given to the controls and breakaway features can be used in the instrument panel.

## Post-Crash Factors

All too frequently occupants survive the dynamic portion of the crash only to suffer additional injury or death because they could not exit the damaged cockpit in time. Fire is by far the most common post-crash factor and includes burning and smoke inhalation and is a major problem on motorised fuel carrying aircraft. The other primary factor is merely the fact that the occupants are unable to evacuate the damaged aircraft in time. It can be argued that by applying the four above mentioned design considerations, the occupant’s chances of being conscious and able to exit after the crash will be improved.

The post-crash factor design consideration implies the provision of a container that could be evacuated and restraints that could be released after a crash. It must also include the possibility of a mid air evacuation after a mid air collision. Container and restraint design must also allow evacuation after:

- A wheels up landing
- A water landing
- Landing in bushes or swampy terrain
- A roll-over landing

## **2.6 Impact Injury Criteria**

A range of impact trauma which may be used to establish bases for accepted levels or performance criteria in the evaluation of occupant survivability in aircraft are described in Advisory Circular (1985). The Advisory Circular stated that the scientific study of human body response to impact exposure began during World War II when the development of ejection seats for high-speed aircraft was initiated. Geertz and Ruff (Advisory Circular 1985) from Germany develop basic criteria for evaluating seat and restraint performance, which are still in use today. After the war the U.S Military continued the research through Colonel Stapp and other scientists, which were summarised by Eiband. The concern for automobile crash safety, which developed in the 1950’s and 1960’s, resulted in a great expansion to increase impact injury protection offered to the civil population.

Injury criteria describes the trauma limits of individual human body components and are therefore used to measure the injury or potential of injury to humans supported and restrained in a certain configuration while they are subjected to impacts. To evaluate the performance of a protection system without the risk of injuring a human subject an Anthropomorphic Test Device (ATD) may be used instead of a biological surrogate or human. Many dummies have been manufactured, but the only standardised ATD generally available is the Hybrid III crash test dummy described in 49 CFR 572. Impact injury criteria should be expressed in parameters that can be measured on an ATD.

Impact injury criteria have been dominated by historically measurement of acceleration but this can however be contributed to the ready availability of accelerometers rather than the significance of acceleration as a factor of injury. In short duration decelerations (e.g. less than 0.02 seconds) which usually occur during impacts, the injury limit would rather be body structural and would better be expressed in terms of body stresses and strains. It should however be understood that no universally accepted handbook values for impact injury criteria exist, as there would be for properties of materials used in aircraft construction. If the criteria and methods of demonstrating compliance with those criteria are not prescribed by an authority like the automotive industry, military or aviation authorities, the responsibility for selecting the appropriate criteria and test methods lies with the designer of the specific system.

## Head Injury

Head injuries cause a third of all aviation fatalities and should thus receive extra attention (The Naval Flight Surgeon's Pocket Reference to Aircraft Mishap Investigation 1995). Head injuries can either be fractures or concussions and the mechanism of injury depends on the energy of the impact, the rotation and translation of the head relative to the body, the characteristics of the impact surface and the site and direction of the load vector. The Wayne State University Concussion Tolerance Curve (WSUCTC) proposed by Lissner, et al in 1960 (Advisory Circular 1985) forms the bases for most current head injury criteria. One of the popular representations of the WSUCTC suggested by Versace (Advisory Circular 1985) is called the Head Index Criterion (HIC) and is specified in Federal Motor Vehicle Safety Standard (FMVSS) no. 208. The HIC requires a measurement of the acceleration of the CG of the head to be inserted into the following equation.

$$HIC = \left[ \frac{1}{(t_2 - t_1)} \int_{t_1}^{t_2} a(t) dt \right]^{2.5} (t_2 - t_1)$$

Where:

$a(t)$  is the time history of the acceleration at the head's CG expressed as a multiple of  $g$ .

$t_1$  and  $t_2$  are any two points in time during the impact separated by no more than 36 milliseconds time interval.

The value of HIC must not exceed 1000 at any calculated interval.

## Neck Injury

According to Eppinger et al. (1999), the current Federal Motor Vehicle Safety Standard (FMVSS) No. 208 includes criteria for neck injury consisting of individual tolerance limits for neck compression, neck tension, neck shear, flexion moment (forward bending of the neck) and extension moment (rearward bending of the neck). Tolerance values were derived from selected voluntary, cadaver and dummy tests and includes the following.

- Axial compression ( $-F_z$ )                                     -4000N
- Axial tension ( $+F_z$ )                                             3300N
- Shear ( $F_x$ )                                                             3000N
- Extension moment ( $-M_y$ )                                     -57Nm
- Flexion moment ( $+M_y$ )                                         190Nm

The above formulation does however not consider the combined effect of extension moment and tension force and therefore the concept suggested by Prasad and Daniel to evaluate combined loads on the neck was included. The resulting neck injury criteria called  $N_{ij}$  propose critical limits for all four possible modes of neck loading and is defined as the sum of the normalised loads and moments.

$$N_{ij} = \frac{F_z}{F_{int}} + \frac{M_y}{M_{int}}$$

Where:

- $F_z$          =         axial load (tension or compression)
- $F_{int}$        =         corresponding critical intercept value of load used for normalisation
- $M_y$          =         flexion/extension bending moment
- $M_{int}$        =         corresponding critical intercept value of moment used for normalisation
- $N_{ij}$          =         neck injury criteria value with performance limit of 1.0

$F_z$  and  $M_y$  are measured at the same point in time and  $N_{ij}$  should be calculated for each instance in time. For the Hybrid III mid-sized male the acceptable region for a combination of neck forces and moments are indicated by the grey region in Figure 2.5 where flexion moment is represented by the positive x-axis and extension moment by the negative x-axis. Neck axial force is represented by the y-axis with tension force indicated by positive y and compression by negative y. Boundary values for the acceptable region are determined by the critical intercept values  $F_{int}$  and  $M_{int}$  for the specific dummy type. Values for  $F_{int}$  and  $M_{int}$  for different dummy sizes are listed in Table 2.2.

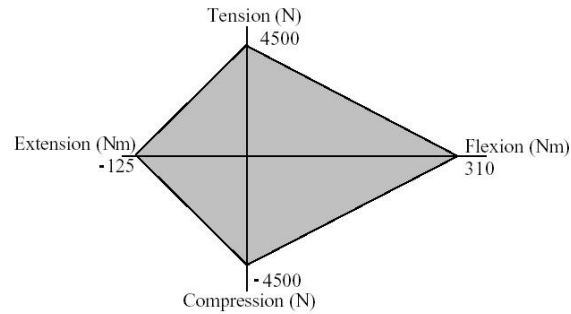


**Figure 2.5: Acceptable range of neck loading modes for the Hybrid III mid-sized male (Eppinger et al. 1999)**

**Table 2.2: Critical Intercepts for Neck Injury Criteria (Eppinger et al. 1999)**

| Dummy Type                  | Fint        |                 | Mint         |                |
|-----------------------------|-------------|-----------------|--------------|----------------|
|                             | Tension (N) | Compression (N) | Flexion (Nm) | Extension (Nm) |
| CRABI 1-year-old infant     | 1465        | 1465            | 43           | 17             |
| Hybrid III 3-year-old child | 2120        | 2120            | 68           | 27             |
| Hybrid III 6-year-old child | 2800        | 2800            | 93           | 39             |
| Hybrid III small female     | 3370        | 3370            | 155          | 62             |
| Hybrid III mid-sized male   | 4500        | 4500            | 310          | 125            |
| Hybrid III large male §     | 5440        | 5440            | 415          | 166            |

### Chest Injury

Upper torso injuries can be both skeletal or soft tissue related. Neathery (Advisory Circular 1985) suggested that chest injury could be related to chest deflection and recommended a sternal deflection limit of 75mm. This deflection represents severe but nonlife threatening chest injury for a 45-year-old mid-sized male. The problem with this criterion was to make a good single measurement that would represent the complex thorax behaviour under all the conditions of an impact.

## University of Pretoria etd – Meintjes, S W v d M (2004)

An alternative easily measured criterion suggested by Eppinger (Advisory Circular 1985) was to measure the shoulder belt load during impact. As a result of thoracic fractures in cadaver tests, he suggested that an upper torso diagonal belt load of 5.8 – 6.7kN during a 13.4m/s frontal impact would produce the minimum average number of thoracic fractures in the automobile population. Federal Aviation Regulation (1997) Part 23.562 specifies that the load in individual shoulder straps may not exceed 7780N. When dual straps are used the total strap loads may not exceed 8900N. These results are however influenced by belt geometry, a factor not represented in the analysis.

### Abdominal Injury

The research accomplished to date to define a suitable abdominal injury criterion has been limited, therefore no practical criteria exists. Considering the potential severity of abdominal loading, it is recommended to avoid loading of the abdominal area. Lap belts should be designed not to slip from the pelvis to the abdomen.

### Leg Injury

#### Femur

Early studies by Patrick, et al and Melvin, et al (Advisory Circular 1985) on the patella-femur-pelvis complex of cadavers indicated an injury threshold of between 6.2 and 13.3kN impact compression force essentially inline with the femur. The current limit specified in FMVSS 208 is 10kN, which is an appropriate criterion in aircraft.

#### Patella

Concentrated impact loading of the patella by impactors having circular or ring shapes less than 16mm in diameter demonstrated failures as low as 2.5kN.

#### Tibia

According to Young (Advisory Circular 1985), transverse loading of the lower leg resulted in tibia fracture at forces from 4.45 – 6.67kN. Kramer (Advisory Circular 1985) found a 50% fracture limit of the tibia to lie between 3.3 and 4.4kN.

### Spinal Injury

Compression loads on the spine frequently causes damage to the vertebral column, particularly to the upper lumbar and lower thoracic segments. This is especially true in aircraft accidents when the impact load normally involves a high magnitude vertical component.

#### Dynamic Response Index (DRI)

Stech and Payne (Advisory Circular 1985) modelled this longitudinal impact to the spine as a single degree of freedom spring-damper-mass system assuming that the total body mass, which acts on the spine could be represented as a rigid mass. This model was then used to predict the total deformation and force in the spring, which represents the spinal column for a given input acceleration-time history pulse. The acceleration input pulse could be measured on a structural member e.g. the seat pan of an ejection seat. The injury criteria that resulted from this model were called the Dynamic Response Index (DRI). The U.S Military suggested the following DRI limits for uniaxial spinal compression fractures.

|            |                                        |
|------------|----------------------------------------|
| DRI = 18.0 | Less than 5 percent risk of injury     |
| DRI = 20.4 | Less than 20 percent risk of injury    |
| DRI = 23.0 | Greater than 50 percent risk of injury |

The DRI criterion was successfully used in several military programs because these programs provided well designed restraint systems which prevented bending loads on the spine. In many civil and commercial applications this was, however, not the case and therefore an alternative criteria had to be constructed.

#### Lumber Load Criteria (LLC)

Chandler (Advisory Circular 1985) conducted tests using a modified part 572 Anthropomorphic Test Dummy with a load cell inserted into the pelvis of the dummy to measure the force transmitted to the pelvis through the spinal column. This compressive force was related to the potential of injury to the lumbar spine due to upward acceleration of the body. Chandler found that a lumber load of 6672N correlated with a DRI of 19, which indicated a low to moderate risk of injury. This method has more general application and is suggested for use in aircraft.

## **2.7 Crash Pulse Shapes**

One of the most difficult tasks of the aircraft accident investigator after an aircraft mishap is to decide what acceleration pulse shape would most likely describe the crash event. Some years ago NASA conducted a series of old aircraft structure crashes under very controlled and instrumented conditions (Wood & Sweginnes 1996). The acceleration with respect to time on the structure, displayed by an oscilloscope showed that the impact is a series of ragged peaks for short duration of time. Each of these oscilloscope displays had a characteristic shape based on the nature of the impact and could however be approximate by a curve with a simple geometry e.g. a rectangular or a triangle.

### Rectangular Pulse Shape

This pulse requires unchanging acceleration over the impact period and implies minimum peak G's sustained by the object. Examples include normal landings with constant braking and wheels up landing on snow or ice (See Figure 2.6).

### Triangular Pulse Shapes

These events include constantly changing acceleration levels, either increasing, decreasing or a combination. Examples of increasing acceleration (Figure 2.7) include impacting mud, dirt or a crash that creates a deep crater.

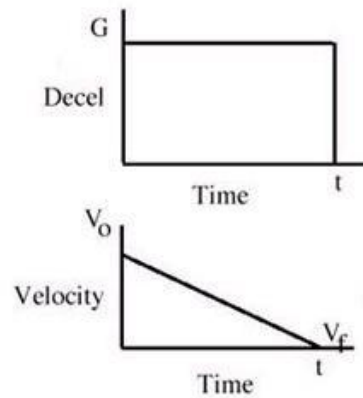


**Figure 2.6: Rectangular acceleration pulse shape (The Naval Flight Surgeon's Pocket Reference to Aircraft Mishap Investigation 1995)**

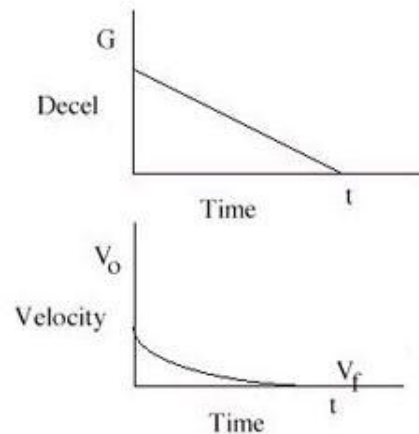


**Figure 2.7: Increasing acceleration pulse shape (The Naval Flight Surgeon's Pocket Reference to Aircraft Mishap Investigation 1995)**



Examples of decreasing acceleration (Figure 2.8) include skidding on pavement or impacting an object that gradually gives way i.e. a tree.

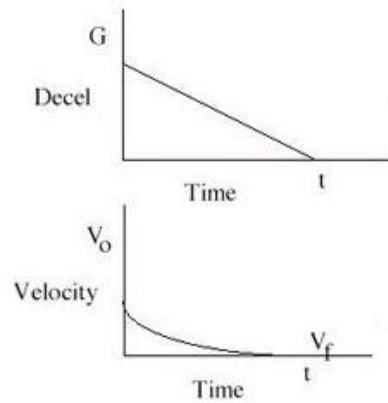


**Figure 2.8: Decreasing acceleration pulse shape (The Naval Flight Surgeon's Pocket Reference to Aircraft Mishap Investigation 1995)**

According to The Naval Flight Surgeon's Pocket Reference to Aircraft Mishap Investigation (1995), the most common acceleration pulse shape encountered in aircraft mishaps is the increasing-decreasing pulse shape shown in Figure 2.9. Although this crash pulse shape is an approximation at best it represents the worst case scenario when peak accelerations are greatest e.g. aircraft flying through trees or a shallow angle water entry.

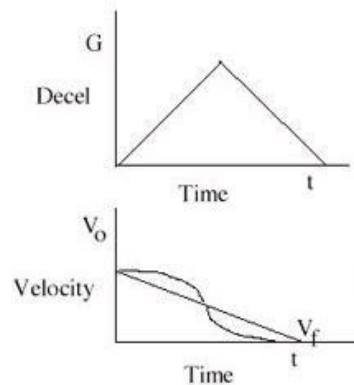


**Figure 2.9: Increasing decreasing acceleration pulse shape (The Naval Flight Surgeon's Pocket Reference to Aircraft Mishap Investigation 1995)**

In The Naval Flight Surgeon's Pocket Reference to Aircraft Mishap Investigation (1995) and Wood & Sweginnes (1996), it is stated that in the case of a general aviation accident the rectangular pulse shape shown in Figure 2.6 would always represent the best case scenario and the equilateral triangle of Figure 2.9 would represent the worst case scenario.

## 2.8 Dynamic Crashworthiness Testing

According to Nicholson & Chapman (199-?), the Dynamic Crashworthiness Requirements for light aircraft were introduced by the FAA in August 1988 and is contained in FAR Part 23.562 – Emergency Landing Dynamic Conditions. FAR Part 23.562 were included in an attempt to improve the crashworthiness of light aircraft in response to a perceived need. The National Transportation Safety Board conducted a study on general aviation crashworthiness using the crash data of 1982. They concluded that the use of shoulder harnesses in aircraft might have prevented 76% of the fatalities and 79% of the serious injuries. A similar study on the proposed use of energy absorbing seats in general aviation aircraft indicated that 2% of fatalities may have been prevented and 38% of the serious injuries may have been prevented by the use of energy absorbing seats.

FAR Part 23.562 requires that the seat and restraint system undergo dynamic testing using a typical crash pulse. Two tests are required to demonstrate compliance with FAR Part 23.562 with the purpose to demonstrate that crash forces on the occupant have been attenuated to within human tolerances. Additional requirements of FAR Part 23.562 state that the tests must be conducted using an ATD specified by 49 CFR Part 572.

Because of the relevance of these tests to this study, it was decided to use them during one of the analysis described in Chapter 4. The two dynamic tests that are required for compliance with FAR Part 23.562 are specified as follow.

*B. Except for those seat/restraint systems that are required to meet paragraph (d) of this section, each seat/restraint system for crew or passenger occupancy in normal, utility, or acrobatic category aeroplane, must successfully complete dynamic tests or be demonstrated by rational analysis supported by dynamic tests, in accordance with each of the following conditions. These tests must be conducted with an occupant simulated by an anthropomorphic test dummy (ATD) defined by 49 CFR Part 572, Subpart B or a FAA-approved equivalent.*

*(1) For the first test, the change in velocity may not be less than 31 feet per second. The seat/restraint system must be oriented in its nominal position with respect to the airplane and with the horizontal plane of the airplane pitched up 60 degrees, with no yaw, relative to the impact vector. For seat/restraint systems to be installed in the first row of the airplane, peak deceleration must occur in not more than 0.05 seconds after impact and must reach a minimum of 19g. For all other seat/restraint systems, peak deceleration must occur in not more than 0.06 seconds after impact and must reach a minimum of 15g (see Figure 2.10).*

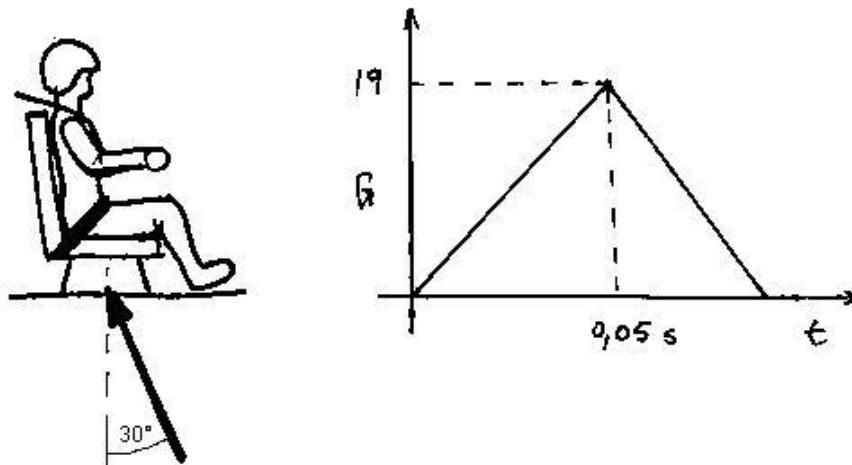


Figure 2.10: FAR 23.562 dynamic Test 1

(2) For the second test, the change in velocity may not be less than 42 feet per second. The seat/restraint system must be oriented in its nominal position with respect to the airplane and with the vertical plane of the airplane yawed 10 degrees, with no pitch, relative to the impact vector in a direction that result in the greatest load on the shoulder harness. For seat/restraint systems to be installed in the first row of the airplane, peak deceleration must occur in not more than 0.05 seconds after impact and must reach a minimum of 26g. For all other seat/restraint systems, peak deceleration must occur in not more than 0.06 seconds after impact and must reach a minimum of 21g (see Figure 2.11).

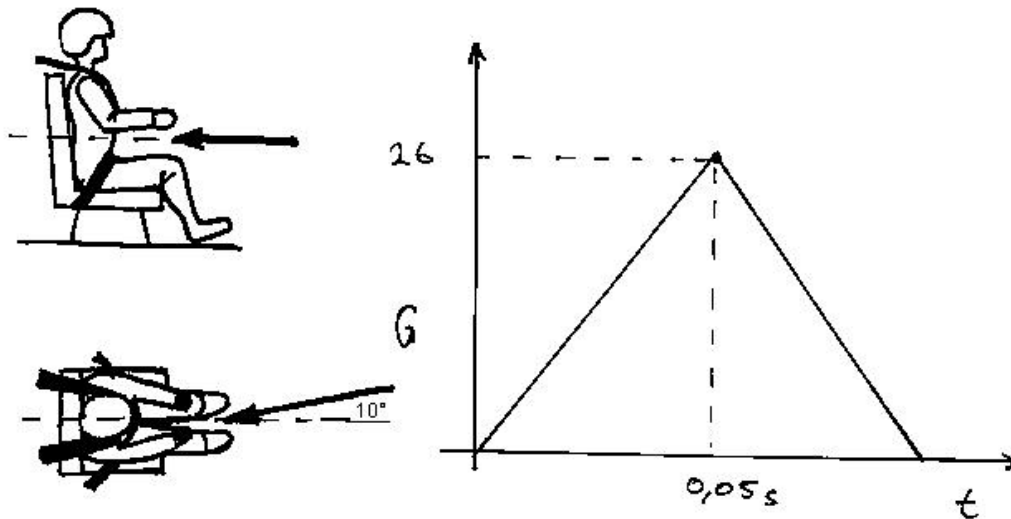


Figure 2.11: FAR 23.562 dynamic Test 2

## University of Pretoria etd – Meintjes, S W v d M (2004)

During these two tests the following requirements must be met in order to comply with the requirement.

*C. Compliance with the following requirements must be shown during the dynamic tests conducted in accordance with paragraph (b) of this section:*

- (1) The seat/restraint system must restrain the ATD although seat/restraint system components may experience deformation, elongation, displacement, or crushing intended as part of the design.*
- (2) The attachment between the seat/restraint system and the test fixture must remain intact, although the seat structure may have deformed.*
- (3) Each shoulder harness strap must remain on the ATD's shoulder during the impact.*
- (4) The safety belt must remain on the ATD's pelvis during the impact.*
- (5) The results of the dynamic tests must show that the occupant is protected from serious head injury.  
(i) When contact with adjacent seats, structure, or other items in the cabin can occur, protection must be provided so that the head impact does not exceed the head index criteria (HIC) of 1000.*
- (6) Loads in individual shoulder harness straps may not exceed 1750 pounds. If dual shoulder straps are used for retaining the upper torso, the total strap loads may not exceed 2000 pounds.*
- (7) The compression load measured between the pelvis and lumbar spine of the ATD may not exceed 1500 pounds.*

The exact same emergency landing dynamic condition is also specified in JAR-23 (2001). This specification together with some other regulations on pilot protection in light aircraft is contained in Appendix C.

### **2.9 Pilot Support Positions**

#### **The Normal Seated Position**

The normal seated position probably dates back even far before the origin of the first chair and is the most popular sitting position. Every day, most people spend some time sitting in the normal seated position and therefore it is assumed that the reader is familiar with this position. It is also the most common occupant support position used in transportation today. Thousands of automobiles produced all over the world implemented the normal seated position. In aviation every commercial, commuter and almost every civil and military aircraft has implemented this position. It is fair to say that the normal seated position is the norm in aviation occupant support (see Figure 2.12).

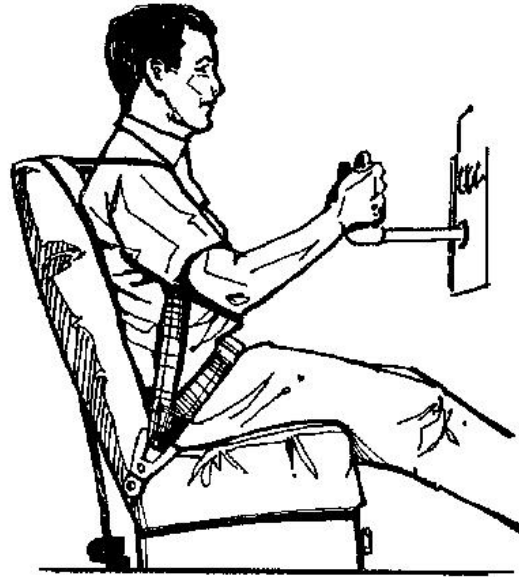


**Figure 2.12: Aviator in the normal seated position (Advisory Circular 1993)**

The advantage of such a universally accepted standard is that a lot of information concerning occupant protection in this position already exists and was published. Some other advantages of the normal seated position are that it offers a good field of vision and good comfort. It provides the pilot with a big volume in which controls would be accessible and easy to reach. In civil aircraft, occupants in the normal seated position are normally restrained by a three point restrained system as shown in Figure 2.13, while aerobatics and military pilots are restrained by four or five point restraint systems shown by Figures 2.14(a) and 2.14(b) respectively.

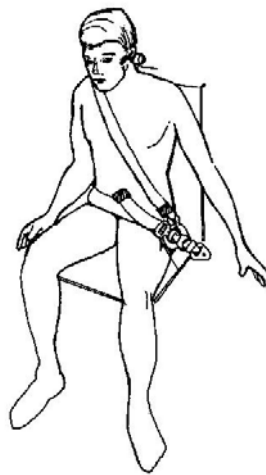


**Figure 2.13: Three-point restraint (Advisory Circular 1993)**

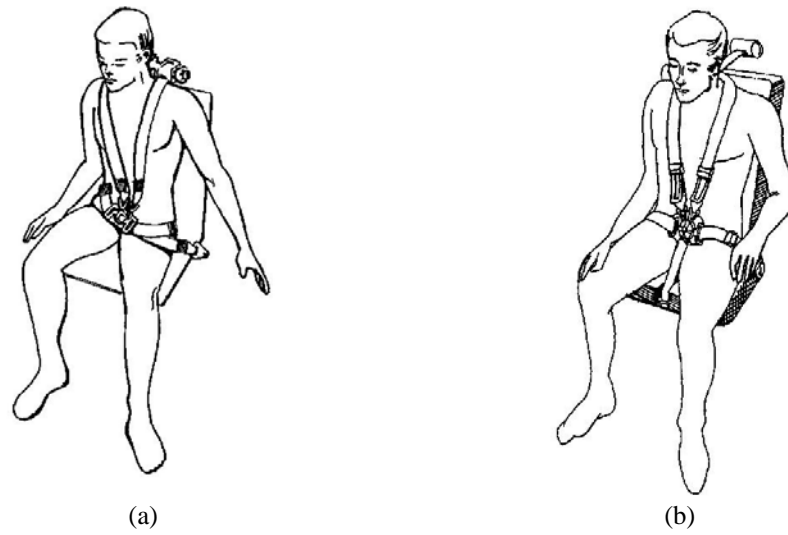


**Figure 2.14: Four and five-point restraint (Advisory Circular 1993)**

The major disadvantages of this position are that the normal seated position would require a relative large frontal fuselage area to house the pilot and seat construction. Head injury could most likely occur in this position. This is especially true for pilots sitting in the cockpit area facing the instrument panel and control stick. Head injury usually result from inadequate torso restraint due to slack in the shoulder straps or failure of the torso restraint system. According to Richards & Podob (1997), compression of the lower lumbar spine during high impact emergency landings often resulted in back injury to occupants in the normal seated position. Additional injury due to arrestment by the webbing restraint system with little distribution of impact pressure is also a disadvantage of this position. In conclusion the major advantages and disadvantages are summarised.

#### Advantages

- Conventional, it has been implemented with success and a lot of data exist for this position
- Comfortable
- Good field of vision
- Provides a large volume with easy reachable flight controls

#### Disadvantages

- Results in a large frontal fuselage area
- Potential for head injury
- Potential for back injury during likely crash scenarios
- Potential for additional injury by webbing and buckles of restraint system

## The Prone Position

Although the historic flight by Orville Wright on 17 December 1903 (Figure 2.15) was done in the prone position it intuitively seems odd and rather dangerous to fly an aircraft in this position. Interestingly enough, some discoveries made during the literature survey concerning the causes of aviation injury and fatalities and human tolerance to high magnitude deceleration suggested otherwise. Nature also tells a different story. If a cat leaps down from a height, it does so in the prone position landing on the front legs. Birds fly with their heads first, which could arguably be referred to as the prone position. Since the early days, concepts of the prone flying position have been investigated and some have even been implemented in a few aircraft. In this paragraph some of the advantages and disadvantages of supporting a human in the prone position would be discussed.

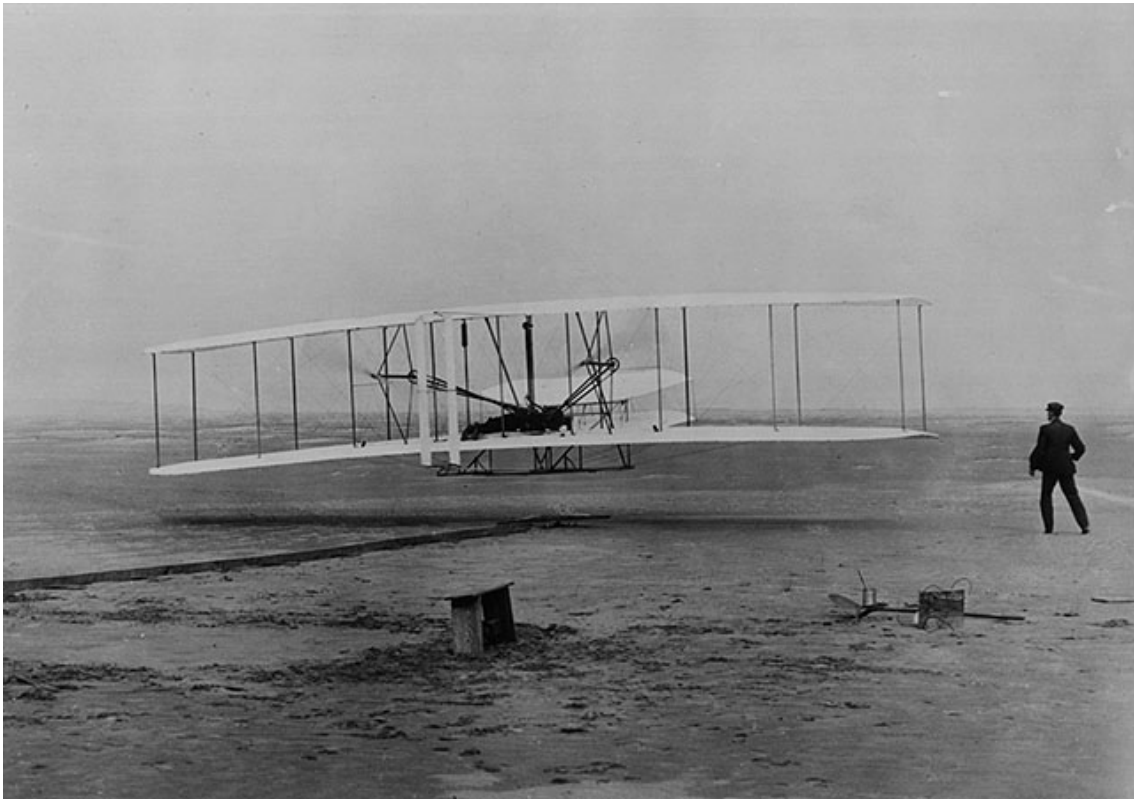


**Figure 2.15: Historic flight by Orville Wright on 17 December 1903, note the prone position (Bradshaw 1996)**

The conventional hang glider (Figure 2.16) is probably the best example of humans flying in the prone position. Some other flying machines utilising the prone position have also found their way into the history books e.g. the Berlin B-9 and the Horten Ho IV shown in Figures 2.17 – 2.19.



**Figure 2.16: Hang glider with pilot in prone position (Couto 1999)**



**Figure 2.17: The Berlin B-9 prone pilot aircraft (Luftfahrt International 1975)**





**Figure 2.18: The Horten Ho IV flying wing with the pilot in the prone position (RFRL)**



**Figure 2.19: A close-up of the Ho IV showing the prone pilot position (RFRL)**

Other interesting prone pilot position concepts under development are the MasterBlaster project (Testi 1998) and the Exulans II glider shown in Figures 2.20 and 2.21.

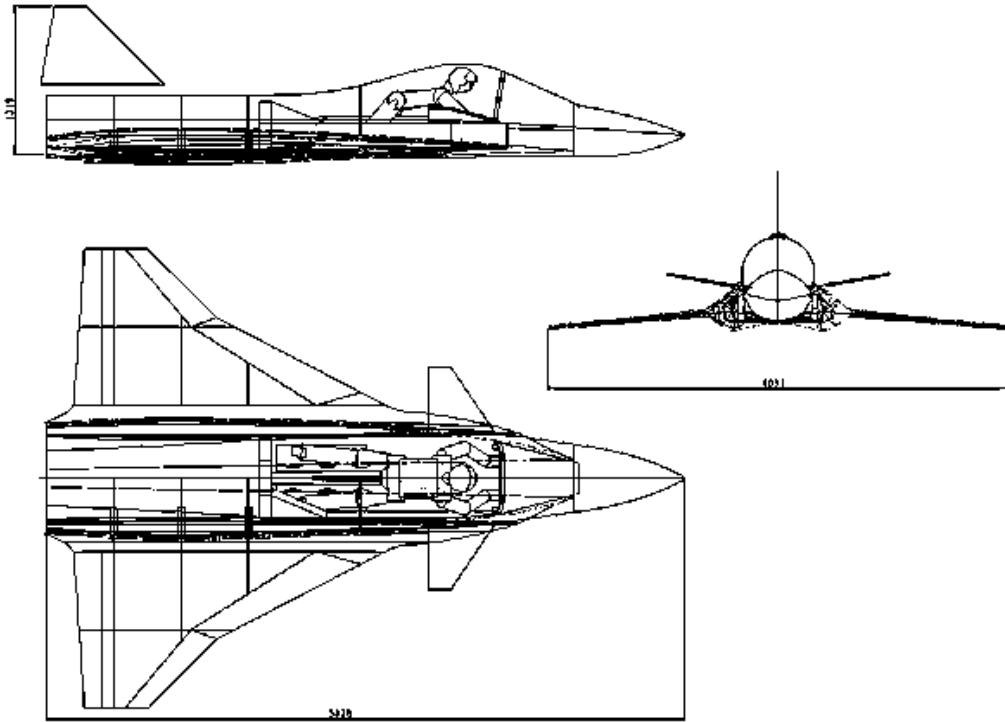


Figure 2.20: The MasterBlaster aerobatics aircraft concept with prone pilot (Testi 1998)

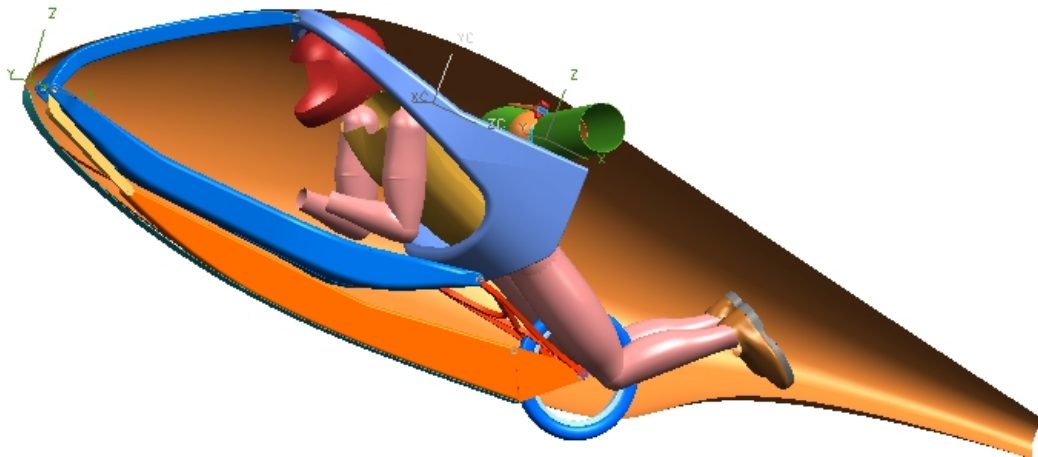


Figure 2.21: Exulans II glider with prone pilot

Racing motor cyclists travelling at speeds in excess of 250km/h are also supported in the riding position, which shows a close resemblance with the prone position (Figure 2.22).



**Figure 2.22: The rider of a super bike in the riding position (Valencia 2003)**

Experiments with the prone pilot position started in the 1930's when the DVL (German Aviation Experimental Establishment) initiated a study to enable dive-bomb pilots to withstand higher G values during the pull out. In 1937 the flight technical study group of the Berlin-Charlottenburg Technical High School had build a small prone pilot aircraft the Berlin B-9 (Figure 2.17) to participate in this research program. Early battle experience during World War II had indicated that the frontal area of a Focke-Wulf 190 provided a target that could be hit by a B-17 gunner at a range of more than 1000 yards. With the issue of the German Air Ministry of a requirement for a small target defence interceptor, it was logical to propose a prone position for the pilot to reduce the frontal area to the bare minimum.

In 1941 Alexander Lippisch also suggested the prone position as a flying position to enable pilots to withstand higher low magnitude accelerations (less than 10g, longer than 1second) and to minimise the fuselage frontal area. For the same reasons the Royal Air Force (RAF) Institute of Aviation Medicine required an aircraft that could be flown by a pilot in the prone position. In 1954 the Gloster Meteor F8 (Prone Position) shown in Figure 2.23 joined the Institute of Aviation Medicine and after 55 hours of flight testing it was concluded that the prone position concept was feasible. The development of special aviation

clothing however, offered a simpler solution to the counteracting of high g-forces and therefore the prone position was abandoned (RAF MUSEUM). Although minimising the aircraft's frontal area to avoid being hit by a shell from a gunner is not a requirement of this project. A small frontal area implies less drag, which leads to a higher efficiency aircraft, which is indeed a requirement of the Exulans project.



**Figure 2.23: Gloster Meteor F8 prone pilot experimental aircraft (RAF MUSEUM)**

Alexander Lippisch claims that the major drawback of flying in the prone position was the insufficient field of vision enjoyed by fighter pilots. The fact that breathing discomfort could easily result from applied pressure on the stomach and lower torso imply that special attention should be given to comfort and support in the prone position. Another disadvantage is merely the fact that very little information on the prone position is available in literature. To conclude this sub chapter the main advantages and disadvantages of the prone position are summarised below.

#### Advantages

- The ability to withstand higher G-forces
- Allows for a smaller fuselage frontal area
- Higher human impact tolerance to likely crash scenarios
- Provides improved passive restraint opportunities
- Arguably smaller flailing envelope
- Eliminates the potential for “submarining”
- Occupant supporting structure offers protection to chest and abdominal penetration
- Lower chances for back injury due to vertebra compression
- Provides good opportunity for foot launching

#### Disadvantages

- Support needs special attention to provide sufficient comfort
- Often criticised for being harsh on neck muscles
- Unconventional, very little information available

### The Supine Seated Position

The supine position is generally associated with soaring and most modern sailplane designs have implemented this support position (Figure 2.24). The difference in body position between the supine position and the normal seated position is that the upper body is supported at a much lower angle with respect to the aircraft's longitudinal axis. The occupant's feet are also supported almost in the same horizontal plane as the hip centre. This reclined body position offers excellent comfort and sufficient field of vision and as with the prone position it allows for a small frontal fuselage area providing the aircraft with a relative high efficiency necessary for gliding.

Restraint in this position is normally achieved with the 4-point or 5-point restraint system recommended lap and shoulder belt attachment points are shown in Figure 2.25. The fact that "submarining" is likely to occur in this position calls for the implementation of the crotch strap and therefore the use of the 5-point system is recommended. Another disadvantage of this position is that a likely accident with both horizontal and vertical deceleration components will cause the impact load to compress the spinal column due to the reclined body position. It can also be seen that most sailplanes do not have sufficient space between the occupant's buttocks and the fuselage floor to implement a load-limiting device.



**Figure 2.24: The supine position used in sailplanes (GFA)**

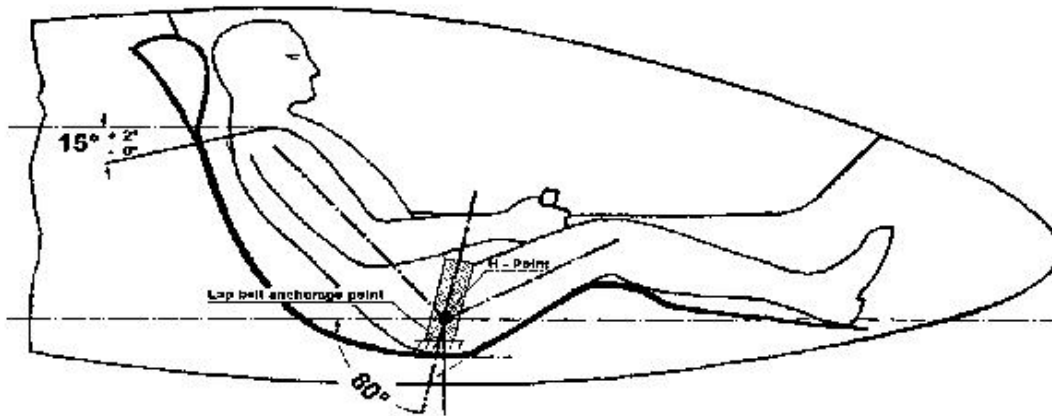


**Figure 2.25: Recommended lap and shoulder belt attachment point in supine position (JAR-22 2001)**

The advantages and disadvantages of the supine position are summarised below.

#### Advantages

- Extremely comfortable
- Good field of vision
- Allows small fuselage frontal area

#### Disadvantages

- Minor accidents can result in back injury caused by spinal compression due to body position
- Submarining is likely to occur in this position
- Very little energy absorbing distance between seat and fuselage floor
- Potential for additional injury by webbing and buckles of restraint system

## **2.10 Summary**

In Conclusion to this literature study it is the opinion of the author that free information on the topic of occupant protection in aircraft is relatively limited. Basically every bit of information that was found during this phase of the project was included in this chapter. No information was excluded on second thought because of insufficient relevance. This is however not the case concerning the topic of occupant protection in motor vehicles and one would feel that this shortfall could be overcome.

## University of Pretoria etd – Meintjes, S W v d M (2004)

The majority of the work done on this topic was focused on military application, especially on U.S Military helicopters with pilots supported in the normal seated position. Virtually no data exist for occupants supported in flying positions other than the normal seated position. Although energy absorption and restraint are only two of the five crash survival design considerations, it seems that these two factors were the most popular topics in the variety of past load limiting seat/restraint systems research projects. The subject of airframe crashworthiness or “container” design deserves more attention and it seems that the recommendations in the literature concerning this subject are much more severe than those found in the aviation regulations.

The literature study provided useful insight and essential data to the project. The thesis specifications and the concept proposal for the Exulans pilot protection system were based on the findings of the literature study and are contained in the following chapter.

## CHAPTER 3: PROPOSED CONCEPTS

### Preview

1. The thesis specifications are stated in non-specific terms as an introduction to this chapter.
2. The pilot support concept is proposed to the reader followed by the philosophy behind this proposal.
3. Some results of the ergonomical investigation are also contained in this chapter.
4. Concepts for the structural and systems design of the Exulans II fuselage are proposed under the headings of the five CREEP design factors.



### **3.1 Thesis Specifications**

As part of the development of a pilot protection system for Exulans, this thesis will investigate pilot protection in light aircraft in general but more specifically it will launch a comparative study into different pilot support positions. The specifications for this thesis are listed as follow:

1. Investigate common causes of aviation fatalities
2. Investigate human impact tolerance limits and injury thresholds
3. Investigate occupant crash protection requirements set by the authorities
4. Investigate different pilot support positions
5. Investigate restraining methods
6. Compare the crash response of a pilot in the prone position to that of other support positions
7. Generate recommendations and guidelines for the design of the Exulans II pilot protection system

Although meeting all the requirements of the specifications for the development of the pilot protection system for Exulans II is not considered a goal for this thesis, they were also included as background information. These specifications are categorised below as ergonomical and structural specifications.

#### **ERGONOMICAL SPECIFICATIONS**

1. Investigate the following ergonomical challenges:
  - Getting in and out of the glider
  - Pilot support and restraint
  - Flight control actions in the support position
  - Layout of controls and instrument panels
  - Pilot field of vision
2. Provide a pilot support system that is both comfortable and safe. The support system must be designed for a pilot wearing a personal parachute
3. One flight may last several hours therefore the pilot should be able to relax in the support position without excessive strain on any part of the body.
4. Provide comfortable restraining methods that will not contribute to injuries during a crash. Restraints should be applied to portions of the body best able to withstand high impact forces and accelerations like the shoulders and pelvis.
5. The restraint locking mechanisms should be reachable and detachable during every instance and aircraft attitude.

## STRUCTURAL SPECIFICATIONS

1. Provide a container that would maintain an occupiable space during a survivable crash (It is recommended that the container should be designed for a 40g ultimate load).
2. The design of the container should allow it to be deflected or rotated into an attitude where energy absorption could proceed in a controlled manner.
3. The container should have the smallest possible frontal area and roll over protection should be considered.
4. Provide energy absorbing mechanisms and materials in the structural design that would attenuate crash forces to tolerable levels during a survivable crash.
5. Provide a cockpit environment cleared from any potentially harmful objects.
6. Implement breakaway features in the control stick and apply padding at potential impact surfaces.
7. Push rods close to the pilot must be placed strategically, not in line with any part of the body.
8. Provide the fuselage with a ballistic parachute.
9. Provide a method to evacuate the fuselage after a survivable crash.
10. On the ground the pilot must be accessible from outside the fuselage.
11. Provide a method for a mid-air bailout.

### **3.2 Proposed Pilot Support Position**

During this subchapter the proposal of the prone pilot position for Exulans is introduced to the reader. Previous studies by the author (Meintjes 1999) and Hanique (2002) investigated the ergonomical feasibility of the prone position as a pilot support position specifically for Exulans. These studies concluded that the pilot's upper torso should be supported onto a chest plate and leg supports should be applied above and below the knees. To provide the necessary comfort, the supports must be lined with a soft material. The pilot's feet should rest on feet supports and connecting the pilot's harness to the airframe structure would provide restraint and additional support. The detail of the proposed prone pilot support position is included in the ergonomical investigation below and is followed by a subchapter stating the reasons that led to this proposal.

#### The Ergonomical Investigation

A previous study by the author (Meintjes 1999) suggested that the pilot's chest should be supported at an angle between 25° and 30° for optimum comfort. This study also indicated that support beneath the elbows greatly enhanced the pilot's comfort by especially relieving some of the pressure experienced on the chest (see Figure 3.1).



**Figure 3.1: Prone pilot position ergonomical investigation (Meintjes 1999)**

During a further study by Hanique (2002), a steel frame mock-up (Figure 3.2) was constructed to investigate the following ergonomical aspects:

- Getting in and out of the prone seat
- The supporting method
- The restraining method
- Pilot comfort
- Flight control actions in the prone position
- Pilot field of vision
- Layout of controls and instrument panel



**Figure 3.2: Steel frame mock-up (Hanique 2002)**

In this mock-up the pilot was supported on a fixed chest plate with an angle of approximately  $30^\circ$  with respect to the horizon. The hip bones in the pelvic region provided good supporting points and additional comfort was achieved with the padded upper leg supports. The knee supports prevented the pilot from slipping down the angle created by the chest plate and also removed some of the pressure from the chest. The pilot's feet were supported on a footrest and support beneath the elbows was provided as suggested previously.

### **3.3 Reasons Leading to the Pilot Support Proposal**

Several reasons led to the suggestion of supporting the Exulans pilot in the prone position. During the literature study it was discovered that the human body could tolerate the highest impact load in the chest to back or eyeballs out ( $-G_x$ ) direction. During a likely crash scenario this would also be the direction of application of a crash load to a pilot in the prone position as indicated by Figure 3.3

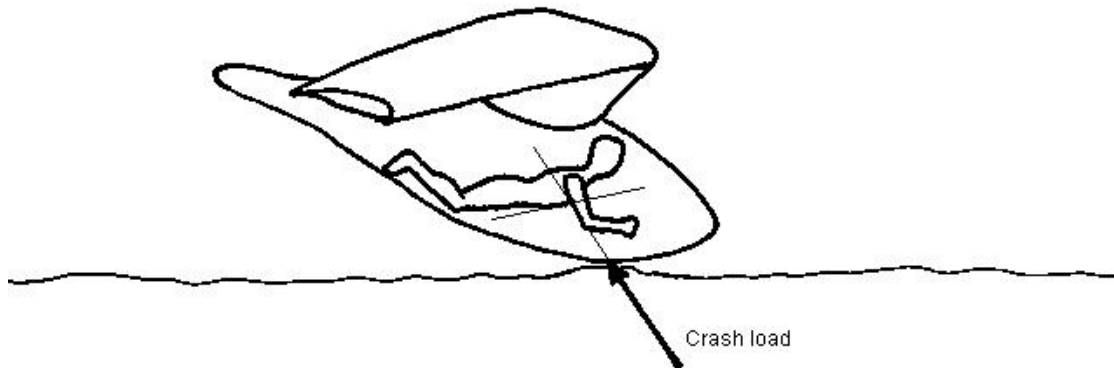


**Figure 3.3: Direction of impact load on prone pilot during likely crash scenario**

Head injury is responsible for a third of all aviation fatalities and is often due to improper torso restraint (The Naval Flight Surgeon's Pocket Reference to Aircraft Mishap Investigation 1995). The prone position would offer excellent opportunity to support the pilot's torso onto a passive restraint system or mechanism. Back injury would also be limited in the prone position due to the fact that there would be no seat structure behind the pilot that would apply a dangerous compressive force to the spine during a crash. Internal organ damage caused by impact into the restraining webbing and "submarining" would also be eliminated and it could be argued that the pilot in the prone position would have a small flail volume.

The capability of Exulans to perform a high angle of attack or flared landing due to its tailless configuration was previously mentioned. This action is executed during the landing, just before touchdown and implies that pilot error during this manoeuvre could be fatal due to the fact that the aircraft would have no altitude to recover from the mistake. Looking at the dynamics of the flared landing action represented in Figure 3.4 it seems that performing this action in the normal seated or supine seated position would compromise the pilots safety and field of vision as indicated in Figure 3.4 (a). The prone position would however result in an almost upright body position with respect to the landing surface as shown by Figure 3.4 (b). Finally the prone position offers excellent field of vision and would result in a much smaller fuselage frontal area required for high efficient flight.

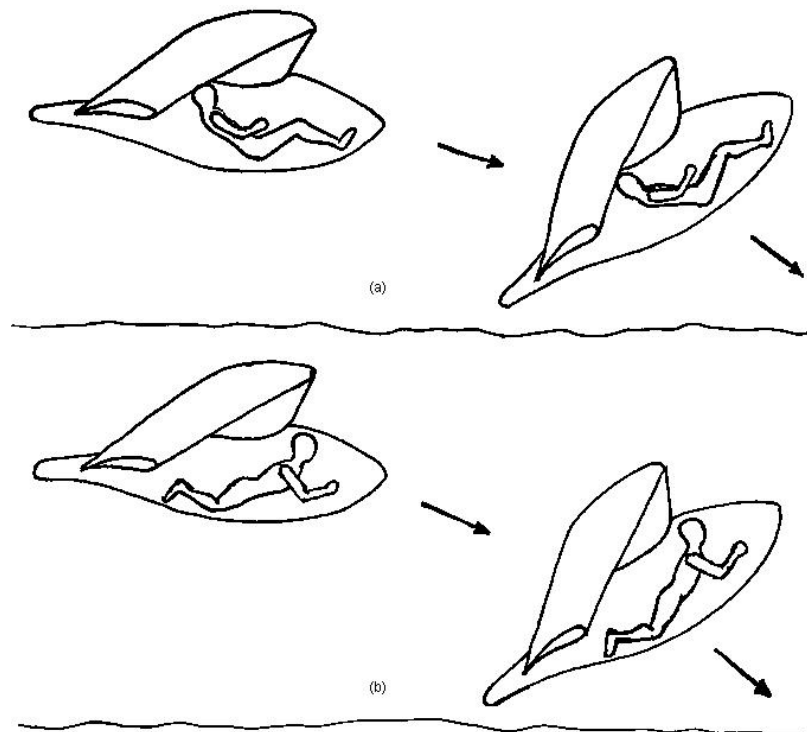


**Figure 3.4: High angle of attack landing executed in different pilot positions**

The ultra-light construction of Exulans together with the proposal of the prone pilot position offered an excellent opportunity to implement and introduce this proposal to the aviation community. It was also learned from the literature study that designing a crashworthy aircraft involves the consideration of five factors known as the CREEP design factors. During the following subchapter concepts for the structural design of the fuselage are proposed in consideration with these factors.

### 3.4 CREEP Concept Design Proposals

#### 3.4.1 Container Concept

The Exulans airframe or container concept is shown as a CAD drawing in Figure 3.5. The aim of the container design is to establish a very strong lightweight construction that would not fracture but rather be deflected into an attitude where energy could be dissipated in a controlled manner. To achieve the rigid lightweight construction, the parts could be manufactured from carbon fibre composite material with high-density polystyrene as the sandwich material. It is desirable to design these parts for a 40g ultimate load as stated by The Naval Flight Surgeon's Pocket Reference to Aircraft Mishap Investigation (1995) and Wood & Sweginnes (1996). The strength of these parts is however limited by the strict weight limitation of this ultra-light glider.

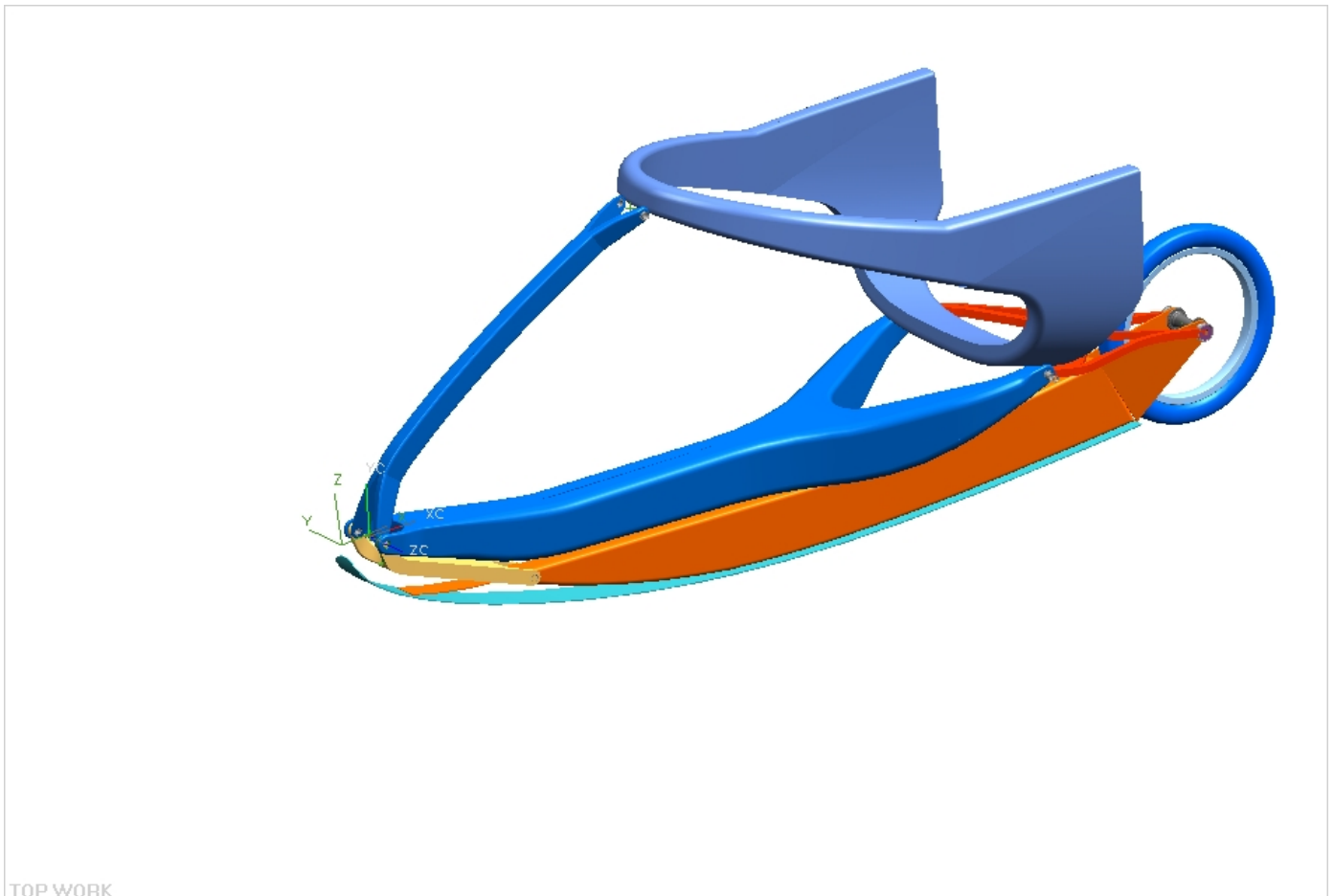


Figure 3.5: Exulans II container concept

### 3.4.2 Restraint Concept

The exceptionality of the prone pilot position implies that no conventional restraining method for this position exists. As with the pilot support position proposal, the restraining method would be a unique concept and should be designed following the basic restraining guidelines. One concept for a restraining system in the prone position is the custom manufactured chest plate harness shown in Figure 3.6. The pilot would fit the harness and tighten the belts to a comfortable fit before entering the cockpit. The harness consists of a rigid chest plate and 45mm webbing extending from the chest plate over the shoulders, through the legs, back to the chest plate. The blue padding between the composite chest plate and chest and between the legs is provided to enhance the comfort of the harness.



**Figure 3.6: Pilot wearing the custom manufactured harness**

Inside the cockpit the pilot would connect the chest plate to the supporting structure through an energy absorber, hence the passive torso restraint. Additional belts extending from the hips would restrain the pelvis to the supporting structure. It is suspected that sufficient pelvic restraint in the prone position would provide the advantage of tension rather than compression loading of the lumbar spine. This would be contributed to the fact that the upper torso would displace forward during a crash. As the torso displaces forward it will tension the spine which is restraint at the base by the pelvic belts. The harness connections to the supporting structure could all be of the quick release type and the emergency parachute would also be connected to the buckles on the harness's shoulder straps. The legs would be supported above and below the knees on padded leg supports and would be free to move from and to the supports as required. Footrests would be provided.

### 3.4.3 Energy Absorption Concept

Energy absorption in Exulans is primarily achieved by three mechanisms. The first mechanism is the collapsible landing skid shown in Figure 3.7. The collapsible landing skid mechanism consists of the skid, skid strut, wheel strut and the energy-absorbing element. This mechanism operates on the basis of a parallelogramming motion energy absorber described by Winkelman & Laananen (1996). Pivots at both ends of the skid strut and wheel strut permits the parallelogramming motion of the landing skid mechanism while the elongation of the diagonal energy-absorbing element absorbs energy.

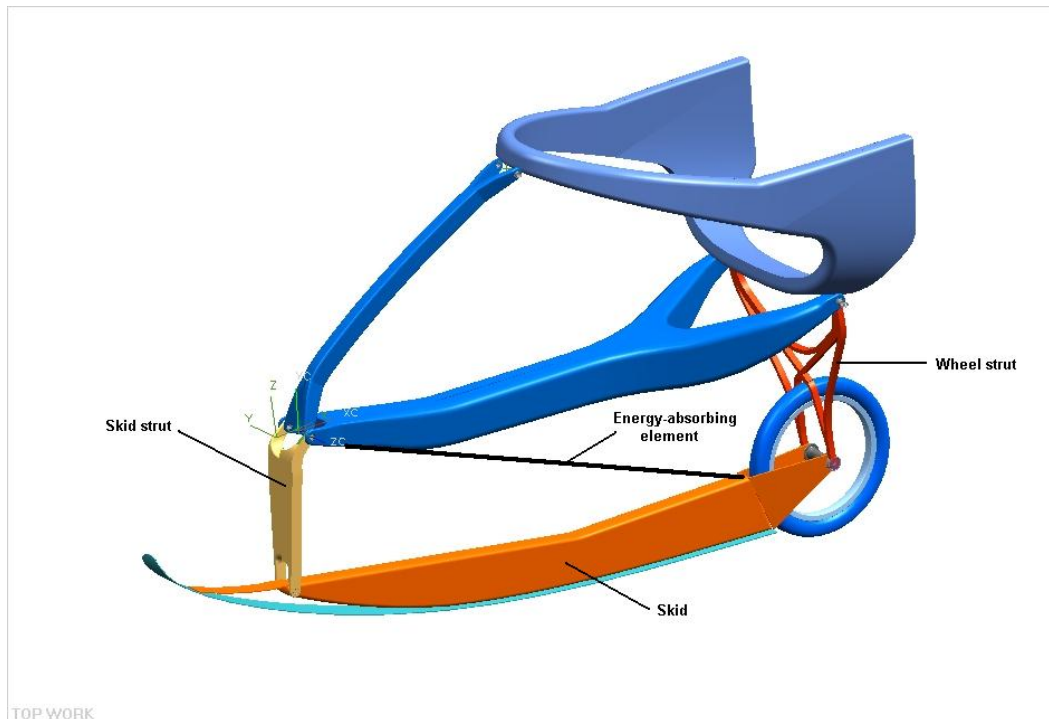


**Figure 3.7: Collapsible landing skid mechanism**



The intention of the landing skid is that the pilot would manually retract it after take-off to avoid excessive drag during flight. Before a landing or during an emergency situation the pilot would move the skid to its extended position. The diagonal energy-absorbing element should preferably be an inexpensive readily available component e.g. a rope, wire or strap, that could be replaced after a hard landing or specified time in service.

Secondly, energy would be absorbed in the connection between the pilot's chest plate and the aircraft structure. This implies that the chest plate would be connected to an energy-absorbing material or mechanism that would "stroke" or deform under a predefined load, subjecting the pilot to a lower acceleration while crash energy is absorbed.

Thirdly it is assumed that the crushing and plastic deformation of the aircraft structure would absorb a portion of the crash energy. Several studies including the publication by Farley (1983) suggested that high-energy absorption could be achieved by the crushing of composite structures. The airframe of Exulans is mainly constructed from carbon fibre sandwich components with high-density polystyrene as the core material. It is however important that the fuselage structure does not fracture to such an extent that the required living space could not be maintained.

#### 3.4.4 Environment Considerations

It was previously mentioned that a clean environment should be provided within the occupant's flailing envelope. In the Exulans cockpit this would be achieved by eliminating any protruding sharp objects from the pilot's flail volume. Where objects could not be removed padding would be provided to protect the pilot from injury. Energy-absorbing padding would also be provided at potential impact surfaces and brake away features could be implemented into the controls.

#### 3.4.5 Post-Crash Factors

Crash Survival Design Considerations states that the occupants should be able to evacuate the aircraft as fast as possible after an emergency landing or high impact event. It could be argued that complying with the first four factors of the CREEP considerations in the aircraft's design, would limit injury to the occupant. Without injury it is more likely that the occupants could escape additional injury or death caused by post-crash factors.

To prevent the pilot from drowning after a water impact a fuselage structure that would float on water is proposed. Furthermore, the Exulans fuselage would be provided with a quick-release fuselage back part that would enable the pilot to create an exit by splitting the fuselage into two halves. Accessibility to the

occupant from the outside should also be provided in the design. Finally, the detachable fuselage back part would also provide a means for a mid-air bailout and quick release from the restraining belts would also be necessary.

### **3.5 Conclusion**

In conclusion it could be stated that the aim of the Exulans II cockpit design is to establish a very strong lightweight container that would provide and maintain the required living space of the pilot during a crash. Sufficient restraint and energy-absorbing materials and mechanisms in the supporting structure and the landing skid would avoid high crash loads applied to the pilot. Where body parts could not be restrained, a clean environment would be provided and a mechanism for quick escape from the fuselage and restraints after a mishap would be established.

Conceptually the fuselage layout and pilot protection strategy have been proposed. The next challenge would be to compare the dynamic response of the proposed prone position with other pilot positions. The dynamic analysis would also aid as a tool to quantify the forces and maximum accelerations in the structure during impact scenarios.

## CHAPTER 4: DYNAMIC ANALYSIS

### Preview

1. This chapter contains the technical information of the dynamic analysis.
2. Initially the approach that was followed and the tools used during the analysis are discussed where after the reader is formally introduced to the Hybrid III test pilots.
3. The models used for bench marking are then discussed under the heading of Validation and Verification.
4. The two sets of dynamic analysis are then introduced to the reader and relevant results and preliminary findings are also contained in this chapter.
5. Detailed discussions of each impact simulation analysis typically involve assumptions, modelling techniques and input values.

#### **4.1 The Approach**

Growing computer technology and current event simulation software packages encourage engineers to do a complete design and operation simulation of a mechanical system on the computer before spending any time and money on prototype development. Due to the possible destructive nature of impact experiments it was thought best to initially follow the computer analysis path in order to save both time and money.

Models of human pilots in the three different support positions were constructed and at first subjected to an approximated crash pulse shape on a virtual test sled. The three pilots were then individually confined to an aircraft cockpit to undergo a series of specified crash scenarios. Considering the difference in the restraint methods and body tolerance to impact in the different positions, the response of the pilots in each case was compared to each other and to injury criteria norms.

The two pilot positions that were compared against the prone position was the normal seated position found in most motorised aircraft and the supine seated position found in many sailplane designs. During a comparative study it is important to assure that apples are being compared to apples. Although it does not always happen in reality it was assumed that the two pilots in the normal seated and supine seated positions were restrained with optimum restraint configurations as specified by the aviation regulations. Because of the fact that the aviation authorities have specified no restraining method for the prone position, different configurations were investigated during the analysis. The best prone position restraining configuration was selected for the comparison.

#### **4.2 The Analysis Tools**

The program ADAMS was used to run the impact simulations. It is a product of Mechanical Dynamics Incorporated (MDI) and has the ability to simulate the dynamics of any mechanical system by generating and solving the equations of motions for the system. The human models were obtained from FIGURE human modeller, which is an add-on to ADAMS. A variety of human and other biological subjects are available in FIGURE but the model with the Hybrid III Crush Dummy properties as specified in 49 CFR 572 was used for this study. Specified injury criteria was used to evaluate the impact effect on the Hybrid III dummy and to compare the results obtained in the three different occupant support positions. The capabilities and additional technical information on ADAMS and FIGURE are contained in Appendix D.

### **4.3 Meet the Pilots**

The three pilots that will be exposed to crash pulse shapes on the test sled and who will crash the fuselage airframes into the ground in the three different support positions will from now on be referred to as the following:

|                                         |   |                         |
|-----------------------------------------|---|-------------------------|
| The pilot in the normal seated position | - | The normal seated pilot |
| The pilot in the prone position         | - | The prone pilot         |
| The pilot in the supine seated position | - | The supine seated pilot |

All three the pilots have a mass of 77kg and stand at a height of 1.778m. They are also referred to as Anthropomorphic Test Devices (ATD's) and have the dimensions, mass and joint properties of the 50<sup>th</sup> percentile male Hybrid III crash test dummy specified by 49 CFR part 572.

To summarise for all the pilots:

|             |                                               |
|-------------|-----------------------------------------------|
| Age:        | 27 years                                      |
| Gender:     | 50 <sup>th</sup> percentile male (Hybrid III) |
| Weight:     | 77kg                                          |
| Length:     | 1.778m                                        |
| Occupation: | Test Pilot                                    |

#### **The Normal Seated Pilot**

The normal seated pilot will feature in all the normal seated configuration analysis and can be recognised by the normal seated position and blue coloured body parts as indicated in Figure 4.1. ADAMS measurements and results for the normal seated pilot will always be represented by a blue coloured curve on graphs.

#### **The Prone Pilot**

The prone pilot will test all the prone support position configurations. The prone pilot can be recognised by the prone position and red coloured body parts as indicated by Figure 4.2. ADAMS measurements and results for the prone pilot will always be represented by a red coloured curve on graphs.

#### **The Supine Seated Pilot**

The supine seated pilot will be used during the supine seated impact analysis. The supine seated pilot can be recognised by the supine position and green coloured body parts. The supine seated pilot is shown in Figure 4.3. ADAMS measurements and results for the supine seated pilot will always be represented by a green coloured curve on graphs.

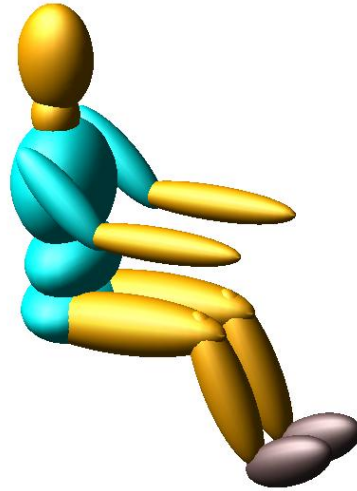


**Figure 4.1: The normal seated pilot in the normal seated position**



**Figure 4.2: The prone pilot in the prone position**

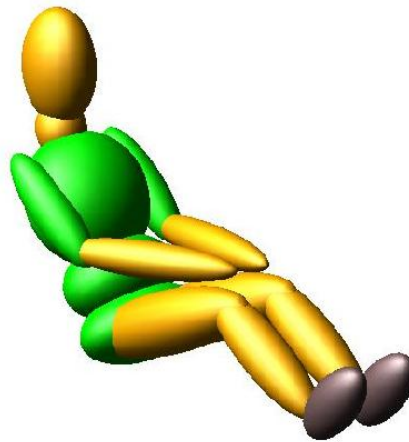


**Figure 4.3: The supine seated pilot in the supine position**

#### 4.4 Validation and Verification

##### Objective

The objective of the result verification process was to validate data obtained from the ADAMS impact analysis by comparing the results to that obtained from a similar impact experiment. It is normally good practice to verify results obtained from computer analysis with experimental results. Due to technical and limited time and financial factors it was, however, not feasible to perform the impact experiments similar to the virtual impact tests described in this chapter and an alternative route to validate the ADAMS data had to be followed. Using existing data from an experiment of the same nature seemed to be the next logical solution. Land Mobility Technologies (LMT) in association with Armscor has been involved in evaluating human response to impact and, much appreciated by the author, have agreed to provide the data on a previous vertical impact experiment.

##### Experimental Set-up

The experiment by Armscor and LMT involved a vertical upward 26g impulse applied to a 50<sup>th</sup> percentile male Hybrid III ATD. The normal upright seated ATD was placed onto a steel rig that was bolted to a hydro pulse actuator (Figure 4.4). The ATD was restrained with a lap belt and the required maximum acceleration was achieved by applying a rapid displacement (see Figure E1) to the seat rig. Measurements taken from the ATD included spinal compression force  $F_z$ , spine acceleration  $A_z$ , ankle compression  $F_z$ , neck compression  $F_z$ , neck shear  $F_x$  and neck bending moment  $M_y$ , head accelerations  $A_x$ ,  $A_y$ ,  $A_z$  and the lap belt force (see Figure A4 for axes definition).

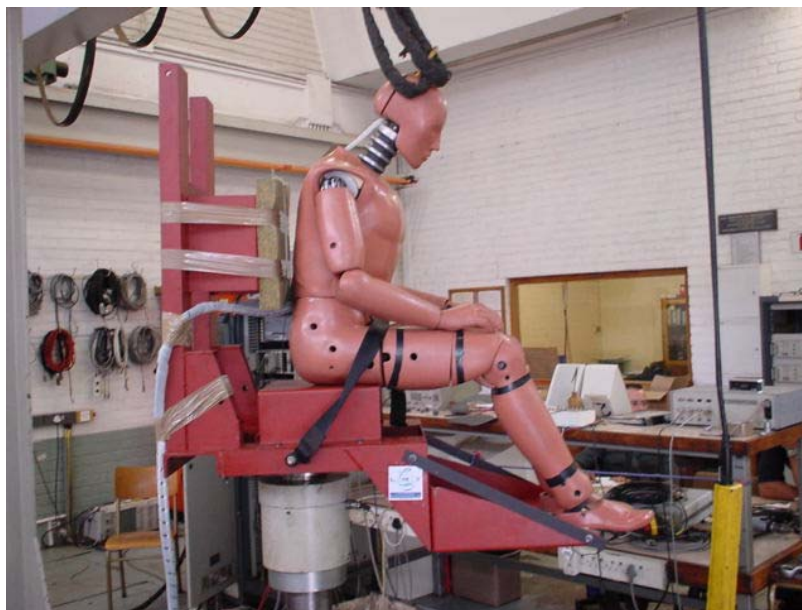
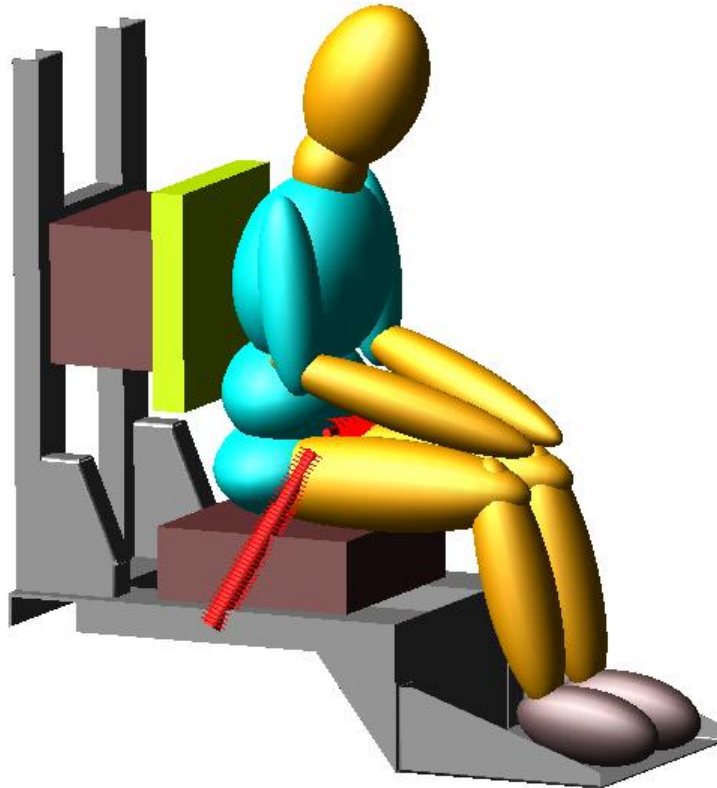


Figure 4.4: Vertical impact experiment with Hybrid III ATD (Courtesy of Armscor and LMT)

### The ADAMS Model

The ADAMS model consisted of the steel test rig modelled as a rigid body, the steel seat blocks also modelled as rigid bodies and the FIGURE 50<sup>th</sup> percentile male Hybrid III ATD. The body position of the ADAMS dummy was adjusted to that of the experimental dummy and the lap belt was simulated with three non-linear spring-dampers (one on each side and one over the dummy's lap). As in the experiment the seat rig acceleration was achieved by applying a rapid upward displacement to the rig. The ADAMS model is shown in Figure 4.5.



**Figure 4.5: ADAMS model of vertical impact experiment**

### Validation Results

The measurements used to compare the ADAMS results with the experimental results were the lumbar spine force  $F_z$  (Figure 4.6) for evaluating the LLC and the dummy's head acceleration magnitude (Figure 4.7) to calculate the HIC value. In the following graphs the ADAMS results (red) were superimposed onto the experimental results (blue).



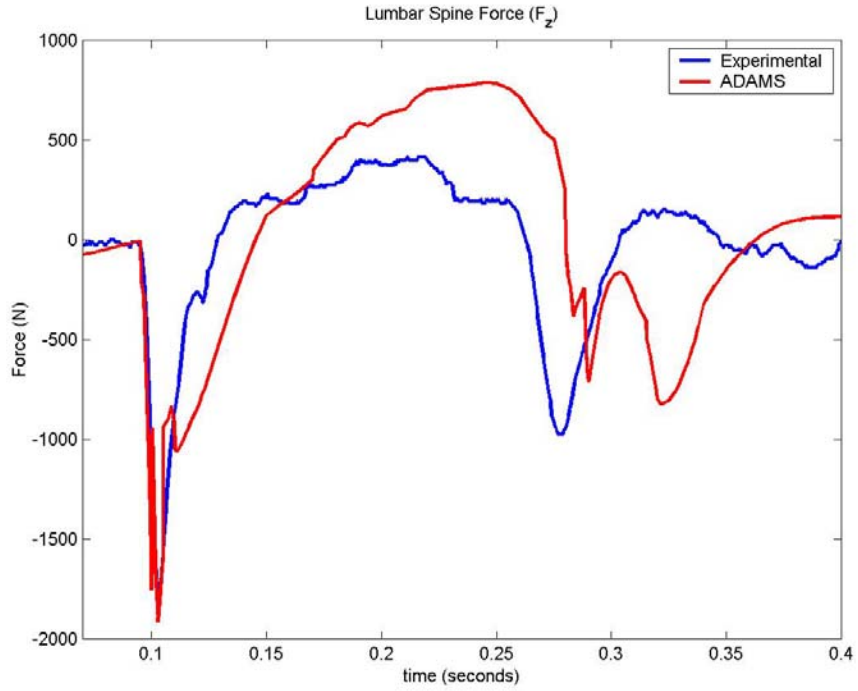


Figure 4.6: Lumbar spine force comparison

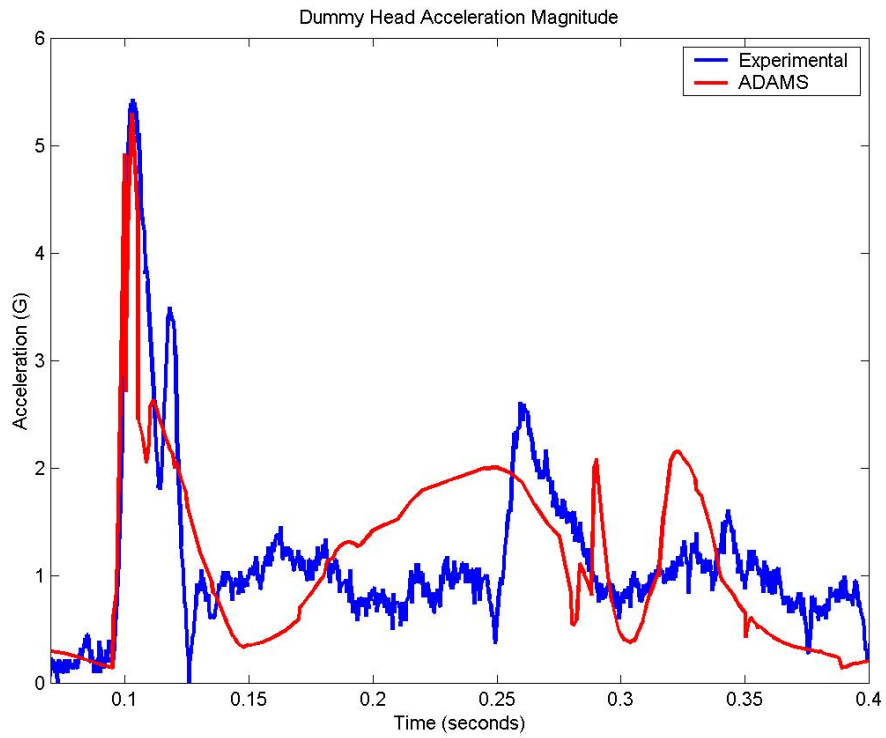


Figure 4.7: Head acceleration magnitude comparison

Although a slight deviation from the experimental results was observed towards the end of the impact response, good correlation between the ADAMS and experimental data was obtained for the initial force and acceleration peaks. Injury criteria are measured from the peak forces and accelerations and therefore it is a fair assumption to look only at these peaks and to ignore the rest of the data. The dummy's lumbar spine force peak and head acceleration magnitude peak are shown in Figures 4.8 and 4.9 respectively.

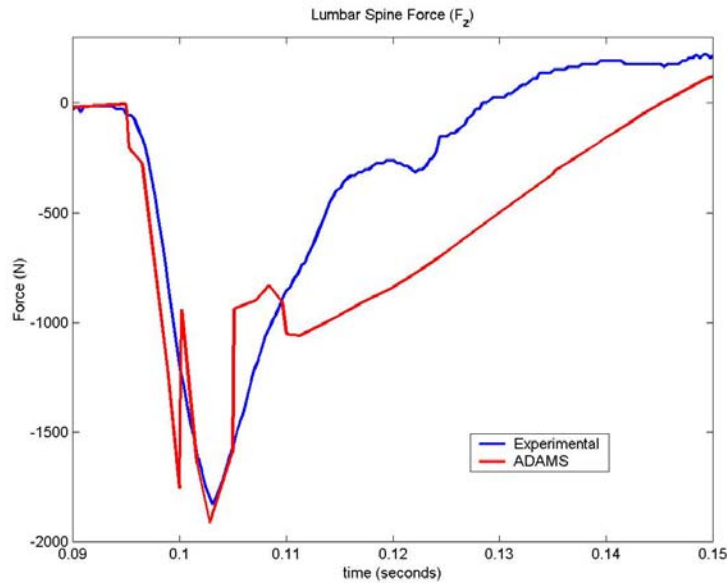


Figure 4.8: Lumbar spine force peak comparison

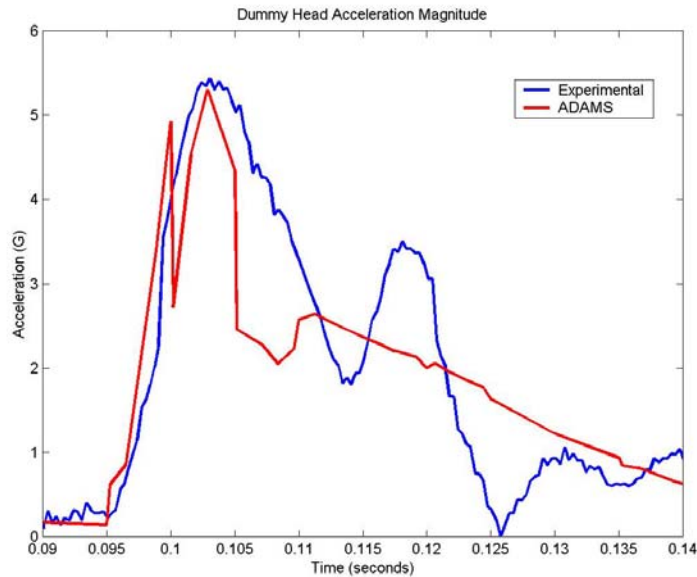


Figure 4.9: Head acceleration magnitude peak comparison

Values for the LLC and HIC were calculated from the ADAMS results and are listed in Table 4.1.

**Table 4.1: Validation injury criteria comparison**

| DATA         | LLC < 6700N | HIC < 1000 |
|--------------|-------------|------------|
| Experimental | 1829        | 0.379      |
| ADAMS        | 2322        | 0.320      |

It is noted that these values are way below the injury threshold and therefore it can be concluded that the severity of the vertical impact was very low.

### Seat Characterisation

It was previously explained that pilots in three different seating configurations would be subjected to different impact scenarios during the analysis. To obtain realistic contact properties between the seat and the dummy a soft material of a certain description was modelled as the seat cushion. To obtain the stiffness and damping properties of the seat cushion used during the analysis, LMT and Armscor provided the data of a static compression-rebound test performed on a typical seat cushion. The test involved measuring the force and displacement of an artificial human buttock being pressed into the seat base cushion. The test set-up for the experiment is shown in Figure 4.10 and a photo of the artificial buttock and seat cushion is shown in Figure 4.11. The resulted stiffness data obtained from this experiment are shown in Figure 4.12. This experiment was simulated with ADAMS to obtain the contact properties that would resemble the seat-buttock contact behaviour during the analysis.

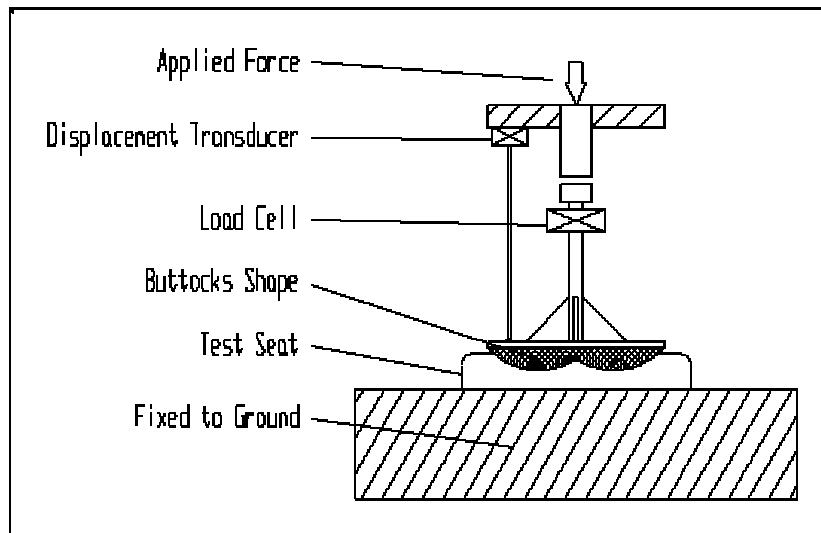


**Figure 4.10: Static seat characterisation experimental test set-up (Courtesy of Armscor and LMT)**



Figure 4.11: Artificial buttock with typical seat cushion (Courtesy of Armscor and LMT)

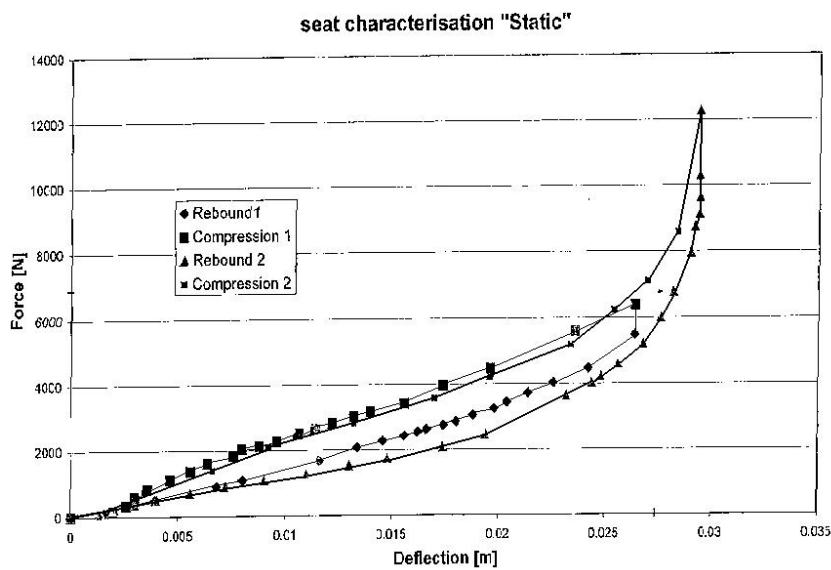


Figure 4.12: Seat stiffness data obtained from static test (Courtesy of Armscor and LMT)

During the ADAMS simulation of this experiment a trail and error method was used to obtain the contact coefficients. The lower torso (pelvis) of the 50<sup>th</sup> percentile FIGURE male Hybrid III model was used as the artificial buttock. The pelvis was forced into a block resembling the seat cushion (see Figure 4.13). The ADAMS contact coefficients were modified until a similar force-displacement curve was obtained for the ADAMS seat cushion model as indicated in Figure 4.14. The experimental result is indicated in blue while the ADAMS result is shown in red.

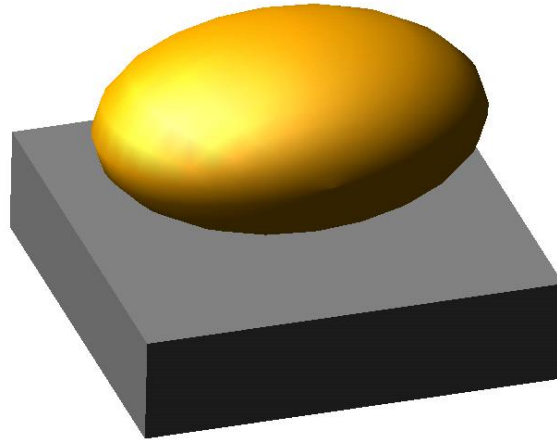


Figure 4.13: ADAMS model of seat characterisation experiment

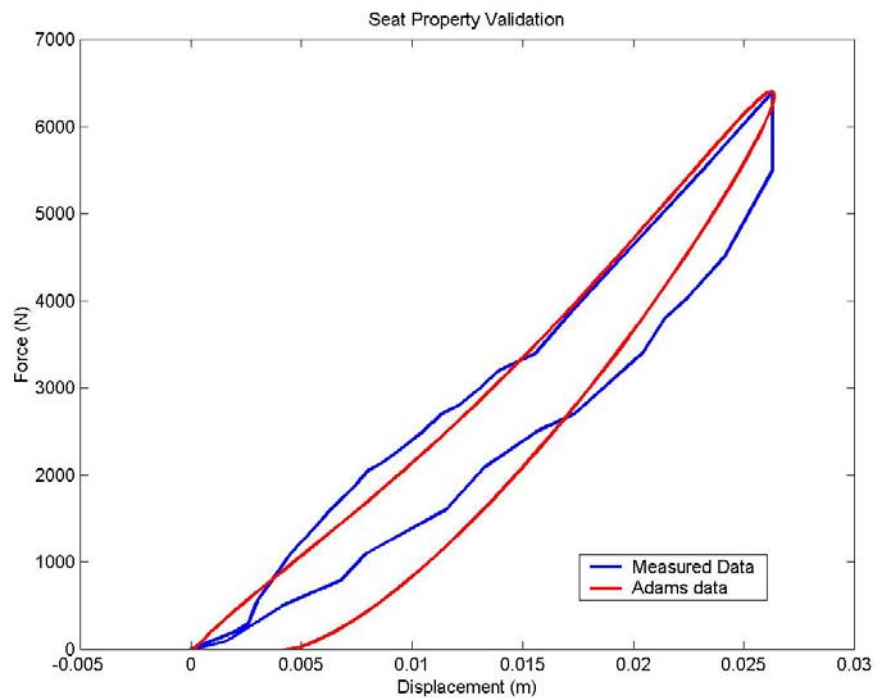


Figure 4.14: Experimental and ADAMS seat stiffness data

The values that resembled the experimental buttock-seat contact trend were found to be the following:

- Contact stiffness  $K = 1.499e6$  N/m
- Contact damping  $C = 9000.0$  Ns/m
- Force exponent  $e = 1.5$
- Penetration depth  $d = 0.0001$ m

During the following dynamic analysis, all contact between the pilot and the support will be modelled using the above coefficients. A more thorough discussion of the above coefficients can be found in Appendix D.

#### 4.5 Sled Impact Tests

It was previously mentioned that in order to make sensible comparisons between the three support concepts, it is important to insure that apples are being compared to apples. The test sled was therefore introduced to compare the different pilot positions under similar dynamic conditions. Models of the different seat-restraint configurations was placed on the virtual test sled and exposed to exactly the same impact pulse shape. Conventional restraining methods found in light aircraft were used for the normal seated and supine seated positions. No conventional restraining methods exist for the prone position and therefore the sled impact test provided a golden opportunity to test different restraining concepts. The results of these tests were then evaluated with the specified injury criteria and compared with each other.

According to FAR Part 23.562, the ATD on the sled should be subjected to two different dynamic tests. The first test generally involves a vertical drop with the aircraft seat pitched 30° downward from the horizontal plane. The second test involves a horizontal frontal impact with the seat yawed 10°. As in real life, the test sleds were modelled in such a way that it could only translate in the direction of the track, constraining all rotations and other translations. The translation constraints and applied acceleration vector for Test 1 and Test 2 are shown by Figure 4.15 and Figure 4.16 respectively.

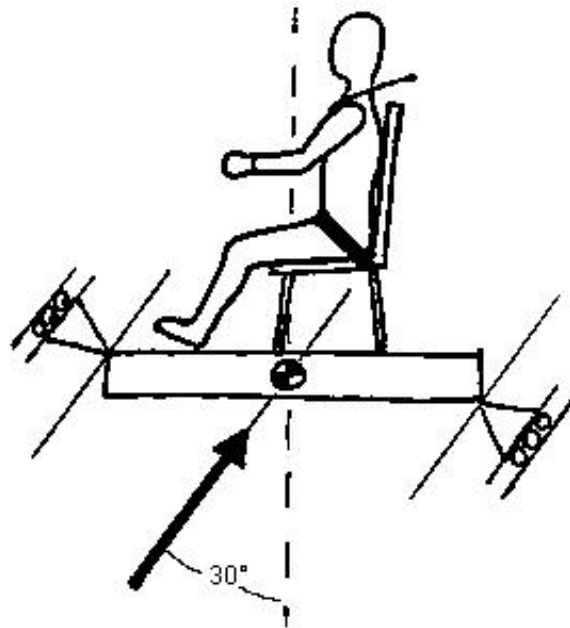


**Figure 4.15: Test 1 model with translation constraints and applied crash pulse vector.**

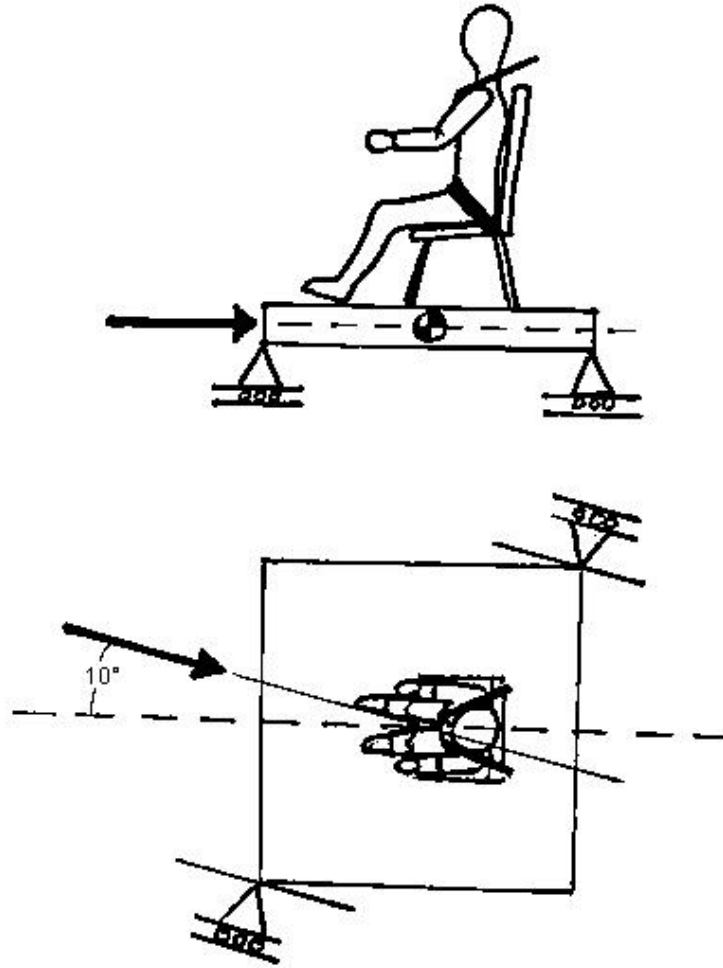


**Figure 4.16: Test 2 model with translation constraints and applied crash pulse vector.**

The seat structures were modelled as rigid bodies fixed to the sled, resulting in no elastic or plastic deformation of the seat structure, thus leaving the seat structure with no energy-absorbing capabilities. The pilots were constrained to the seats with the respective restraint systems modelling the belts as 50mm Nylon webbing as specified in Appendix B. The webbing was modelled as one directional non-linear spring-dampers that could only transmit tension. According to Appendix B, Nylon webbing would show an elongation of 17% under a load of 11120N while Dacron webbing would show an elongation of only 8% under the 11120N load. This information could be translated as one point on the force-displacement curve of the two different materials. Assuming that the webbing would possess a non-linear increasing stiffness due to the geometrical effect of the fibre weave, the shape of the stiffness curves were plotted as indicated in Figure 4.17 for the two different materials, blue representing Nylon and red representing Dacron. The elongation for each belt in the ADAMS models was scaled according to the blue Nylon curve.

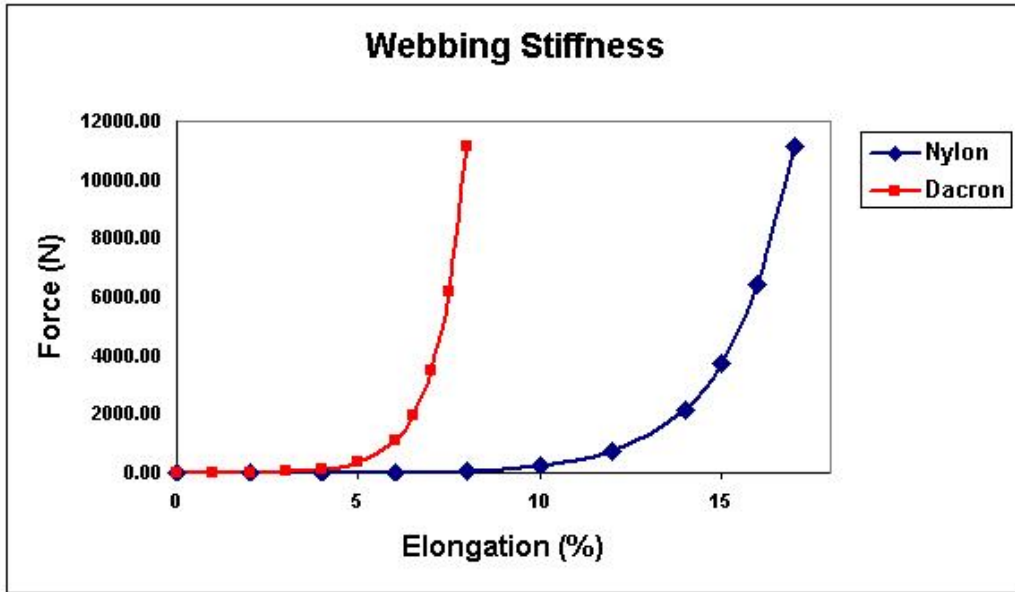


Figure 4.17: Webbing stiffness curves

Belt slack and belt pretension was modeled using the ADAMS spline function. An example of this technique is shown in Figure 4.18. From the belt pretension curve it can be seen that there is already a 2000N pretension force in the belt at zero elongation and from the belt slack curve it can be seen that there is approximately 2% elongation of the belt at zero force. This zero force elongation represents the slack in the belt that has to be taken up before the belt is actually tensioned.

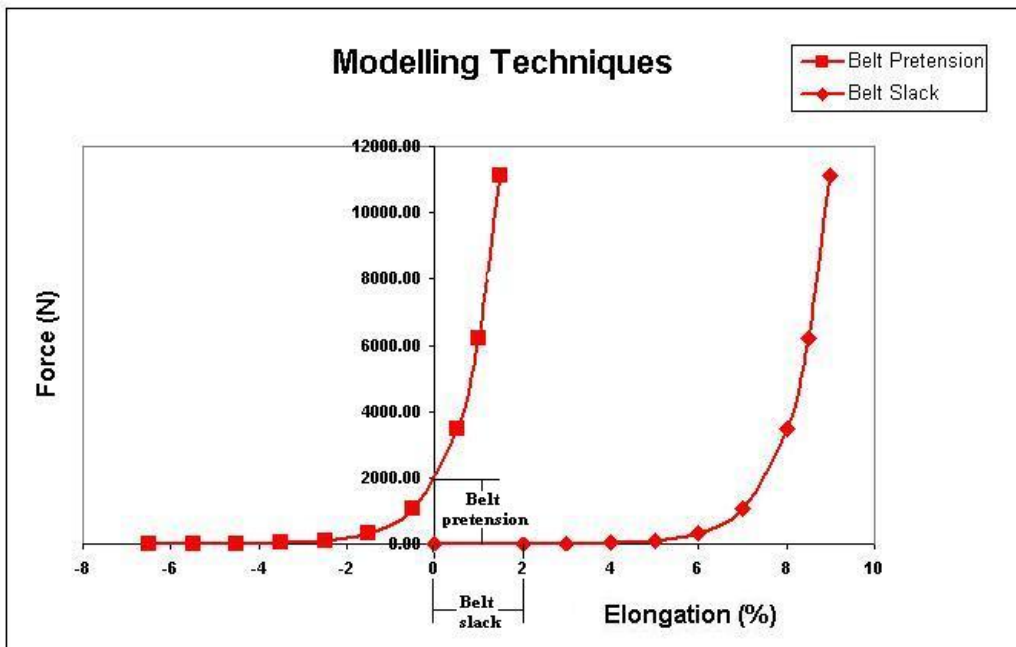


Figure 4.18: Modelling belt slack and belt pretension with the ADAMS spline function



During the sled impact tests for all three seating configurations, energy absorption in the seat or support padding was modelled by specifying a contact stiffness and damping between the ATD and the seat or support. The magnitude of these values was obtained during the seat validation process described in the previous subchapter.

The pulse shape specified by FAR Part 23.562 is the triangular increasing decreasing pulse with a velocity change of no less than 9.45 m/s, a rise time of no more than 0.05 seconds and a peak deceleration of no less than 19G for the first test. For the second test the change in velocity must be no less than 12.8 m/s with a rise time not exceeding 0.05 seconds and a minimum peak deceleration of 26G. Using the specified limit values the pulse shapes for the sled tests could be calculated using the formulas found in Simula Incorporated (1980). The pulse shape calculation for Test 1 is shown in Figure 4.19 and Figure 4.20 shows the calculation for Test 2.

$$\begin{aligned}\Delta V &= 9.45 \text{ m/s} \\ t_m &= 0.05 \text{ sec} \\ G_m &= \frac{\Delta V}{gt_m} = \frac{9.45}{(9.81)(0.05)} = 19.27 G\end{aligned}$$

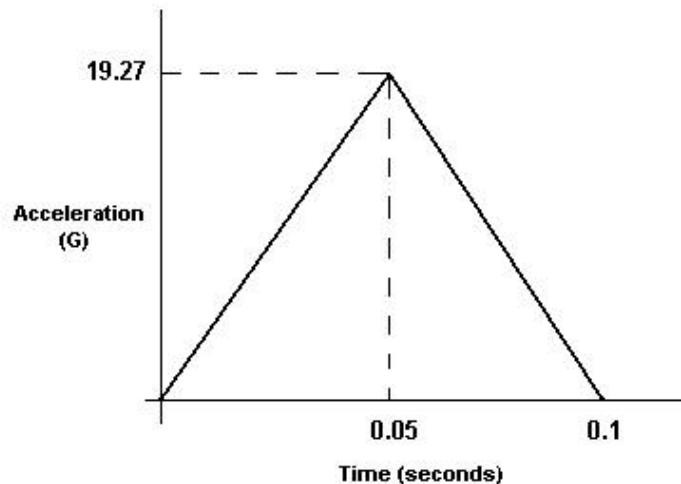
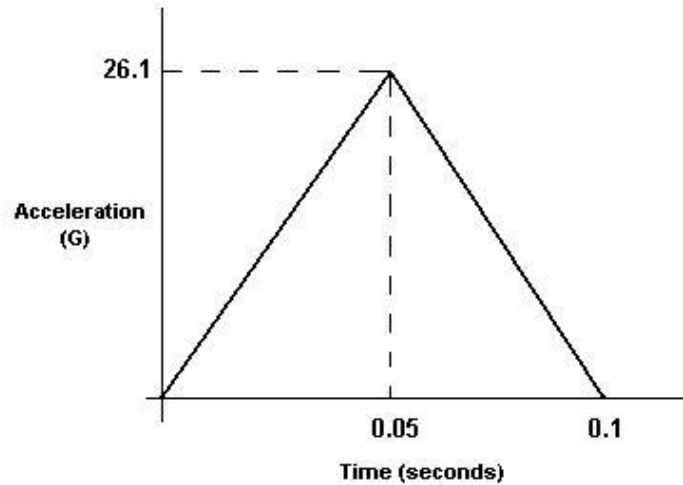


Figure 4.19: Pulse shape calculation for Test 1

$$\Delta V = 12.8 \text{ m/s}$$
$$t_m = 0.05 \text{ sec}$$
$$G_m = \frac{\Delta V}{gt_m} = \frac{12.8}{(9.81)(0.05)} = 26.1G$$



**Figure 4.20: Pulse shape calculation for Test 2**

A major advantage of a computer impact simulation is that the impact event can be modelled without any unwanted structural failure, and even where structural failure is modelled, there is no injury risk or structural damage involved in the failure.

FAR 23.562 requires the application of the HIC, the LLC and the measuring of shoulder strap loads to evaluate injury during the dynamic tests. In ADAMS the chest of the FIGURE Hybrid III ATD is modelled as a rigid body with no deflection. This modelling technique however does not provide realistic belt-chest interaction and therefore the shoulder strap load criteria was traded for the neck injury criteria ( $N_{ij}$ ) explained in Chapter 2.7. The reason for selecting the neck injury criteria was purely based on the high neck deflections viewed in the animations of the sled impact tests.

#### 4.5.1 Normal Seated Position

The normal seated pilot was placed on a seat in the upright normal seated body position simulating a grip on to the control stick. The ADAMS contact properties resulting from the seat characterisation described in Chapter 4.4 were used to simulate realistic dummy-seat contact. The normal seated pilot was restraint with the four-point restraint system indicated in Figure 2.15(a). The trailing lengths of the shoulder straps were connected to the seat structure at the prescribed range of angles with the shoulder's connection point as indicated in Figure B11. Belt slack in the shoulder straps was introduced by modelling the non-linear shoulder strap spring dampers with a 100mm no resistance elongation as explained in Figure 4.18. The lap belt was connected to the seat structure at the recommended angle of 45° to limit both forward and upward motion of the pelvis (Figure B4). A pretension of 100N was modelled in the non-linear lap belt spring dampers as explained in Figure 4.18. The ADAMS model of the normal seated pilot on the test sled is shown in Figure 4.21. In this figure and following figures, a belt connection to the structure will be indicated by a triangular symbol while a belt connection to the pilot's body will be indicated by a circular symbol.

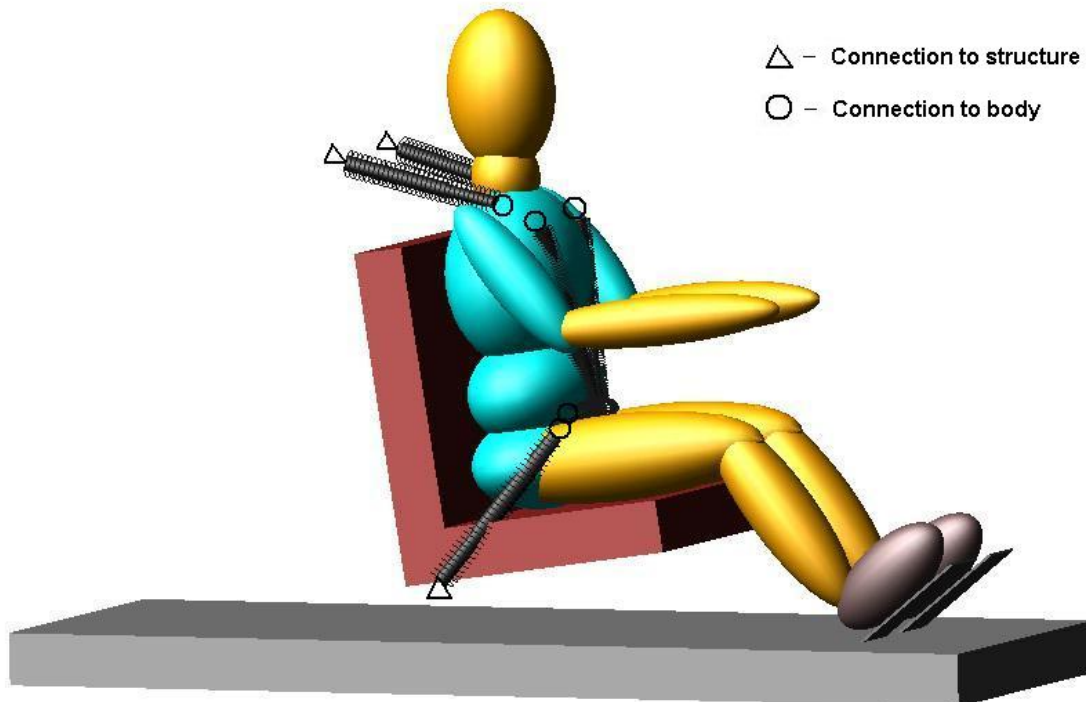


**Figure 4.21: Test sled with normal seated configuration**

#### 4.5.2 Prone Pilot Position

To obtain the best prone pilot support-restraint configuration, different restraining methods were evaluated during these tests. Initially the prone pilot was restraint onto the prone seat with the restraining concept proposed in Chapter 3.4.2 (Figure 4.22). Reviewing the animation and some preliminary results of this restraint concept indicated that some improvements were necessary to obtain the anticipated advantages expected from the prone position.

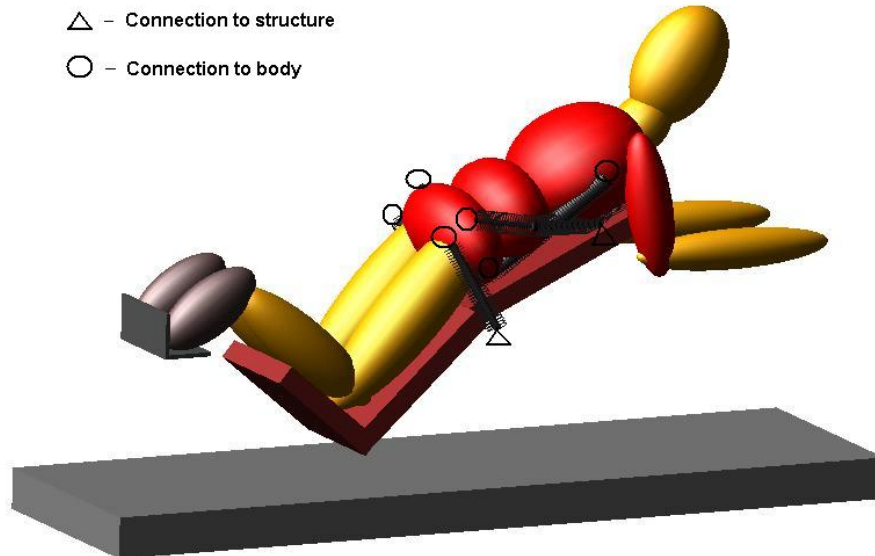


**Figure 4.22: Test sled with prone restraint concept 1**

Two more restraint concept models were created and subjected to the impacts on the test sled. In prone restraint concept two (Figure 4.23) the hip belt angle was changed by moving the end attachment points backward to allow more resistance to forward motion of the pelvis. Additionally this resistance to forward pelvic motion was complimented with two back straps attached to the harness in the lower back region. In prone restraint concept three (Figure 4.24), the back straps were removed but the shoulder strap end attachments were moved to a position above and behind the pilot's shoulders. A soft chin rest was also introduced to relieve the tension of the neck muscles during normal flight and to limit dynamic overshoot of the head during an impact. Although this modification could introduce an additional injury mechanism to the mandible (lower jawbone), it was done under the assumption that the pilot in the prone position would in reality wear a helmet. The helmet would support the jaw and distribute the impact force along the contact surface. From Table 2.1 it is noted that the mandible can tolerate a high acceleration of 40g before a fracture would occur. The impact force of the jaw on the chin rest and the head's CG acceleration were monitored during the sled tests and were included in the results. In each model the seat characterisation contact properties were specified between the dummy and the support. The prone pilot's arms were oriented to simulate a grip on to the Exulans sweep lever controls.

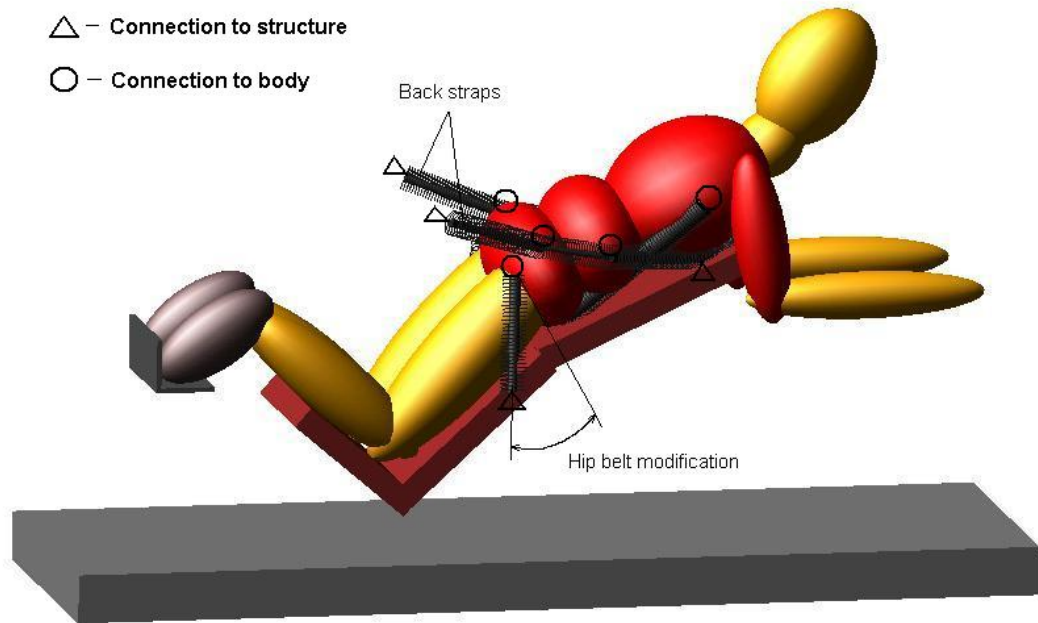


Figure 4.23: Test sled with prone restraint concept 2

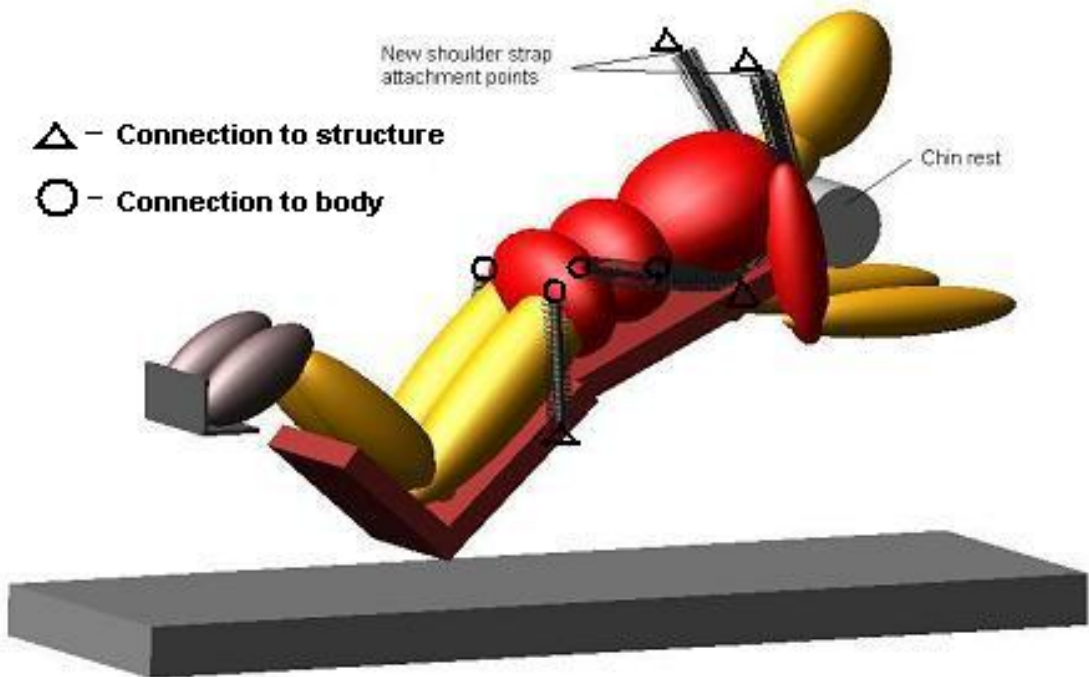
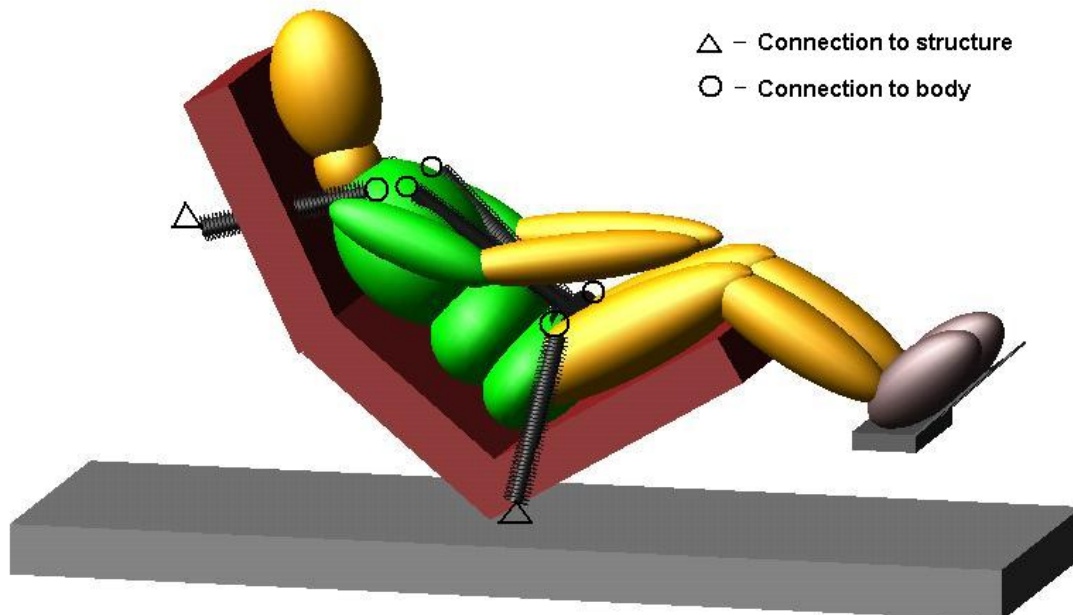


Figure 4.24: Test sled with prone restraint concept 3

#### 4.5.3 Supine Seated Position

The supine seated pilot was placed in the supine seated configuration with his right arm positioned to simulate a hold onto the control stick. The supine seated pilot was restrained with the recommended five-point restraint system, which includes a crotch strap between the legs. The crotch strap was included to prevent submarining which is believed to occur most likely in this reclined body position. The trailing lengths of the shoulder straps were connected to the seat structure at an angle of  $15^\circ$  below the longitudinal tangent to the occupant's shoulder and the lap belt connection points were constructed at an angle of  $80^\circ$  from the longitudinal as indicated by Figure 2.25. The shoulder and crotch straps were joined at the centre of the lap belt. As with the normal seated pilot, shoulder strap belt slack and lap belt pretension was included into the model. Figure 4.25 shows the ADAMS model of the pilot in the supine seated configuration on the test sled.



**Figure 4.25: Test sled with supine seated configuration**

#### 4.5.4 Sled Test Results

##### Dynamic Test 1

From the ADAMS simulation results of dynamic test 1 it was discovered that both the normal seated pilot and the supine seated pilot exceeded the LLC (-6700N). As expected, the prone position configuration performed exceptionally well in this category. This can be attributed to the orientation of the body with respect to the impact direction, which means that the impact force acted transverse to the spine and did not have a large component acting inline with the spine as in the normal seated and supine seated configurations. The lumbar spine force for each position is indicated in Figure 4.26

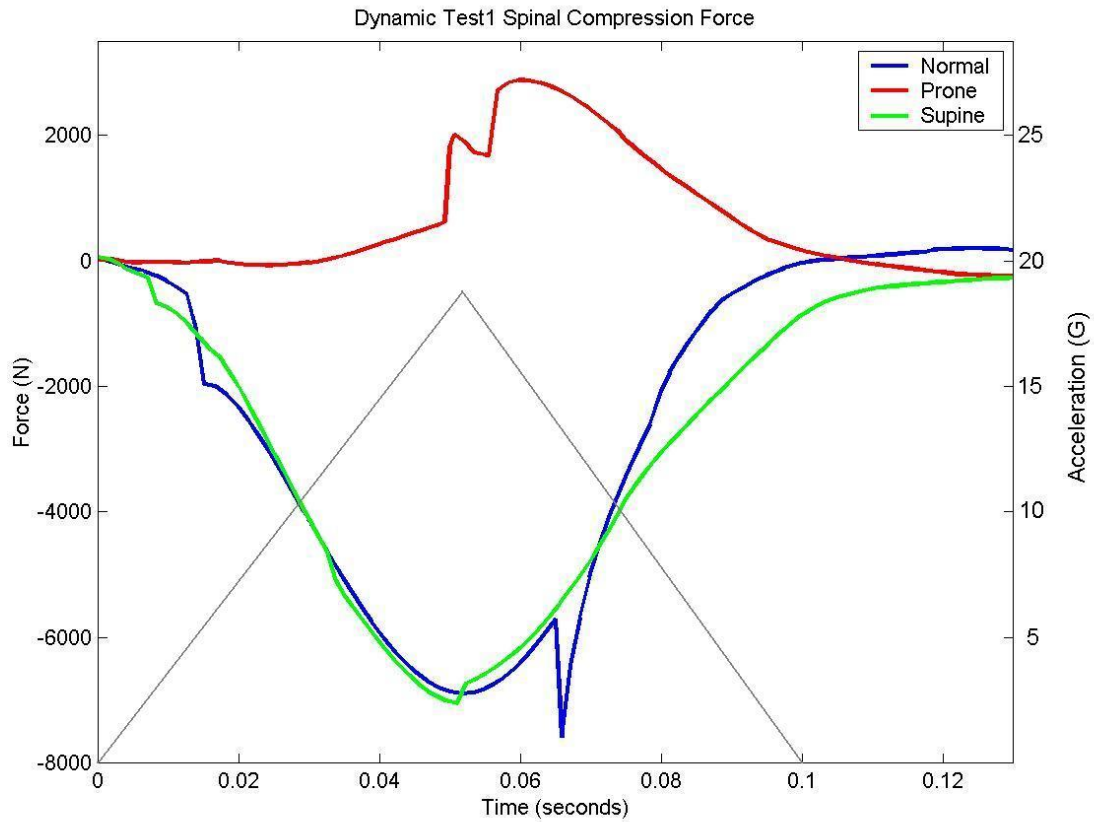


**Figure 4.26: Dynamic Test 1: lumbar spine force results calculated by ADAMS with grey acceleration pulse scaled to right vertical axis**

Due to the impact direction and the absence of secondary head impact into the surrounding cabin, the head accelerations were relative low and the HIC values for all the positions were way below the limit value of 1000. The lowest HIC value for the supine position can be attributed to the application of the impact vector inline with the spine neck and head causing a low rotational moment on the neck. Although the normal seated position also had a low HIC value, the normal seated pilot's body accelerated through a much bigger flail volume with respect to the other pilots. If the normal seated pilot had been sitting inside a cockpit, head and chest impact into the instrument panel and controls would have been unavoidable. The chin rest implemented in the third restraint concept of the prone pilot indicated good improvement of the HIC value and flailing volume of the pilot. The head acceleration magnitude for each position is indicated in Figure 4.27 and the flailing envelopes for each position are shown in Figure 4.28.

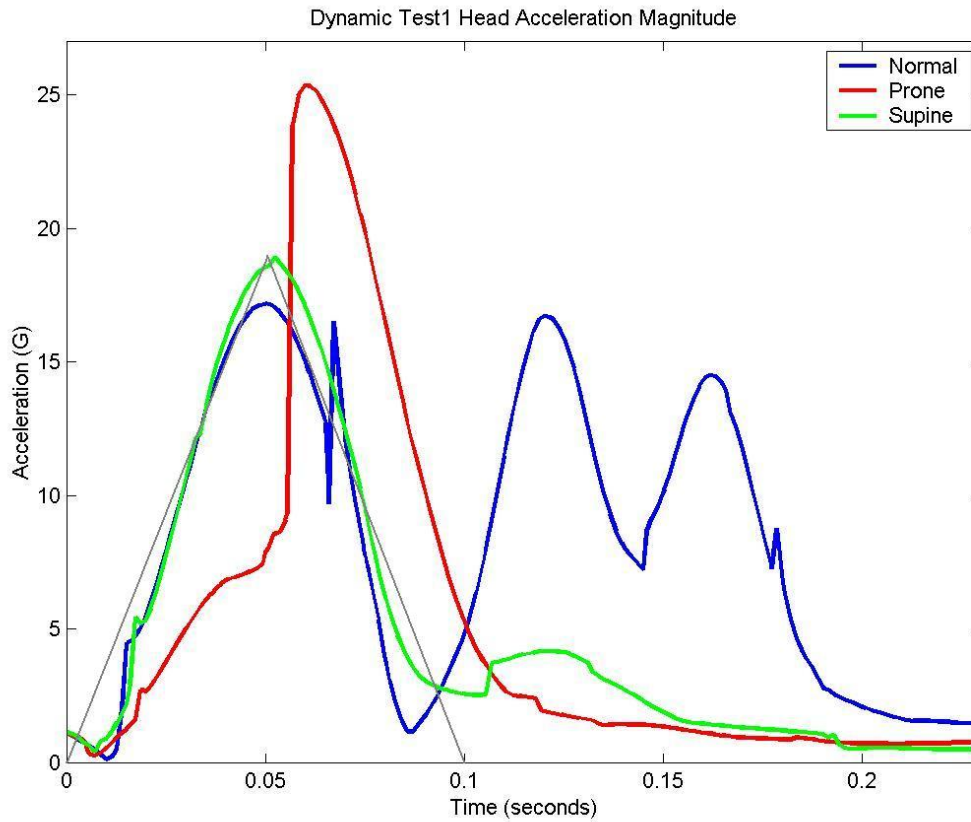
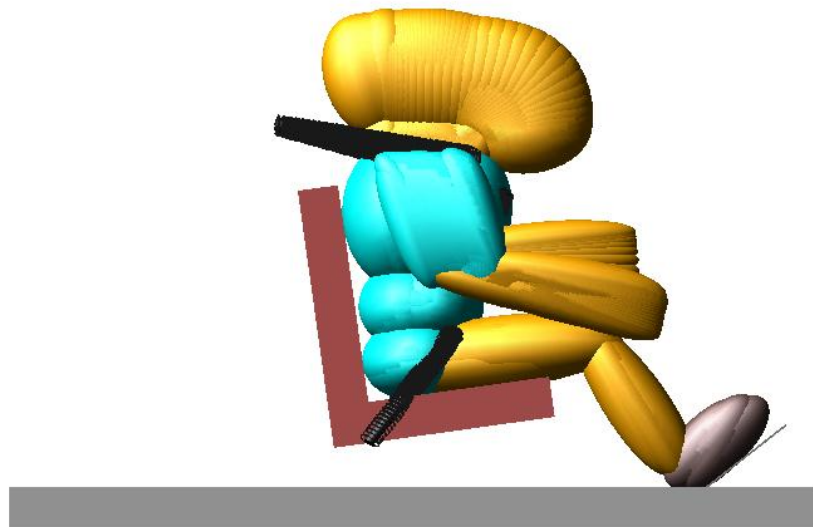


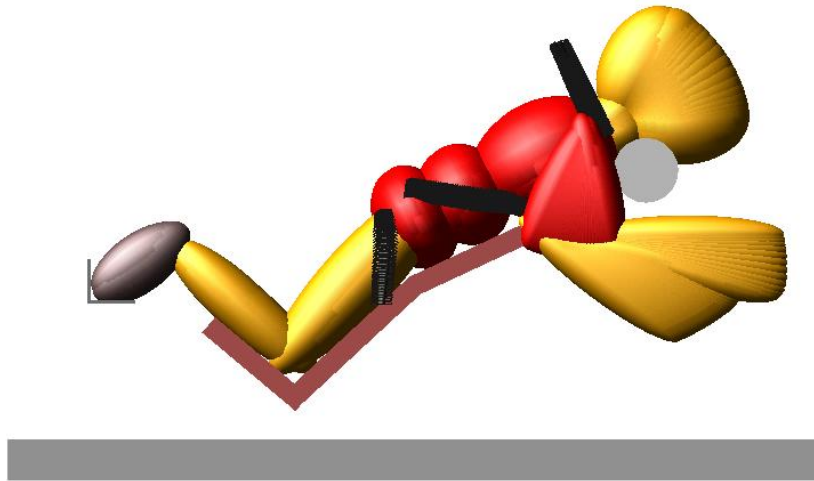
**Figure 4.27: Dynamic Test 1: head acceleration magnitude results calculated by ADAMS with grey acceleration pulse on scale**

Due to the body position of the pilot in the prone position, a higher axial force was applied to the neck. This resulted in a high value of 0.979 for  $N_{ij}$  but was still within the limits. The  $N_{ij}$  value for the normal seated pilot was also relative high due to dynamic overshoot of the head. The supine position indicated a good value for  $N_{ij}$ . The results of the lumbar load and head acceleration comparison between the three prone concepts are contained in Figures E2 and E3 and the results of the injury criteria for dynamic test 1 are listed in Table 4.2.

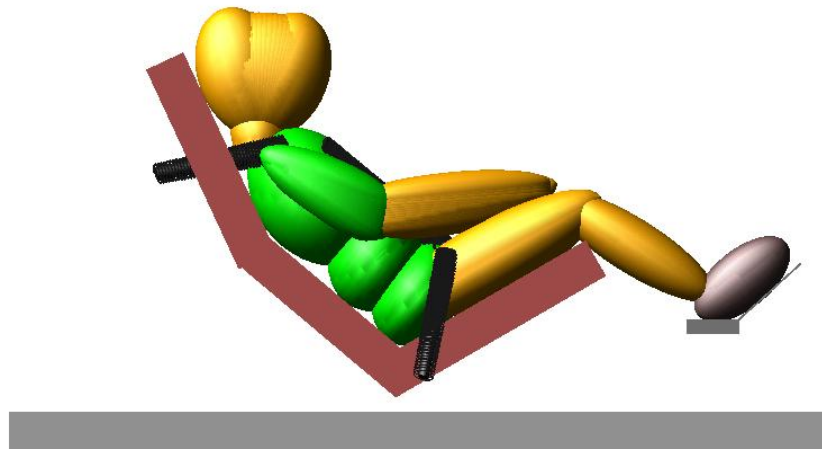




(a)



(b)



(c)

Figure 4.28: Dynamic Test 1: flailing envelopes calculated by ADAMS

## Dynamic Test 2

The magnitude of the spinal compression loads of the normal seated pilot and the supine seated pilot during Test 2 were lower due to the direction of the frontal impact load transverse to the spine. Spinal compression loads were however induced by wedging of the upper body between the angled shoulder straps and the seat base but the LLC was not exceeded.

During the frontal impact of the first restraint concept of the prone pilot as indicated in Figure 4.22, a massive spinal compression force was induced by the mass of the upper body and pelvis impacting into the shoulder straps. This led to the conclusion that sufficient pelvic restraint was vital to avoid high compression loads to the spine in a frontal impact scenario. The animation of the impact revealed that the hip belts did not restrain the pelvis from displacing forward because the attachment angle was of such a nature that the belts were not elongated but only rotated around the seat attachment points by the pull of the pelvis.

In the proposal of the second restraint concept indicated in Figure 4.23 the end attachments of the hip belts were moved backwards to offer more resistance to the forward pull of the pelvis. More belt slack was modelled in the shoulder straps and the two back straps achieved additional pelvic restraint. On review of the results it seemed that this proposal was somewhat of an over kill and a huge tension force was induced in the lumbar spine. From this exercise it was however realised that there would exist a combination of belt slack and pretension between the pelvic restraints and shoulder straps that would result in an acceptable spinal loading scenario between the extreme tension and compression cases.

In the third restraint concept indicated in Figure 4.24 the back straps were removed and the shoulder strap end attachments were moved to a position above and behind the pilots shoulders. This was done to eliminate the sudden direct pull of the straps on the shoulders during a frontal impact. The results of the spinal force of the three pilots during Test 2 are indicated in Figure 4.29. (The spine force result of restraint concept three were used)

During Test 2 the impact into the restraint systems were quite severe and resulted in high head accelerations for both the normal seated and supine seated positions (see Figure 4.30). Dynamic overshoot of the head following from inadequate torso restraint due to shoulder strap slack resulted in exceeded HIC values for these two positions. The orientation of the body with respect to the horizontal impact load, the passive torso restraint and the arrestment of the head by the chin rest achieved an acceptable HIC value for the prone pilot. This achievement is also reflected in the results of the flailing volumes for the three different positions indicated in Figure 4.31. In the pictures of the flailing envelopes the pilot's right arm was removed to display the movement of the head, which is the most vulnerable part of the body.

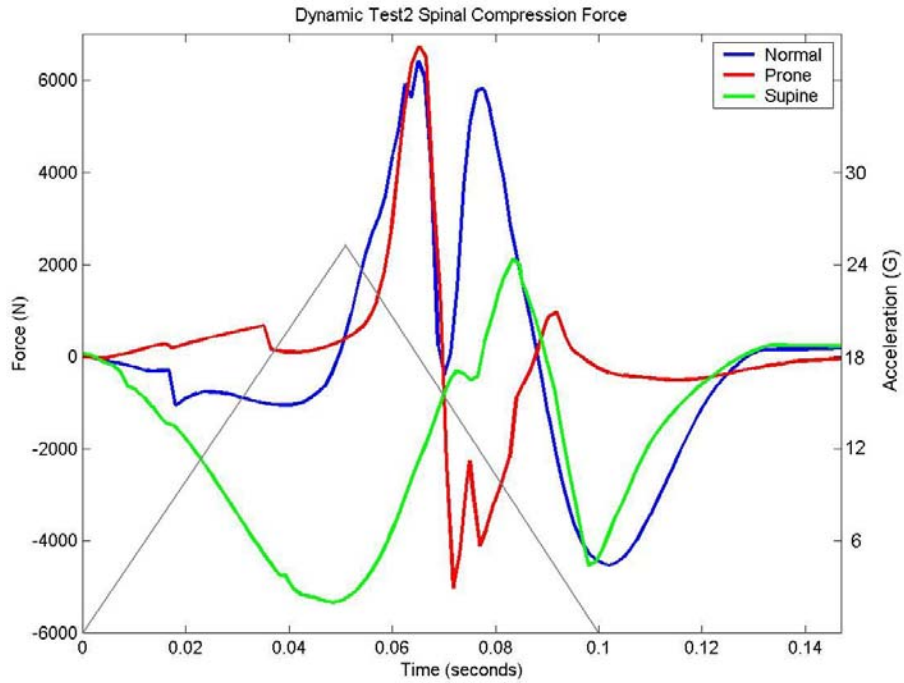


Figure 4.29: Dynamic Test 2: lumbar spine force results calculated by ADAMS with grey acceleration pulse scaled to right vertical axis

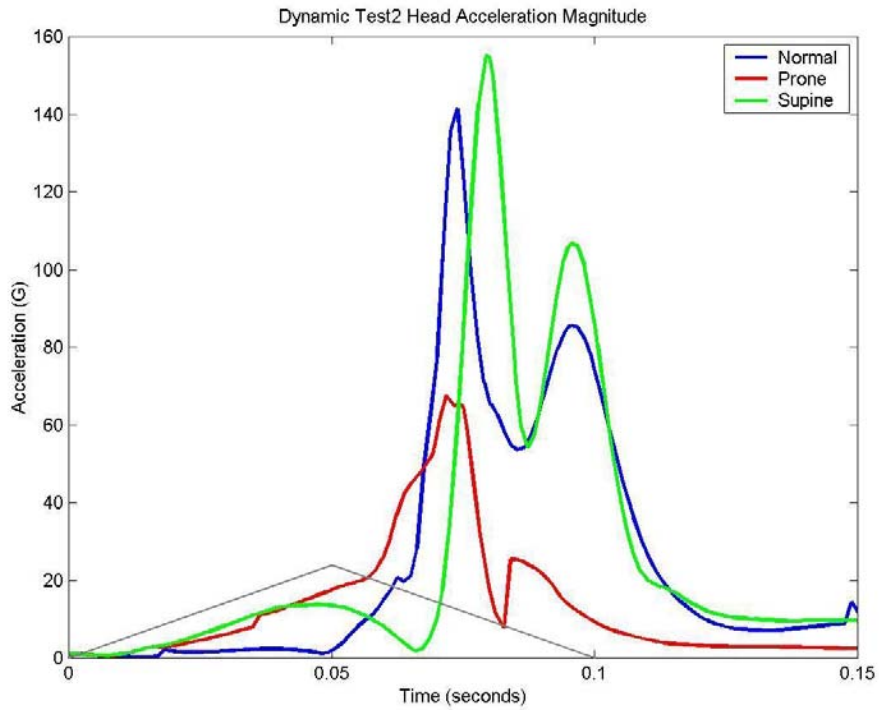
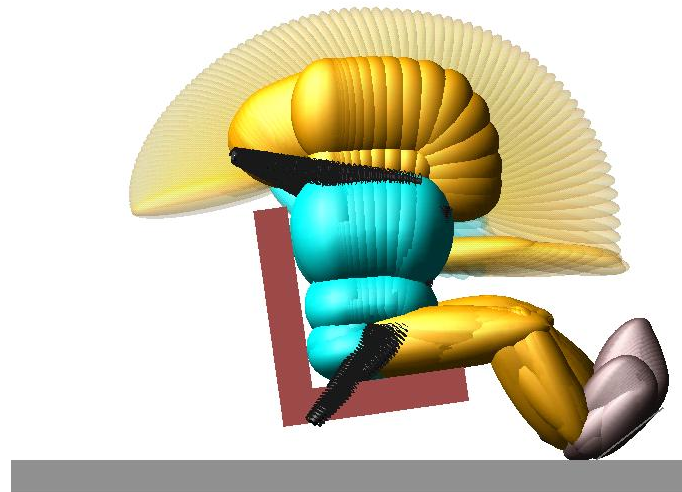
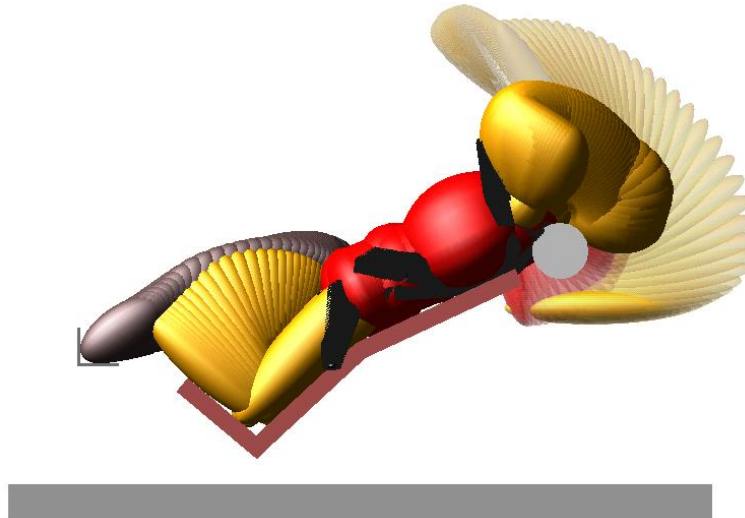


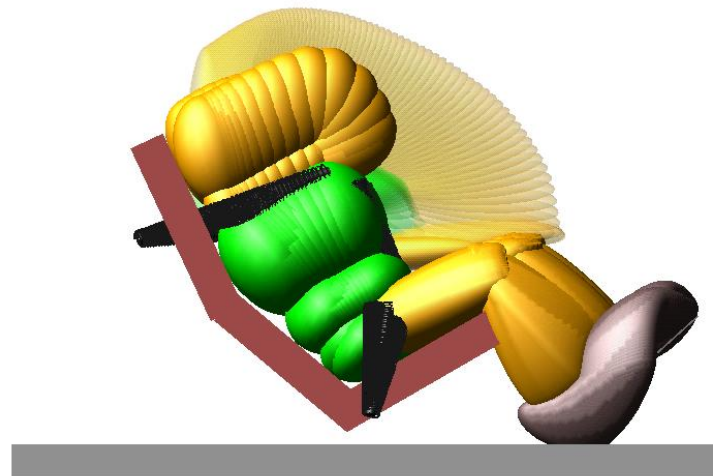
Figure 4.30: Dynamic Test 2: head acceleration magnitude results calculated by ADAMS with grey acceleration pulse on scale



(a)



(b)



(c)

Figure 4.31: Dynamic Test2: flailing envelopes calculated by ADAMS

The dynamic overshoot of the head due to the slack in the shoulder belts of the normal seated pilot and the supine seated pilot induced massive tension forces and extension-bending moments in the neck, which resulted in exceeded  $N_{ij}$  values. The direction of the impact force during Test 2 resulted in a high-tension force applied to the prone pilot's neck. Compared to the other positions, the prone pilot had the lowest  $N_{ij}$  value but still over the limit. The injury criteria values for Test 2 are contained in Table 4.2. The lumbar spine load and head acceleration results for the three prone concepts are contained in Figure E4 and E5 respectively.

**Table 4.2: Sled test injury criteria results**

| Analysis    | Pilot Position | Injury Criteria (IC) |          |         | # of IC exceeded | Best Performance |        |        |
|-------------|----------------|----------------------|----------|---------|------------------|------------------|--------|--------|
|             |                | LLC<6700             | HIC<1000 | Nij<1.0 |                  | LLC              | HIC    | Nij    |
| Sled Test 1 | Normal Seated  | 7599                 | 31.49    | 0.882   | 1                |                  | Normal |        |
|             | Prone Seated   | 240                  | 57.97    | 0.979   | 0                | Prone            |        |        |
|             | Supine Seated  | 7045                 | 39.19    | 0.446   | 1                |                  |        | Supine |
| Sled Test 2 | Normal Seated  | 4527                 | 1905     | 4.011   | 2                | Normal           |        |        |
|             | Prone Seated   | 5017                 | 270      | 1.416   | 1                |                  | Prone  | Prone  |
|             | Supine Seated  | 5335                 | 2432     | 3.755   | 2                |                  |        |        |

#### 4.5.5 Conclusion

The sled tests revealed valuable information regarding the restraining problems and the advantages of the different pilot positions. Dynamic overshoot of the head due to inadequate torso restraint remains a problem in both the normal seated and supine seated positions. Although compression of the spine in the conventional pilot position can be limited by following the recommended shoulder harness and safety belt installations, it will always be present due to the resultant force caused by the angle of the shoulder straps and the seat structure below the pilot.

Although the prone pilot's lumbar load during Test 1 was exceptionally low, adequate pelvic restraint balanced with sufficient upper body restraint in the prone position during Test 2 proved to be crucial in obtaining acceptable loads in the spine. The passive torso restraint in the prone position displayed remarkable potential for minimising head injury and flailing volume and was improved with the addition of the chin rest. It also limited forward bending of the neck, contributing to the improvement of the neck injury criteria.

From the injury criteria results the following conclusions could be derived. The normal seated position failed some of the injury criteria three out of the possible six times and therefore received a score of 3/6. The prone position scored an acceptable 5/6 and the supine position also received a 3/6. Furthermore, the normal seated position was awarded the title of best performance in a specific injury criterion twice, while

the prone position received the title three times. The supine position only received this title once. From these results it can be concluded that the best support-restraint system for the dynamic tests specified in FAR 23.562 was unarguably the proposed prone pilot position.

Response of the pilots to very controlled impacts was achieved with the sled tests. A need to compare actual crash situations where the dynamics of the fuselage would also influence the response of the pilot still exists. The fuselage crash test was therefore introduced to simulate actual crash scenarios with the three different pilot support positions.

## **4.6 Fuselage Crash Tests**

There are quite a number of ways in which an aircraft can impact into the ground or into other objects. To design a crashworthy aircraft it is important to evaluate every possible crash scenario in order to provide occupant protection during as many as possible of the crash scenarios. As an introduction to the fuselage crash test analysis, some of the likely crash scenarios and possible reasons leading to these scenarios are discussed below.

### **4.6.1 Crash Scenarios**

To protect the occupant from the inherent risk of flight it would be desirable to offer protection during the termination of flight in any thinkable terrain out of any thinkable flight manoeuvre. It should, however, be realised that it would be impossible to provide optimum protection during every possible scenario and therefore the following group of scenarios was considered.

#### **Forced Landing**

A forced landing is the unplanned termination of flight without the proper choice of a landing site, forced onto a pilot by reasons varying from engine failure, cabin fire, severe weather conditions or medical conditions. Lock-up in terrain could occur if an aircraft becomes trapped in a valley or mountainous region where there would not be sufficient space for the aircraft to turn or enough engine power/lift to gain sufficient altitude. This category of emergency implies that the aircraft is aerodynamically intact and controllable until it impacts into the ground and is also referred to as controlled flight into terrain (CFIT). CFIT could lead to a variety of aircraft impact attitude scenarios, but the most likely scenarios conceivable during CFIT are the following:

#### High Impact Belly Landing

Resulting in a high vertical load on the airframe, this scenario can be caused by excessive airspeed during a forced landing. Landing on high crops can result in a high impact belly landing if the top edges of the crops are assumed to be the landing surface. Mushing is the term used when the aircraft is in an aerodynamic state that results in a very high sink rate. Mushing into the ground would also result in a high impact belly landing scenario.

#### Nose Impact

Controlled flight into sloped terrain or a stall from low altitude would result in a nose impact. Landing on obstacles like anthills, rocks and grass clumps would also result in nose impact.

#### Tail Impact

If the high angle of attack landing manoeuvre of Exulans were not well executed, the glider would gain some height from which it would fall back in a tail slide.

#### Wing Tip Impact

Not keeping the wings level during a landing approach or while flying low-level on sloped terrain or any asymmetric contact with an object will cause the aircraft to rotate around the wing into the ground.

#### Pitch Over

When landing in rough terrain, the friction force on the under carriage can cause the aircraft to pitch over the nose. This is especially true for aircraft having a relative large distance between the centre of gravity (CG) and the landing gear's contact surface.

#### Ground Loop

Generally results from retarding of one wing on the ground causing a rotation around the yaw axis.

#### Cart Wheeling

Cart wheeling is the scenario that occurs when a wingtip or nose impact occurs in such a way that it causes the aircraft to roll over the ground around the yaw axis. Cart wheeling due to contact of one wing would thus result in wingtip-nose-wingtip-tail impact.

#### Bad Landing

A bad landing may include the bad planning of a landing circuit that might bring the aircraft down before (undershoot) or beyond (overshoot) the runway. Bad landing may also include bad judgement of the landing flair, bad judgement of the wind, bad judgement of the terrain and bad judgement of the airspeed. Detriments of the latter could have a pilot landing downwind or in a crosswind or be punished by a strong

wind gradient, turbulence or wind shear. Most of the above scenarios would be considered as landings on appropriate terrain but with unusual contact conditions.

#### High Impact Belly Landing

This scenario would follow from bad judgement by the pilot during a landing attempt and would result in a high vertical impact load on the airframe.

#### Nose Impact

Under shooting or over shooting the runway could result in impact into obstacles like anthills, rocks, trees and grass clumps usually found in the unprepared portion of the runway.

#### Termination of Controlled Flight at Altitude

Scenarios in this category include structural failure in mid air and spinning. For this type of emergency the parachute is provided, which brings down both the pilot and the airframe of the Exulans glider.

#### Mid-air Collision

Flying into another object at altitude. This scenario usually occurs as a result of poor field of vision. For example, if a hang glider or micro light pilot with no field of vision to above would fly in the same vicinity but at a lower altitude than a sailplane pilot with no field of vision to below, a mid-air collision could easily occur.

#### Nose Impact

This scenario could result from a spin or in the case of the Exulans glider a parachute descent caused by a parachute deployment at insufficient altitude.

### 4.6.2 The Analysis

During the analysis the pilots in the three different positions were placed in an arbitrary fuselage structure or cage (see Figure 4.32). The pilots were restraint in exactly the same manner as in the sled tests using restraint concept 3 for the prone position. The cage was then subjected to different crash scenarios by modelling impact of the cage into the ground with different airframe attitudes. In other words, the cage was dropped from a specified height with a specified initial forward velocity and various rotations were applied to the CG of the cage to attain the different airframe impact attitudes of the specified crash scenarios. The two most likely crash scenarios selected for this comparing analysis was the high impact belly landing and the nose impact as described above. Two variations of the nose impact scenario were modelled with Crash Scenario 3 having a higher impact angle as Crash Scenario 2.



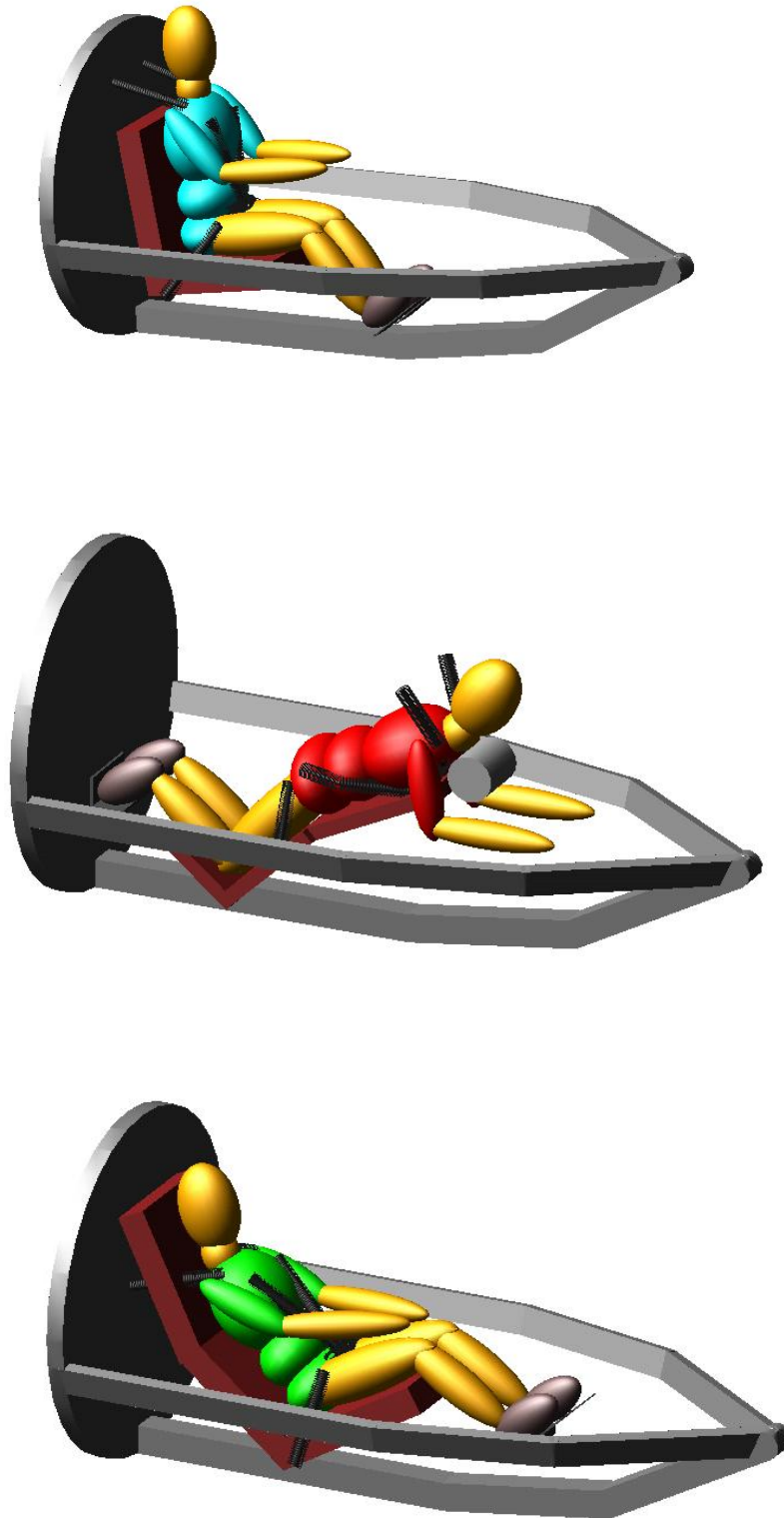
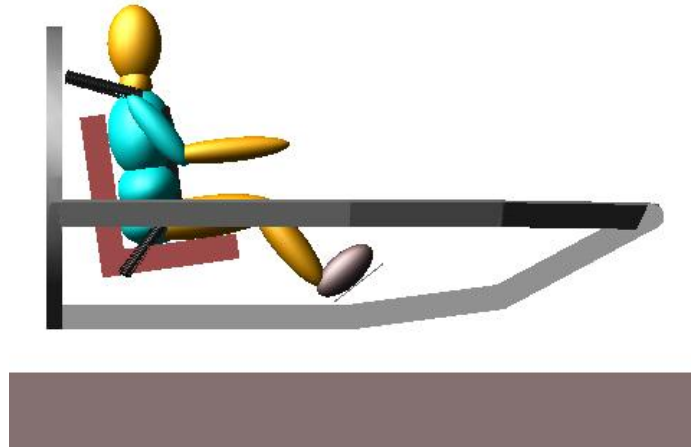


Figure 4.32: Fuselage crash test cage with pilots in different positions

The initial velocity condition applied to the cage was a forward velocity of 60km/h (16.7m/s) and the cage was dropped from heights varying from 1.5-2.0 meters. The cage was modelled as a rigid body construction with a mass of approximately 300kg. Contact between the cage and the ground was modelled with stiffness and damping values that would represent the properties of a soft soil. Friction between the cage and ground was also included in the model.

#### Crash Scenario 1: High Impact Belly Landing

This scenario usually results from bad judgement by the pilot during landing or too much airspeed during a forced landing. To achieve this scenario the cage was dropped from a height of 1.5m with a forward velocity of 60km/h. No rotation was applied to the fuselage and the scenario was simulated for all three pilot support positions. To visualise this scenario, the cage with the normal seated pilot is show in Figure 4.33 just before impact. As usually the specified injury criteria was monitored and used in the comparison of the different positions.



**Figure 4.33: Airframe impact attitude of Crash Scenario 1**

#### Crash Scenario 2: Nose Impact (shallow angle)

This scenario usually results from controlled flight into sloped terrain or a stall from low altitude. The impact force resultant following from impact into an object during a landing will also cause a nose impact scenario. In ADAMS this scenario was modelled by applying a forward initial velocity of 60km/h to the cage and dropping it from an approximate height of 1.7 meters. The nose impact was achieved by applying an initial angular velocity to the CG of the cage that resulted in downward pitching of the nose. Figure 4.34 shows the prone pilot in the cage with an impact angle of approximately 20°.

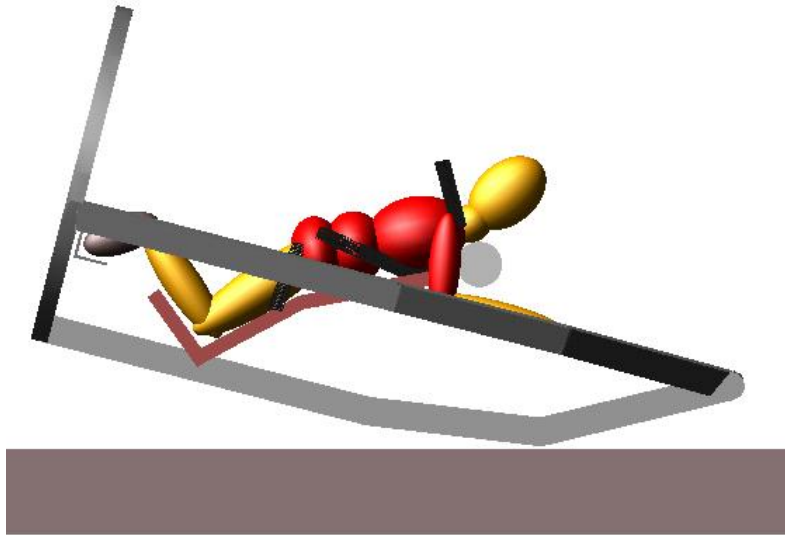


**Figure 4.34: Airframe impact attitude of Crash Scenario 2**

Crash Scenario 3: Nose Impact (steep angle)

Because of the likelihood of a nose impact crash during aircraft accidents another nose impact scenario with a steeper impact angle was modelled as scenario 3. The same forward initial velocity condition of 60km/h was applied but the initial angular velocity around the CG was increased and the cage was dropped from an approximate height of 2 meters. During this scenario the impact angle was increased to approximately  $40^\circ$  as indicated by the cage impact attitude shown in Figure 4.35 with the supine seated pilot.

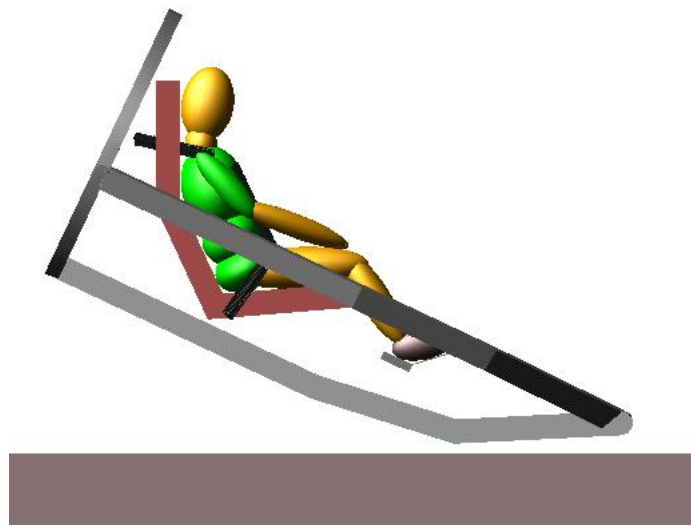


**Figure 4.35: Airframe impact attitude of Crash Scenario 3**

#### 4.6.3 Crash Test Results

During the fuselage crash tests the peak forces and accelerations on the pilots resulted from the initial impact into the ground and were never exceeded by the response due to the fuselage dynamics. During the crash scenarios the orientation of the spine (inline with the vertical crash load on the cage) caused exceeded LLC values for both the normal seated and supine seated positions. This was however not the case for the prone position and this can be attributed to the transverse application of the crash load to the spine as explained previously. Due to the absence of the cockpit parts like the instrument panel and the controls, no secondary head impact occurred during the fuselage crash test. This implied that the HIC values were low for all three the positions.

As explained in Chapter 2.6 the  $N_{ij}$  value is evaluated by considering a combination of neck axial force and bending moment. On evaluation of these forces and moments it seemed that the neck tension force was constantly the highest in the case of the prone position. Although the prone pilot never exceeded the criterion, it resulted in high values during all three scenarios. The reason for these high neck tensions could be explained by the fact that the upper body was restrained by the shoulder straps but the head was still free to displace forward therefore pulling on the neck.

This is actually exactly the same scenario that was obtained with the second prone position restraint concept during the sled tests where the unbalanced pelvic and shoulder strap restraint caused a huge tension force in the spine. Although  $N_{ij}$  was not exceeded, the values were on the limit and the added mass of a helmet worn by the pilot might cause a problem. Dynamic overshoot of the pilot's head during the high impact angle of Crash Scenario 3 resulted in a high  $N_{ij}$  value for the normal seated pilot. The results of the three specified injury criteria for the fuselage crash tests are contained in Table 4.3. Graphs containing the neck axial force and bending moment for each scenario and an example calculation of  $N_{ij}$  were included in Appendix E. The value for  $N_{ij}$  was calculated at each point in time but only the peak value was used for comparison. The values used in the evaluation of the worst case  $N_{ij}$  for all the analysis are listed in Table E1.

**Table 4.3: Fuselage crash tests injury criteria results**

| Analysis   | Pilot Position | Injury Criteria (IC) |          |         | IC exceeded | Best Performance |        |        |
|------------|----------------|----------------------|----------|---------|-------------|------------------|--------|--------|
|            |                | LLC<6700             | HIC<1000 | Nij<1.0 |             | LLC              | HIC    | Nij    |
| Scenario 1 | Normal Seated  | 7619                 | 18.12    | 0.673   | 1           |                  |        |        |
|            | Prone Seated   | 673                  | 12.37    | 0.808   | 0           | Prone            | Prone  |        |
|            | Supine Seated  | 8783                 | 25.03    | 0.377   | 1           |                  |        | Supine |
| Scenario 2 | Normal Seated  | 7921                 | 2.78     | 0.652   | 1           |                  | Normal |        |
|            | Prone Seated   | 3549                 | 5.93     | 0.708   | 0           | Prone            |        |        |
|            | Supine Seated  | 9490                 | 4.77     | 0.378   | 1           |                  |        | Supine |
| Scenario 3 | Normal Seated  | 7754                 | 4.52     | 0.940   | 1           |                  | Normal |        |
|            | Prone Seated   | 2203                 | 14.64    | 0.943   | 0           | Prone            |        |        |
|            | Supine Seated  | 10305                | 8.47     | 0.459   | 1           |                  |        | Supine |

#### 4.6.4 Conclusion

Spinal injury in the normal seated and supine seated position due to vertical crash loads seemed to be the major problem during the fuselage crash tests. This also explains the huge amount of research into load limiting crew seats found in the literature. The head injury criteria values for these analyses were low due to the clean environment provided by the fuselage cage structure. As with the sled test analyses the prone position had a small flailing envelope, which could be attributed to the passive torso restraint and the chin rest. As a result of forward displacement of the head in the prone position the neck injury criteria values were high in comparison and sometimes on the limit.

The injury criteria comparison resulted in the following scores. Both the normal seated and supine seated positions exceeded three of the possible nine injury criteria and therefore receive a score of 6/9. The prone position scored a perfect 9/9. The title of best performance in a specific injury criterion during the fuselage crash tests was awarded twice to the normal seated position and four times to the prone position. The supine position received this title for a competitive three times. These scores indicate that the prone position proposal performed best during the fuselage crash test comparison.

## CHAPTER 5: FINAL CONCLUSIONS AND RECOMMENDATIONS

### ***Conclusions***

The question of safety of a pilot in the prone position during a crash originated long ago with the birth of the Exulans project but was never adequately answered. Not only did this study answer this question but it also shed more light on the whole subject of pilot protection in light aircraft. Crashworthiness are receiving more and more attention during the design of modern aircraft structures and therefore the results of this study would be implemented during the design of the fuselage and pilot protection system of Exulans II.

The literature study revealed that crash survivability is achieved through a combination of five design factors described by the acronym CREEP. These design criteria require the provision of a container that would maintain a living space to the occupant during a crash and sufficient restraint applied to appropriate portions of the body. It also suggested that a clean environment should be provided inside the cockpit with specific attention to the volumes through which unrestraint portions of the body might travel during a crash. Through the implementation of energy absorbing materials and mechanisms in the airframe design, crash forces could be attenuated to tolerable levels during high energy impact scenarios. The literature study further revealed that the majority of aviation fatalities occur post impact. The post-crash design factor takes this fact into consideration when it requires fast and easy evacuation from the fuselage even if damage was inflicted during the crash.

From human impact tolerance limits it was suspected that a pilot could obtain higher crash survivability if supported in the prone position. This statement was further investigated and proved during the dynamic analysis of this study. It was indicated that the prone position could offer better protection to injury if certain guidelines during the support and restraint method were followed.

In comparison with the normal seated and supine seated positions a pilot in the prone position would be exposed to much lower spinal compression forces due to the orientation of the body with respect to a crash load with both vertical and horizontal components. During the dynamic sled test analysis it was however found that this argument could not be presented in the case of a frontal impact and different restraint concepts were evaluated to improve this drawback in the prone position. The results of the different prone concepts indicated that spinal compression during the frontal impact case could be limited if adequate pelvic restraint was provided. On the contrary, if the pelvis was restrained adequately but not with sufficient upper body restraint a huge tension force was induced in the spine. When analyzing the final prone support-restraint proposal, it was however discovered that a good balance between the two restraint systems could result in acceptable spinal loads.

The dynamic analysis also indicated that the passive torso restraint supplied by the chest support limited the dynamic overshoot of the head and resulted in a small flailing envelope for the prone position. It was also discovered that due to the same explanation provided for the reason of the huge tension force induced in the spine during the frontal impact test sled simulation, the neck of the prone pilot was also exposed to rather large tension forces. These tension forces produced neck injury criteria values on the limit and might be unacceptable with the inclusion of a helmet.

It was also discovered that dynamic overshoot of the head and extension of the neck of the pilot in the prone position was limited by the inclusion of a chin rest. The chin rest did however induce an additional injury mechanism to the jaw but due to the high tolerance of the mandible and the addition of a helmet serious injury was assumed to be unlikely. This subject is however recommended for further investigation. From the results of the dynamic analysis it is suspected that additional head restraint would result in a much higher crash survival rate for all three pilot positions. Whether this would be possible to accomplish without restricting the necessary freedom of the pilot's head is still a topic that needs further investigation.

Connecting the helmet to the existing harness system of the prone positioned pilot will go a long way to alleviate these problems without restricting the head's freedom of movement. A similar system called the HANS (Head and Neck Support) is currently used by Formula 1 racing drivers. In this system the driver's helmet is loosely connected to a yoke through several tethers ensuring free movement of the head. The yoke is on its turn fixed to the torso by belts thus providing helmet restraint relative to the torso. According to Wright (2000) frontal impact tests with a Hybrid III ATD wearing the HANS system produced similar results as that with an airbag system.

### ***Recommendations***

Although some of the recommendations were not directly derived from the analysis results, they were included due to their relevance to the Exulans project. The consideration of the five CREEP design factors during a fuselage design was strongly emphasized throughout the literature study and therefore the first recommendation is to structure the design of the Exulans II fuselage according to these factors. This calls for the following:

#### Container

- The container should be designed for a 40g ultimate load
- To achieve a very strong light-weight construction the use of composite materials are recommended
- Provide a structure that would deflect wires from fences and electrical cables away from the pilot
- Provide roll-over protection

## University of Pretoria etd – Meintjes, S W v d M (2004)

- Due to the fact that head injury often result in aviation fatalities it is recommended that the head should be contained in a helmet

### Restraint

- Support the Exulans II pilot in the prone position
- Provide passive torso restraint
- Use Nylon webbing with a minimum width of 50mm and a minimum thickness of 1.5mm.
- Three restraining concepts for the prone pilot were evaluated during the sled test analysis. The best results were obtained with restraint concept 3 and is therefore recommended for use in the Exulans II pilot protection system
- For added comfort and limited neck flexion a chin rest is recommended
- Additional head restraint is recommended to limit dynamic overshoot and neck injury

### Energy Absorption

- The collapsible landing skid should be used as the primary energy absorbing mechanism
- The energy absorbing element used in the collapsible landing skid should be cheap, light and easy replaceable. A kinetic rope or strap is recommended
- An energy absorbing mechanism or material should be used between the pilots chest support and the fuselage
- Due to the ultra-light construction of Exulans II it is possible and recommended to equip the fuselage with a ballistic parachute
- Equip the pilot with a parachute

### Environment

- Line the inside of the fuselage structure with kevlar fiber to contain fracturing of structural elements
- Provide a soft energy-absorbing material lining at potential impact surfaces
- Avoid the use of cables and push-rods close to the pilot

### Post-Crash Factors

- Design the fuselage back part to be detachable for fast and easy escape from the cockpit
- Provide a means for a midair bailout
- Make the fuselage floatable on water
- Make the pilot accessible from outside



Recommendations for Future Work

- Perform the crash test analysis with the prone pilot in the Exulans II fuselage with the recommended energy absorbing mechanisms.
- Investigate the crash response in different prone body positions
- Investigate additional jaw injury mechanism due to impact into chin rest
- Investigate the HANS system
- Perform a finite element fuselage crash test analysis that would include fuselage deformation
- Optimize the energy absorbing mechanisms by investigating different available energy absorbing materials
- Perform an impact experiment using a Hybrid III ATD and a prototype Exulans II fuselage

In the fuselage crash test analysis the airframe containing a pilot in a specific support restraint method was supplied with a forward velocity and dropped from a specific height. During these analyses an idea for evaluating the crash forces on the airframe during a survivable crash was conceived and the author would like to propose this idea for use in the design of the Exulans II fuselage. The idea involves the use of ADAMS as a design tool and basically states that the forward velocity and initial height components could be converted into an energy value.

With an ADAMS model of the Exulans II fuselage and the proposed pilot protection system, the energy of the crash could systematically be increased while injury criteria are monitored on the pilot. The moment when the injury criteria are exceeded the crash would no longer be survivable and integrity of the structure beyond this point would be useless. At this moment the forces on the airframe could be retrieved from ADAMS and used as input design criteria. This process could be repeated for different crash scenarios to obtain the worst case scenario. It is however realized that the feasibility of the resulting design would be determined by the strict weight requirements set by the Exulans II project.

## REFERENCES

- ADVISORY CIRCULAR. 1985. *Injury Criteria for Human Exposure to Impact*. U.S Department of Transport, Federal Aviation Administration. Advisory Circular AC No 21-22.
- ADVISORY CIRCULAR. 1993. *Shoulder Harness-Safety Belt Installations*. U.S Department of Transport, Federal Aviation Administration. Advisory Circular AC No 21-34.
- BRADSHAW, G. Wright, S. 1996. *Wright Brothers History, First Flight, 1903*.  
<http://www.wam.umd.edu/~stwright/WrBr/wrights/1903.html> Access: 17 September, 2003
- CAVANAUGH, J. 2000. *The Biomechanics of Thoracic Trauma*. Bioengineering Center. BME 7160. Wayne State University.
- COUTO, G. 1999. *The Arizona Hang Glider Association Photo Gallery*. <http://www.ahga.org/cgi-bin/photo.cgi?gallery/hg0037.jpg> Access 28 October, 2003
- DAVIDSON, B. 1994. *Crash Survivability, Improving Your Odds*.
- EPPINGER, R. Sun, E. Bandak, F. Haffner, M. Khaewpong, N. Maltese, M. Kuppa, S. Nguyen, T. Takhounts, E. Tannous, R. Zhang, A. and Saul, R. 1999. *Development of Improved Injury Criteria for the Assessment of Advanced Automotive Restraint Systems – II*. National Highway Traffic Safety Administration. Final Rule Docket NHTSA-00-7013. Washington D.C.
- EURONCAP. 1997. <http://www.euroncap.com/tests.htm> Access: 28 April 2003.
- FAR. 1997. *Part 23-Airworthiness Standards: Normal, Utility, Acrobatic, and Commuter Category Airplanes*. Federal Register.
- FARLEY, G.L. 1983. *Energy Absorption of Composite Materials*. Journal of Composite Materials, Vol 17, May 1983, Pp 267-279.
- GFA. *The Gliding Federation of Australia*. <http://www.gfa.org.au/Gallery/index4.htm> Access: 28 October, 2003
- GM. *Protecting Occupants* [http://www.gm.com/company/safety/protect\\_occupants/dummies/index.html](http://www.gm.com/company/safety/protect_occupants/dummies/index.html) Access: 15 September, 2003

## University of Pretoria etd – Meintjes, S W v d M (2004)

- HANIQUE, M. 2002. *The Mock-up of the Fuselage of Exulans II*. Bachelors Degree in Mechanical Engineering. Fontys Hogescholen, Eindhoven.
- JAR-22. 2001. *JAR-22: Sailplanes and Powered Sailplanes*. Joint Aviation Authorities. The Netherlands.
- JAR-23. 2001. *JAR-23: Normal, Utility, Aerobatic, and Commuter Category Aeroplanes*. Joint Aviation Authorities. The Netherlands.
- JAR-VLA. 2001. *JAR-VLA: Very Light Aeroplanes*. Joint Aviation Authorities. The Netherlands.
- LABUN, L.C. and Rapaport, M. 1994. *A Third Generation Energy Absorber for Crash Attenuating Helicopter Seating*. Proceedings-50<sup>th</sup> Annual American Helicopter Society Forum, Vol 1, May 1994, pp 521-535.
- Luftfahrt International, 1975. *Berlin B9 Experimental Aircraft*.  
<http://www.luft46.com/prototyp/berlin9.html> Access: 18 September, 2003
- McCORMICK, B.W. 1979. *Aerodynamics, Aeronautics, and Flight Mechanics*. 1<sup>st</sup> ed. John Wiley & Sons, Inc. Canada.
- MECHANICAL DYNAMICS INC. *ADAMS Technical Manual Version 12.0*
- MECHANICAL DYNAMICS INC. 2002. *FIGURE HUMAN MODELLER Technical Manual Version 4.0*.
- MEINTJES, S.W. 1999. *Mock-up of Exulans II Cockpit*. B. Engineer Mechanical. University of Pretoria, Pretoria.
- NASA History Office. 1958. *History of Research in Space Biology and Biodynamics*. Holloman Air Force Base, New Mexico.
- Naval Aerospace Medical Institute. 1991. *United States Naval Flight Surgeon's Manual*. 3<sup>rd</sup> ed. The Society of United States Naval Flight Surgeons.
- NHTSA. *Pedestrian and Applied biomechanics* <http://www-nrd.nhtsa.dot.gov/vrtc/bio/adult/hybIII50dat.htm> Access: 28 April, 2003.

## University of Pretoria etd – Meintjes, S W v d M (2004)

NICHOLSON, C.R. and Chapman, H. *The Dynamic Crashworthiness Testing of the GA-200 Seat and Restraint System to FAR 23.562*. Proceedings of the 5<sup>th</sup> Australian Aeronautical Conference, Part 1 of 2, pp 273-276.

TESTI, M. 1998. MasterBlaster Aircraft Home Page.  
<http://digilander.libero.it/karenfuxia/masterblaster.htm> Access: 17 September, 2003

RAF MUSEUM. *Gloster Meteor F8 Prone Position*. <http://www.rafmuseum.org.uk/gloster-meteor-f8-prone-position.htm> Access: 16 September, 2003.

RAPAPORT, M.B. Yeiser, C.W. and Oslon, M.B. 1995. *Performance Assessment of the V-22 Aircraft Crashworthy Crew Seat With Various Size and Gender Aircrew Using the Articulated Total Body (ATB) Computer Simulation Model*. Proceedings-33<sup>rd</sup> Annual SAFE Symposium, pp 279-304.

RFRL, Raspet Flight Research Laboratory, Department of Aerospace Engineering, Mississippi State University. *History: Horten Ho IV Flying Wing*. <http://www.ae.msstate.edu/rfrl/pages/horten.html> Access: 18 September, 2003

RICHARDS, M.K. and Podob, R. 1997. *Development of an Advanced Energy Absorber*. Proceedings-35<sup>th</sup> Annual SAFE symposium, pp 321-327.

SIMULA INCORPORATED. Tempe, Arizona. 1980. *Aircraft Crash Survival Design Guide. Volume IV- Aircraft Seats, Restraints, Litters, and Padding*. U.S. Department of Commerce, National Technical Information Service.

The Naval Flight Surgeon's Pocket Reference to Aircraft Mishap Investigation. 1995. 4<sup>th</sup> ed. The Society of United States Naval Flight Surgeons.

VALENCIA. 2003. *Superbike Photo Gallery*.  
[http://www.superbike.it/multimedia.asp?p\\_Anno=2003&p\\_S\\_Campionato=SBK&p\\_Tab=2&p\\_Round=ES](http://www.superbike.it/multimedia.asp?p_Anno=2003&p_S_Campionato=SBK&p_Tab=2&p_Round=ES)  
P Access: 28 October, 2003

WINKELMAN, K.L. and Laananen, D.H. 1996. *Analysis of Energy-Absorbing Seat Configurations*. Proceedings-52<sup>nd</sup> Annual American Helicopter Society Forum, June, pp 1319-1323.

WOOD, R.H. and Sweginnis, R.W. 1996. *Aircraft Accident Investigation*.

University of Pretoria etd – Meintjes, S W v d M (2004)

WRIGHT, P. 2000. *Technical: Head and Neck Support (HANS)*. <http://www.grandprix.com/ft/ft00358.html>

Access: 29 October, 2003

## APPENDIX A THE HYBRID III CRASH TEST DUMMY

### *Introduction*

According to the National Highway Traffic Safety Administration (NHTSA) the Hybrid III 50<sup>th</sup> percentile crash test dummy was born in the labs of General Motors in the U.S in 1976. Although this dummy is generally used throughout the world in automotive frontal impact crash evaluations it is also part of the Hybrid III family shown in Figure A1. The family consists of a 3-year-old, 6-year-old, 10-year-old, small adult female, midsize adult male and a large adult male.



**Figure A1. The Hybrid III crash test dummy family (GM)**

The Hybrid III is no ordinary shop window mannequin but rather a very sophisticated piece of engineering equipped with sensors to measure injury risk to various portions of the body in impact events. To achieve this, each dummy must satisfy a number of design criteria. Firstly, the dummy must be anthropometric, meaning that it should have the same dimensions and mass properties as a human in the population group it represents. Secondly, the dummy must be anthropomorphic, which means that it must possess the same mechanical properties as a human. These properties include joint stiffness, joint range of motion, thoracic stiffness and skin force deflection characteristics. If the dummy satisfy both these conditions its kinematics and interaction with the restraint system and vehicle interior should result in a realistic representation of a human in a crash event.

## ***Dummy Measurements***

Measurements in the 50<sup>th</sup> percentile male Hybrid III dummy consist of the following:

### **Head**

The head is made of aluminium and covered with a vinyl rubber 'flesh'. Inside, three accelerometers are set at right angles, each providing data on the forces and accelerations to which the brain would be subjected in a crash.

### **Neck**

The segmented neck shown in Figure A2 is provided with sensors measuring bending, shearing and tension forces as the head is thrown forwards and backwards during impact.



**Figure A2. Hybrid III neck sensors (Euroncap 1997)**

### **Upper Torso**

Six high strength steel ribs covered with polymer base damping material are fitted with measuring equipment to record chest deflection and impact forces (Figure A3).



**Figure A3. Steel ribs with measuring equipment in upper torso (Euroncap 1997)**

#### Lower Torso

The lower torso consist of a curved cylindrical rubber lumber spine, which mounts to the pelvis through a lumber load cell, which provides lumber load information.

#### Upper Leg, Lower Leg, Feet and Ankles

The ball-jointed femur attachments in the pelvis carry bump stops to reproduce the human leg to hip moment/rotation characteristics. The femur, tibia and ankle can be instrumented to predict bone fracture and the knee can evaluate tibia to femur ligament injury. The foot and ankle simulate heel compression and ankle range of motion.

The following tables contain more specifications on the Hybrid III family. In Table A1 the mass, sitting height and stature of the different family members are listed. Table A2 contains the segment masses of the 50<sup>th</sup> percentile dummy. The major dimensions of the 50<sup>th</sup> percentile male Hybrid III are given in Table A3 and Table A4 lists the instrumentation used in the 50<sup>th</sup> percentile male Hybrid III.



**Table A1: Comparison of Weight (NHTSA)**

| <b>Comparison of Weight, Sitting Height, and Stature for HYBRID III Family</b> |                        |                   |                   |                  |                 |
|--------------------------------------------------------------------------------|------------------------|-------------------|-------------------|------------------|-----------------|
|                                                                                | <b>12 MO<br/>CRABI</b> | <b>3 YO Child</b> | <b>6 YO Child</b> | <b>5% Female</b> | <b>50% Male</b> |
| <b>Weight<br/>(lbs.)</b>                                                       | 22.0                   | 34.1              | 51.6              | 108.0            | 172.3.0         |
| <b>Stature<br/>(in.)</b>                                                       | 29.4                   | 37.2              | 45.0              | 59.1             | 69.0            |
| <b>Sitting<br/>Height (in)</b>                                                 | 18.9                   | 21.5              | 25.0              | 31.0             | 34.8            |

**Table A2: Segmented Weights (NHTSA)**

| <b>Segment and Assembly Weight of the HYBRID III 50<sup>th</sup> Percentile Male</b> |                    |
|--------------------------------------------------------------------------------------|--------------------|
| <b>Part</b>                                                                          | <b>Weight (lb)</b> |
| Head                                                                                 | 10.0               |
| Neck                                                                                 | 3.4                |
| Upper Torso                                                                          | 37.9               |
| Lower Torso                                                                          | 50.8               |
| Upper Arms                                                                           | 8.8                |
| Lower Arms and Hands                                                                 | 10.0               |
| Upper Legs                                                                           | 26.4               |
| Lower Legs and Feet                                                                  | 25.0               |
| <b>Total Weight</b>                                                                  | <b>172.3</b>       |

**Table A3: Dimensions (NHTSA)**

| <b>External Dimensions for the HYBRID III 50<sup>th</sup> Percentile Male</b> |                            |
|-------------------------------------------------------------------------------|----------------------------|
| <b>Dimension Description</b>                                                  | <b>Specifications (in)</b> |
| Head Circumference                                                            | 23.5                       |
| Head Breadth                                                                  | 6.1                        |
| Head Depth                                                                    | 8.0                        |
| Erect Sitting Height                                                          | 34.8                       |
| Shoulder to Elbow Length                                                      | 13.3                       |
| Back of Elbow to Wrist Pivot Length                                           | 11.7                       |
| Buttock to Knee Length                                                        | 23.3                       |
| Knee Pivot Height                                                             | 19.5                       |

**Table A4: Instrumentation (NHTSA)**

| <b>Instrumentation Capabilities of the HYBRID III 50<sup>th</sup> Percentile Male</b>       |                      |
|---------------------------------------------------------------------------------------------|----------------------|
| <b>Instrumentation</b>                                                                      | <b># of Channels</b> |
| Head 12 Array x (4), y (4), z (4) accelerometers<br>+ 3 other locations                     | 12                   |
| Thorax x, y, z accelerometers                                                               | 3                    |
| Pelvis x, y, z accelerometers                                                               | 3                    |
| Thorax (Chest Deflection) x rotary<br>potentiometer                                         | 1                    |
| Knee Slider* x linear potentiometer                                                         | 1                    |
| Upper Neck x, y, z forces and moments                                                       | 6                    |
| Lower Neck x, y, z forces x, y moments                                                      | 6                    |
| Lumbar Spine x, y, z forces x, y moments                                                    | 5                    |
| Femur - 1 channel *# z force                                                                | 1                    |
| Femur - 6 channel *# x, y, z forces and<br>moments                                          | 6                    |
| Knee Clevis Load Cell* z (2) force                                                          | 4                    |
| Upper Tibia Load Cell* x, z forces x, y moments                                             | 4                    |
| Lower Tibia Load Cell* x, z forces x, y moments                                             | 4                    |
| Total number of channels                                                                    | 56                   |
| * indicates that right and left instruments are required                                    |                      |
| # the two femur load cells are mutually exclusive; if one is used, the other is<br>excluded |                      |

The axes associated with the ATD are defined as indicated below in Figure A4.

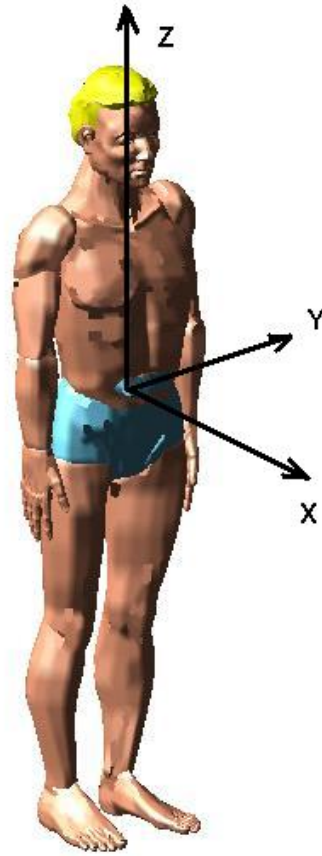


**Figure A4. ATD axes definition**

## **APPENDIX B            SHOULDER HARNESS AND SAFETY BELT INSTALLATIONS**

### ***Experience***

According to the Advisory Circular (1993) experience has shown that the best safety mechanism that a driver and passengers of an automobile has, is the conventional seat belt. Statistics indicate that an airbag, also known as a Supplementary Restraint System (SRS), is only effective if the seat belt is also worn. Of more relevance is that aviation accident experience has provided substantial evidence that the use of a shoulder harness in conjunction with a safety belt can reduce serious injury to the head, neck and upper torso of aircraft occupants. Experience also indicated that the correct application of a shoulder harness and safety belt has the potential to reduce fatalities of occupants involved in otherwise survivable accidents. The same experience has shown that installation geometry, attachment techniques and the cabin area surrounding the seat influence the shoulder harness-safety belt combination that should be selected and the effectiveness of that restraint system.

Most aircraft occupants generally accept the use of a lap belt for restraint during turbulence, aerobatics manoeuvres and agricultural flying. A shoulder harness is however generally associated with the relatively rear occurrence of an accident and it is often heard that a shoulder harness is cumbersome, unwieldy, hot and uncomfortable. Such objections for not installing and using a shoulder harness should be dispelled in view of the benefits gained from using a correctly designed and installed shoulder harness-safety belt system. These benefits range from the prevention of serious head, neck and upper torso injuries in minor accidents to the prevention of irreversible or fatal injuries in more severe accidents.

### ***Shoulder Harness Configurations***

Shoulder harness assemblies are categorised as single shoulder belt assemblies and dual shoulder belt assemblies. The single shoulder belt configuration is normally arranged diagonally across the occupant's chest and is also referred to as a 3-point restraint system (Figure B1). The dual shoulder belt assembly is a symmetrical arrangement of two belts with one belt passing over each of the occupant's shoulders. This arrangement is frequently referred to as a 4-point (Figure B2) or a 5-point (Figure B3) restraint system if a negative-G strap is used. Shoulder harness systems should be designed to meet the requirements specified by the ultimate inertia loads resulting from emergency landing conditions specified in the JAR or the torso restraint system Technical Standard Order (TSO) C114.

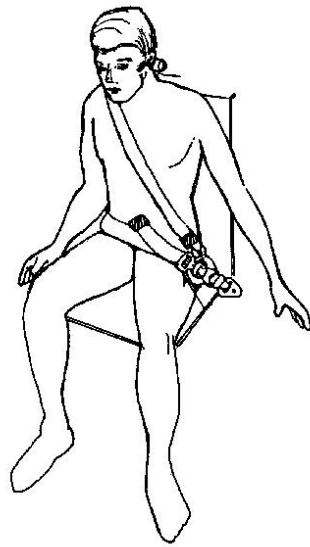


**Figure B1: Single strap 3-point restraint**  
(Advisory Circular 1993)

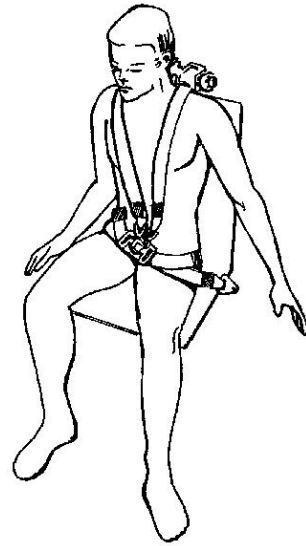


**Figure B2: Dual strap 4-point restraint**  
(Advisory Circular 1993)

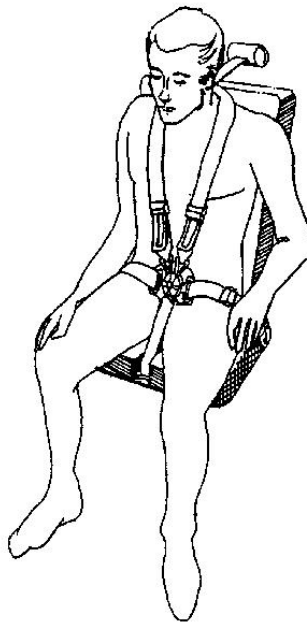


**Figure B3: Dual strap 5-point restraint (Advisory Circular 1993)**

### ***Shoulder Harness Considerations***

The elements that should be considered when installing a shoulder harness restraint system are the webbing, steel cables, energy absorbing devices and buckles. Each of these elements play an important roll in the effectiveness of the restraint system as described in the following paragraphs.

## **Webbing**

Webbing is the one element common to all shoulder harness installations. Webbing should be made from synthetic materials to avoid deterioration by climate exposure. Webbing characteristics to consider are the width, thickness, weave and elasticity.

### **Webbing Width**

Technical Standard Order (TSO) C114, torso restraint systems, allows a minimum webbing width of 1.8 inches (45mm). The majority of shoulder harness-safety belt systems designed for civil aircraft use nominal 2.0 inches (50mm) wide webbing. Webbing widths of 2.25 – 3 inch and associated hardware are also available for special applications. The correct hardware fittings should be used with the appropriate webbing width to avoid wear and cutting of the webbing under strain.

### **Webbing Thickness**

It is again important to match the hardware to the webbing thickness. Some hardware elements such as retractors and manual length adjusters are sensitive to webbing thickness. Nominal webbing thickness of 1.0 and 1.5 millimetres is common in civil aircraft restraint systems but thicker webbing is available for special applications. The thickness of the webbing contributes to the maintenance of the contact between webbing and occupants under load.

### **Webbing Weave**

Herringbone weave is used in most new webbing designs. Hardware should be matched to the correct type of weave because incorrect hardware to webbing adoption could lead to excessive slippage under loads.

### **Webbing Elasticity**

The webbing commonly used in safety belt designs is an elastic material. Nylon is the most common and the 2.0-inch webbing permits a 17 to 20% stretch under a tensile load of 2500 pounds with the herringbone weave. Dacron 2.0-inch webbing with the herringbone weave exhibits an elasticity of 8% under a 2500-pound tensile load. If limited space for occupant displacement is available in the aircraft cabin, substantial elongation of the webbing should not be allowed.

## ***Cables***

The use of steel aircraft cable offers a means of reducing occupant displacement due to unwanted webbing elongation and it is also used to extend belts to suitable attachment points. It is however important to take the necessary precautions when using steel cable and they include the following.

- Use cable flexible in bending to avoid fatigue failure due to flexing
- Avoid sharp bends of the cable. A bend radius of at least 4 times the diameter is recommended
- Selection of any cable clevises needs careful attention

## ***Energy Absorbing Devices***

The use of energy absorbing devices in the webbing of the shoulder harness-safety belt chain is not recommended. This is primarily recommended due to the increased potential for secondary occupant impact. Insufficient torso restraint that could lead to head injury should be expected when energy-absorbing devices are used in the webbing. Energy absorbing mechanisms should be incorporated into the aircraft structure or seat and webbing elongation should be limited.

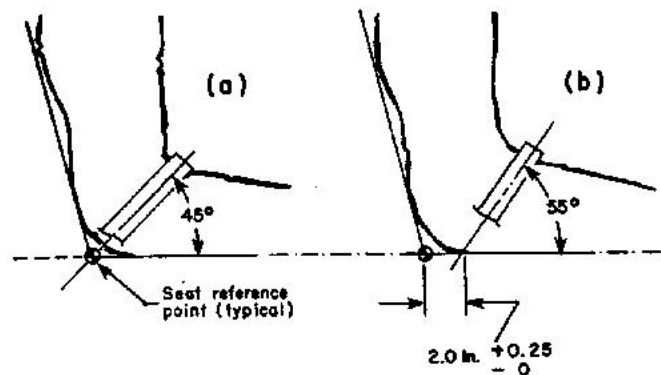
## ***Buckles***

Buckles provide the basic means of securing the various segments of a shoulder harness-safety belt system around the occupant and also allow easy and quick release of the system. According to the FAR metal-to-metal coupling provide improved security and reliability over any method of coupling which rely on clamping of the webbing. The release mechanism of the buckle should be designed to minimise the potential for inadvertent release by the occupant or premature release by inertia forces acting on it. It should also be designed for fast and easy release by one finger after an accident.

## Installation Geometry

### The Safety Belt

The safety belt, also referred to as the lap belt or seat belt restrains the occupant at the pelvic region. Safety belts generally perform best when they act at an angle of  $45^\circ$  with the aircraft's longitudinal axis as seen in Figure B4 (a). Attachment of the safety belt to the floor for an adjustable seat needs special attention in maintaining a proper belt angle for all the seat positions. An angle varying between  $45^\circ$  and  $55^\circ$  are acceptable for adjustable seats as seen in Figure B4 (b).



Figures B4: Acceptable lap belt attachment angles (Advisory Circular 1993)

If the safety belt acts along a shallow angle as shown in Figure B5 (a), it is likely to slip off the pelvis of the occupant applying unwanted loads to the abdomen. In addition, the shallow belt angle is prone to produce anterior wedge fracture of the lumbar vertebra due to flexure of the upper torso over the belt. Muscular resistance to the upper torso flexure is unlikely for even the strongest individuals at decelerations above 3 or 4 G's. If the safety belt is installed at too steep an angle as shown in Figure B5 (b), it will not restrain the forward movement of the occupant until the occupant has displaced to such an extent that the belt angle approaches the recommended  $45^\circ$  angle. This type of steep belt angle permits knee impact with the instrument panel or even worse will allow the occupant to slip off the front edge of the seat creating a shallow belt angle scenario with all the associated potential for injuries including impact into the instrument panel. Furthermore, when selecting the safety belt attachment point, one should consider the length of the webbing and the effect of webbing elongation due to elasticity as mentioned in the previous section.



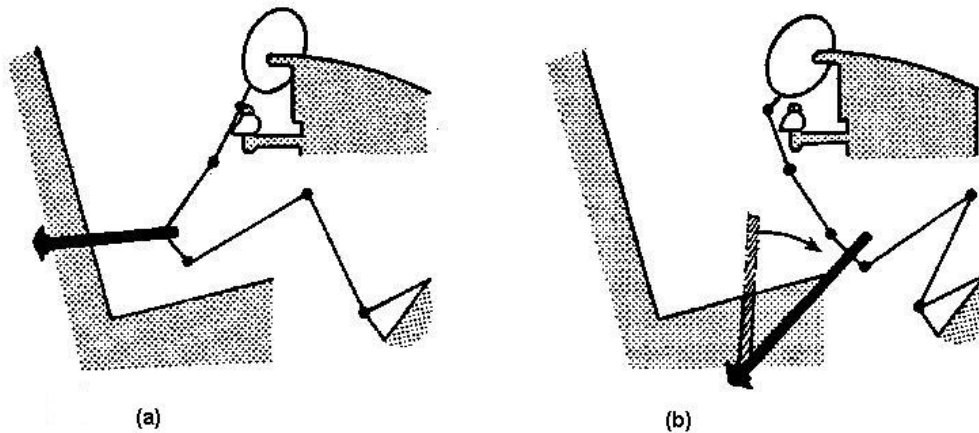


**Figure B5: Incorrect shallow and steep belt angles (Advisory Circular 1993)**

### Single Diagonal Shoulder Harness

These types of restraint systems have been used in automobiles for a number of years and accident experience showed that they perform well. As indicated in Figure B6 (a), the shoulder strap should be positioned to pass the midpoint of the shoulder and should be attached well to the side of the occupant's hip. An improper lower attachment is illustrated in Figure B6 (b). The shoulder belt is attached to a buckle situated near the centre of the pelvis, which renders the diagonal support of the shoulder belt over the occupant's chest ineffective. The shoulder belt passes the torso's centre of mass low and to the side, which will cause the torso to twist and even slide out of the belt in a severe accident.

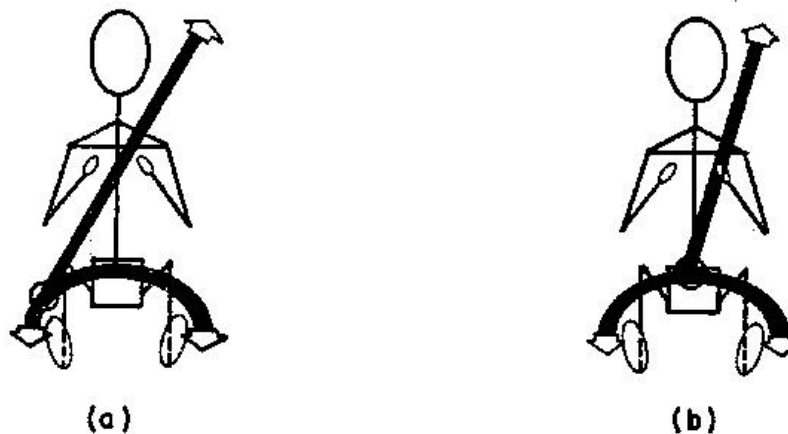


**Figure B6: Correct and incorrect single diagonal shoulder harness attachment (Advisory Circular 1993)**

In selecting the upper end attachment point of the diagonal shoulder belt, precautions should be taken to avoid problems with variation in occupant size. Figure B7 (a) illustrates the situation in which the shoulder belt bears against the neck of a short occupant. A similar situation could develop with a medium size occupant when the upper attachment point is selected to close too the vertical centreline of the seat. This situation is aggravating and discourages the use of the shoulder harness. Figure B7 (b) illustrates how the shoulder belt may tend to fall off the shoulder of a tall occupant or when the upper attachment point is too far outboard or too low with respect to the shoulder midpoint. This situation is aggravating and also discourages the use of the shoulder harness. General anthropomorphic data indicates the sitting height to the midshoulder of a small female at approximately 21.5 inches and that of a large male at 27.5 inches. An upper attachment point at 25 inches is considered as a good starting point.

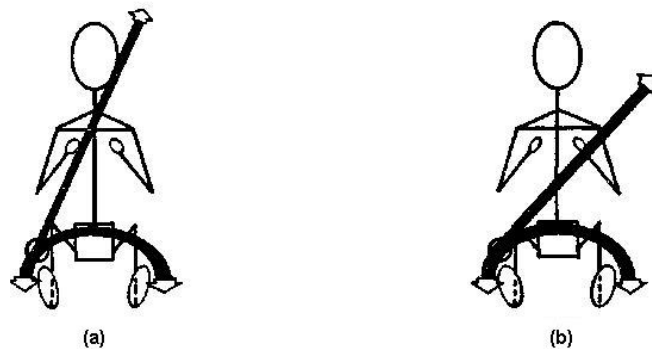


**Figure B7: Incorrect upper shoulder harness attachments (Advisory Circular 1993)**

### Dual Shoulder Harness

A common dual shoulder harness installation is shown in Figure B8 (a) with all the segments joined by the single buckle in the centre of the lap belt. This design allows rapid escape by releasing only one buckle (single point release). An alternative dual shoulder harness system is shown in Figure B8 (b), where the shoulder belts are attached at the lap belt attachment points to the sides of the occupant's hip. A system installed with a shallow angle safety belt will allow the shoulder harness to pull the safety belt up into the abdominal area as illustrated in Figure B9 (a). In addition to the injury potential of a shallow angled safety belt discussed previously, this action also introduces a slack into the shoulder harness that could lead to head, neck and chest injury due to impact into the instrument panel. Again a 45° to 55° belt angle is recommended to permit the safety belt to react to the upward pull of the shoulder straps as indicated by Figure B9 (b). Another method of limiting upward movement of the safety belt is by the use of a negative-G strap also referred to as a crotch strap. A negative-G strap is attached at one end to the buckle and at the other end to the front edge of the seat or airframe under the seat as shown in Figure B10. This method has proved to be very efficient and has been installed on many commercial and aerobatics pilot crew seats.

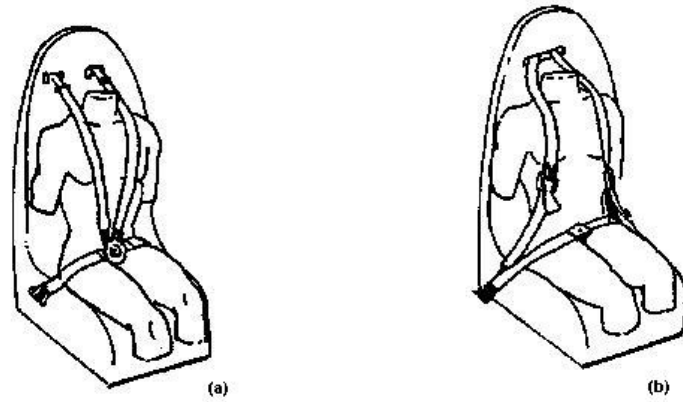


Figure B8: Typical concepts for dual shoulder harness installations (Advisory Circular 1993)

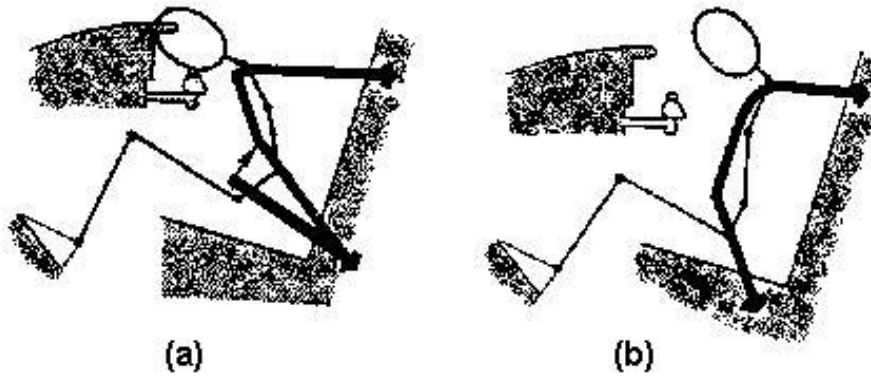


Figure B9: Incorrect and correct shoulder harness safety belt installations (Advisory Circular 1993)

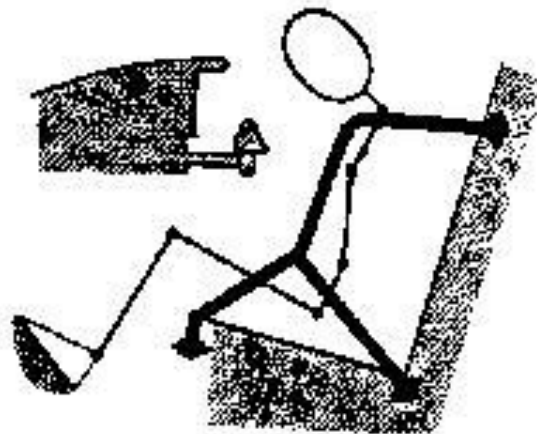
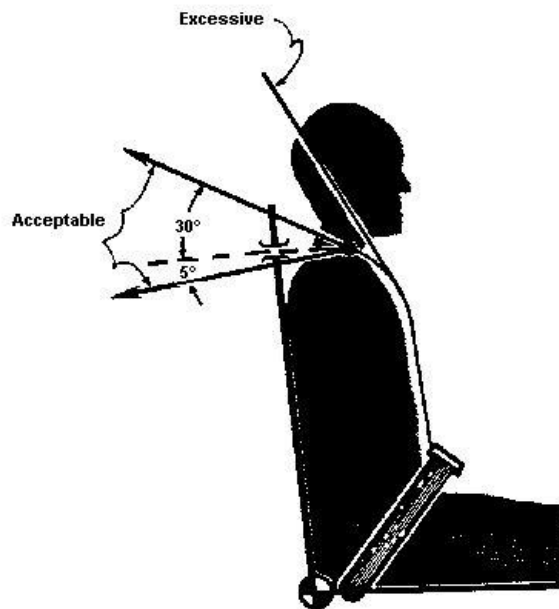


Figure B10: Installation of the negative-G strap (Advisory Circular 1993)

## ***Spinal Compression***

Compression of the spinal column by both single and dual shoulder harnesses should be avoided. This can generally be achieved by selecting the upper attachment points of the shoulder harness such that the trailing length behind the occupant does not fall below an angle of  $5^\circ$  below the longitudinal tangent to the occupant's shoulder as indicated in Figure B11. Spinal compression is likely to occur when the upper end of the shoulder harness is mounted below the occupant's shoulders. This configuration, as illustrated in Figure B12, causes the straps to pull down onto the occupant's shoulders as forward movement is resisted. The resultant restraint force shown in Figure B13 will place the spinal column under compression, which will add to the stress on the vertebra due to the vertical deceleration in an accident. In addition, attaching the upper end of the shoulder harness too high will create additional structural loads and would provide poor restraint to forward displacement of the occupant. A maximum angle of  $30^\circ$  above the longitudinal tangent to the shoulder is recommended as a guideline (refer Figure B11).



**Figure B11: Acceptable range of upper attachment points (Advisory Circular 1993)**

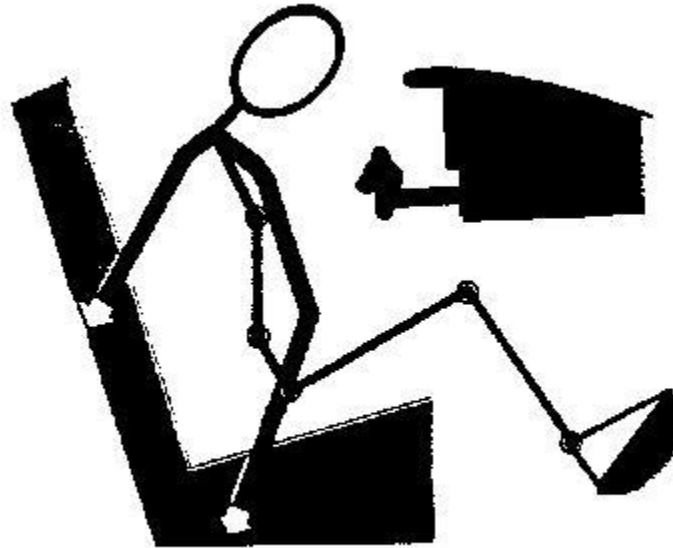


Figure B12: Compression of spine due to incorrect shoulder strap installation (Advisory Circular 1993)

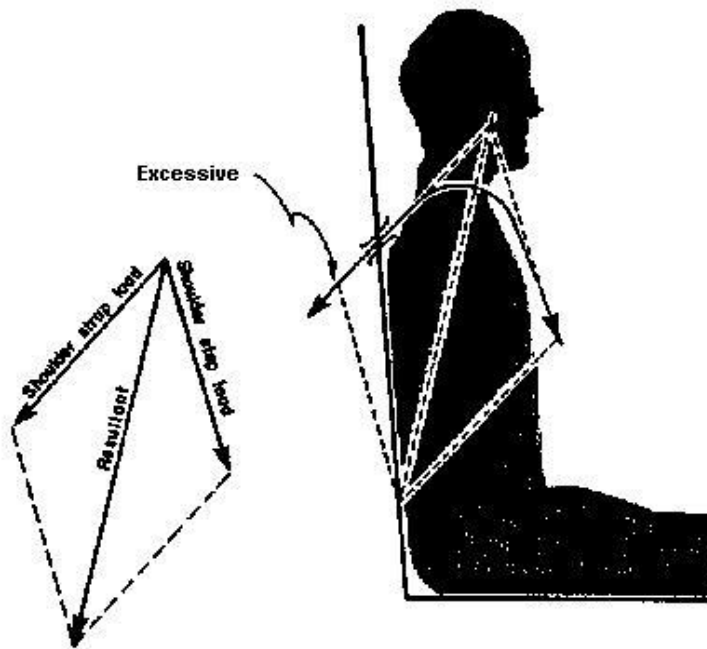


Figure B13: Spinal compression due to resultant restraint force (Advisory Circular 1993)

## **Conclusion**

The intent of the Advisory Circular (AC) was to provide guidance to achieve an effective shoulder harness-safety belt installation in the dynamic loading environment. It is, however, recognised that compromises are necessary due to the absence of sufficient attachment structure in some aircraft. In conclusion the most valuable pointers retrieved from the AC concerning shoulder harness-safety belt restraint systems are listed below.

- Width of webbing in contact with occupant, nominally 2.0 inches or more
- Minimise webbing stretch by minimising webbing length
- Use single buckle for release and escape
- Attachment range for safety belts, between 45° and 55° for all seat positions
- Webbing guides position dual shoulder straps at middle of occupant's shoulders
- Lower attachment of single diagonal shoulder strap to the side of occupant's hip
- Upper attachment of single diagonal strap should provide sufficient restraint for various occupant sizes
- Elevation angle range of trailing shoulder straps between 5° and 30° from longitudinal

## APPENDIX C JOINT AVIATION REGULATIONS SELECTIONS

### JAR-22

The Joint Aviation Regulations requirements for sailplanes and powered sailplanes are stated in JAR-22 (2001). Some of the important requirements concerning pilot protection and occupant safety were summarised in the following paragraphs.

#### JAR 22.561 Emergency Landing Conditions

- a) Although the sailplane may be damaged in emergency landing conditions, it must be designed to protect the occupant under the prescribed conditions.
- b) The structure must be designed to protect the occupant provided that full use is made of seat belts and harnesses under the following conditions.
  - 1) If the occupant experiences separately ultimate inertia forces corresponding to the following accelerations:

|          |      |
|----------|------|
| Upward   | 4.5g |
| Downward | 9.0g |
| Sideward | 3.0g |
| Downward | 4.5g |
  - 2) If an ultimate load of 6 times the weight of the sailplane acting rearwards and upwards at an angle of 45° to the longitudinal axis of the sailplane is applied at the most suitable forward position of the fuselage.
- c) A sailplane with retractable landing gear must be designed to protect the occupant in a landing with wheels retracted under the following conditions.
  - 1) With a downward ultimate inertia force corresponding to an acceleration of 3g.
  - 2) With a coefficient of friction of 0.5 at the ground.
- d) The supporting structure must be designed to restrain under loads specified in sub-paragraph (b)(1) each item of mass that could injure the occupant if it came loose in a minor crash landing.
- e) For a powered sailplane with the engine located behind and above the pilot's seat an ultimate inertia load of 15g in the forward direction must be assumed.

#### JAR 22.785 Seats and Safety Harnesses

- a) Each seat and supporting structure must be designed for an occupant weight in accordance with JAR-22.25 (a)(2) and for the maximum load factors corresponding to the specified flight, ground

and emergency landing conditions prescribed by JAR 22.561. The seat and its supporting structure must also be designed to withstand the reaction to the load specified in JAR 22.397(b).

- b) The seats including the cushions may not deform to such an extent that the pilot is unable to reach the controls safely or operate the wrong controls when subjected to the loads corresponding to JAR 22.581 and JAR 22.583.
- c) The seat design must allow the accommodation of a parachute worn by the occupant and must allow comfortable seating whether the occupant wears a parachute or not.
- d) The strength of the safety harness must not be less than that following from the ultimate loads of the flight and ground load conditions and the emergency landing conditions according to JAR 22.561(b).
- e) Safety harness installations must be designed so that the occupant is safely retained in his initial sitting or reclining position under any acceleration occurring in operation.
- f) Each seat and safety harness installation must be designed to give each occupant every reasonable chance of escaping serious injury under the conditions of JAR 22.561(b)(1).

#### IEM 22.785 Seats and Safety Harnesses

- 1) The arrangement of the safety harness installation should minimise the probability of the occupant's body from sliding underneath the belts or laterally when subjected to inertia loads acting in the forward or sideward direction.
- 2) For semi-reclined seating positions the anchorage points of the lap belt should be located well below and behind the H-Point at an angle between  $80^{\circ} \pm 10^{\circ}$  to the datum line through the H-Point parallel to the longitudinal axis of the sailplane. The H-Point (Hip Point) is the pivot between the torso centreline and the thigh centreline of the occupant.
- 3) The anchorage points of the shoulder belts for a 50 percentile male should be located below and behind the pilots shoulders at an angle of  $15^{\circ} + 2^{\circ} / - 0^{\circ}$  to a line parallel to the longitudinal axis of the sailplane. The lateral separation should not be more than 200mm (see Figure C1).

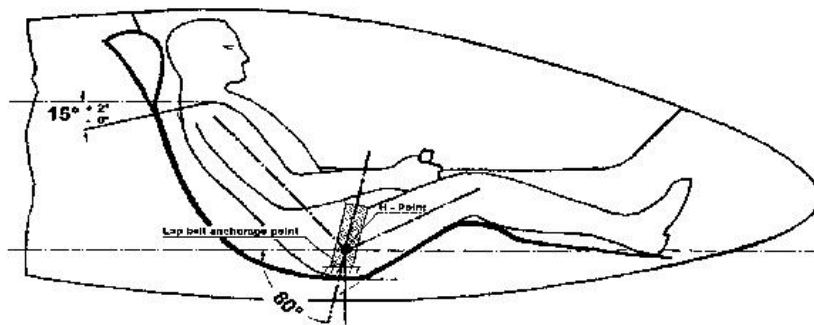


Figure C1: Lap and shoulder belt attachment points in supine position (JAR-22 2001)



## University of Pretoria etd – Meintjes, S W v d M (2004)

### JAR 22.786 Protection from Injury

- a) Rigid structural members or rigidly mounted items of equipment must be padded where necessary to protect the occupant from injury during minor crash conditions.
- b) Structural members which, by the nature of their size or shape are capable of piercing the instrument panel, must be designed or positioned such that under the conditions of JAR 22.561(b)(2) injury to occupants would be unlikely.

### JAR 22.788 Headrests

- a) A headrest must be provided to protect the occupant from rebound injuries in the event of a crash landing. It must be equipped with energy absorbing padding protected against wear and weathering encountered in normal operating conditions. Adjustable headrests must be capable of being positioned such that the point of contact is at eye level.
- b) Each headrest must be designed to minimise the possibility of entanglement with clothing or the parachute when bailing out.
- c) Each headrest must be designed for an ultimate load of at least 135daN acting normal to a vertical plane touching the head contact point when the headrest is in its most critical position.
- d) The width and design of the headrest must not restrict vision from either seat.

### IEM 22.788 Headrests

- a) If possible the structure of the headrest should be integrated into the backrest of the seat.
- b) Each headrest should be designed that protection from injury is ensured whether the occupant wears a parachute or not.

### JAR 22.807 Emergency Exit

- a) The cockpit must be so designed that unimpeded and rapid escape in emergency situations during flight and on the ground is possible with the occupant wearing a parachute.
- b) The opening or jettisoning of the canopy or emergency exit must not be prevented by the presence of aerodynamic forces and/or by the weight of the canopy at speeds up to  $V_{DF}$  or by jamming of the canopy by other parts of the sailplane. The canopy or emergency attachment fittings must be designed to permit easy jettisoning.
- c) The opening system must be designed for simple and easy operation. It must function rapidly and must also be designed for operation by each occupant strapped in his seat and from the outside of the cockpit.

## University of Pretoria etd – Meintjes, S W v d M (2004)

- d) A canopy or emergency exit jettisoning system must be actuated by not more than two controls with one or both which must remain in the open position. The controls must be operated with a pilot effort between 5 and 15daN. If two controls are used they must both move in the same sense to jettison the canopy. If a single control is used it must be designed to minimise the risk of unintentional operation.
- e) In order to enable the occupants to bail out under acceleration conditions, sufficiently strong cabin parts or grab handles must be available and suitably located so that the occupants can lift themselves from their seats and support themselves. These parts must be designed to an ultimate load of at least 200daN in the anticipated direction of force application.

### **JAR-23**

The Joint Aviation Requirements for Normal, Utility, Aerobatics and Commuter Aircraft are contained in JAR-23 (2001). Some of the most relevant requirements concerning pilot protection and occupant safety were summarised in the following paragraphs.

#### JAR 23.561 Emergency Landing Conditions

- a) The aircraft, although it might be damaged in emergency landing conditions, must be designed to protect each occupant under the conditions of this section.
- b) The structure must be designed to give each occupant every reasonable chance of escaping serious injury under the following conditions:
  - 1) When proper use is made of seats, safety belts and shoulder harnesses as provided in the design.
  - 2) When the occupants experience the static loads corresponding to the following accelerations.
    - I) Upward 3.0g for normal, utility and commuter category  
4.5g for aerobatics category
    - ii) Forward 9.0g
    - iii) Sideward 1.5g
  - 3) When the items of mass that could injure an occupant experience the static inertia loads corresponding to the following accelerations.
    - i) Upward 3.0g
    - ii) Forward 18.0g
    - iii) Sideward 4.5g

## University of Pretoria etd – Meintjes, S W v d M (2004)

- c) Each aircraft with retractable landing gear must protect the occupants in the following landing conditions:
- 1) A landing with the wheels retracted.
  - 2) A landing with moderate descent velocity.
  - 3) Assuming a downward ultimate inertia load force of 3.0g and a coefficient of friction of 0.5 at the ground.
- d) If it is not established that a turnover is unlikely during an emergency landing condition, the structure must be designed to protect the occupants in a complete turnover as follows:
- 1) The likelihood of a turnover may be shown by an analysis assuming the following conditions:
    - i) The most adverse combination of weight and CG position
    - ii) A longitudinal load factor of 9.0g
    - iii) A vertical load factor of 1.0g
    - iv) For aircraft with tricycle landing gear, the nose wheel strut failed with the nose contacting the ground
  - 2) An upward ultimate inertia load factor of 3.0g and a coefficient of friction of 0.5 with the ground must be used to determine the loads on the inverted aircraft.
- e) Except as provided in JAR 23.787(c), the supporting structure must be designed to restrain under loads specified in (b)(3) each item of mass that could injure an occupant if it came loose in a minor crash landing.

### JAR 23.562 Emergency Landing Dynamic Conditions

- a) Each seat/restraining system must be designed to protect each occupant in an emergency landing under the following conditions:
- 1) When proper use is made of seats, safety belts and shoulder harnesses provided in the design.
  - 2) When the occupants is exposed to the loads resulting from the conditions prescribed in this section.
- b) Each seat/restraint system must successfully complete dynamic tests or be demonstrated by analysis supported by dynamic tests in accordance with the following conditions. These tests must be conducted with an Anthropomorphic Test Dummy (ATD) seated in the normal upright position.
- 1) For the first test the change in velocity may not be less than 31ft per second. The seat/restraint system must be oriented in its normal position with respect to the aircraft but with the aircraft pitched up 60° with respect to the horizontal plane. For seat/restraint systems installed in the first row of the aircraft, peak decelerations must occur in no more

## University of Pretoria etd – Meintjes, S W v d M (2004)

than 0.05 seconds after impact and must reach a minimum of 19g. For all other seat/restraint systems, peak decelerations must occur in no more than 0.06 seconds after impact and must reach a minimum of 15g.

- 2) For the second test the change in velocity may not be less than 42ft per second. The seat/restraint system must be oriented in its normal position with respect to the aircraft with the aircraft yawed at 10°. For seat/restraint systems installed in the first row of the aircraft, peak decelerations must occur in not more than 0.05 seconds after impact and must reach a minimum of 26g. For all other seat/restraint systems, peak deceleration must occur in no more than 0.06 seconds after impact and must reach a minimum of 21g.
  - 3) To account for floor warpage the floor rails used to attach the seat/restraint system to the airframe structure must be preloaded to misalign with each other by at least 10° vertically (i.e. pitch out of parallel). One of the rails must be preloaded to misalign by at least 10° in roll prior to conducting the test.
- c) Compliance with the following requirements must be shown during the dynamic tests conducted in accordance with subparagraph (b)(2).
- 1) The seat/restraint system must restraint the ATD although the seat/restraint system components may experience deformation, elongation, displacement or crushing intended as part of the design.
  - 2) The attachment between the seat/restraint system and the test fixture must remain intact although the seat structure may have deformed.
  - 3) Each shoulder harness strap must remain on the ATD's shoulder during the impact.
  - 4) The safety belt must remain on the ATD's pelvis during the impact.
  - 5) The results of the dynamic tests must show that the occupant is protected from serious head injury considering the following.
    - i) When head contact can occur, protection must be provided so that head impact does not exceed a Head Injury Criteria (HIC) of 1000.
    - ii) The value of HIC is defined as:

$$HIC = \left[ \frac{1}{(t_2 - t_1)^{\frac{2}{5}}} \int_{t_1}^{t_2} a(t) dt \right]^{2.5} (t_2 - t_1)$$

Where:

$t_1$  is the initial integration time in seconds

$t_2$  is the final integration time in seconds

$(t_2 - t_1)$  is the duration of the major head impact separated by no more than 36 milliseconds

$a(t)$  is the resultant deceleration at the CG of the head expressed as a multiple of g

## University of Pretoria etd – Meintjes, S W v d M (2004)

- iii) Compliance with the HIC limit must be demonstrated by measuring the head impact during dynamic testing as prescribed in sub-paragraphs (b)(1) and (b)(2).
- 6) Loads in individual shoulder harness straps may not exceed 794kg. If dual straps are used to restrain the upper torso, the total strap loads may not exceed 907kg.
- 7) The compression load measured between the pelvis and lumbar spine of the ATD may not exceed 680kg.
- d) An alternative approach that achieves an equivalent or greater level of occupant protection to that required by this section may be used if substantiated on a rational basis.

### **JAR-VLA**

The Joint Aviation Requirements for Very light Aircraft are contained in JAR-VLA (2001). Some of the most relevant requirements concerning pilot protection and occupant safety were summarised in the following paragraphs.

#### JAR-VLA 561 Emergency Landing Conditions

- a) Although the aircraft may be damaged in emergency landing conditions, it must be designed to protect the occupant under the following prescribed conditions.
- b) The structure must be designed to give each occupant reasonable chance of escaping serious injury under the following conditions:
  - 1) If proper use was made of the provided seatbelts and harnesses.
  - 2) If the occupant experiences ultimate inertia load factors corresponding to the following accelerations:

|          |      |
|----------|------|
| Upward   | 3.0g |
| Forward  | 9.0g |
| Sideward | 1.5g |
- c) Each item of mass that could injure the occupant if it came loose must be designed according to the loads stated above. For engines installed behind and above the occupant's seat the engine mount and supporting structure must be designed for an ultimate load factor of 15g.
- d) The structure must be designed to protect the occupant in a complete turnover scenario under the following conditions.
  - 1) An upward ultimate inertia force of 3g.
  - 2) A coefficient of friction of 0.5 at the ground.
- e) Each aircraft with retractable landing gear should be designed to protect the occupant under the following conditions.

## University of Pretoria etd – Meintjes, S W v d M (2004)

- 1) A landing with wheels retracted.
- 2) A landing with moderate descent velocity.
- 3) A landing with a downward inertia load of 3g and a coefficient of friction of 0.5 at the ground.

### JAR-VLA 783 Exits

- a) The aircraft must be designed that unimpeded and rapid escape is possible in any normal and crash attitude including turn over.
- b) No exits may be located with respect to any propeller disc that might endanger persons using that exit.

### JAR-VLA 785 Seats, Safety belts and Harnesses

- a) Each seat and its supporting structure must be designed for an occupant weighing at least 86kg and for the maximum load factors corresponding to the flight load, ground load and emergency landing conditions described in JAR-VLA 561.
- b) Each safety belt with shoulder harness must be approved and must be equipped with a metal to metal latching device.
- c) Each pilot seat must be designed for reactions resulting from the application of the pilot forces to the primary flight controls as described in JAR-VLA 395.
- d) Proof of compliance with the strength and deformation requirements for seat installations must be shown by one of the following:
  - 1) Structural analysis, if the structure conforms to conventional aircraft types for which existing methods are known.
  - 2) A combination of structural analysis and static load tests to the limit loads.
  - 3) Static load tests to ultimate loads.
- e) Each occupant must be protected from serious head injury by a safety belt and shoulder harness that is designed to prevent the head from contacting any injurious object.
- f) Each shoulder harness installed at a pilot's seat must allow the pilot in the seated position to perform all functions necessary for flight operations.
- g) There must be a means to secure the safety belt and shoulder harness when not in use to prevent interference with operations and rapid egress during an emergency.
- h) The seat track must be fitted with stops to prevent the seat from sliding from the tracks.
- i) The cabin area surrounding each seat, within striking distance of the occupant's head or torso must be free of any potential injurious objects. If energy absorbing designs or devices are used to meet this requirement they must protect the occupant against serious injury when ultimate inertia forces as described in JAR-VLA 561 are experienced by the occupant.

JAR-VLA 807 Emergency Exits

- a) Where exits are provided to achieve compliance with JAR-VLA 783(a), the opening system must be designed for simple and easy operation. It must function rapidly and must be designed so that it can be operated by each occupant strapped in the seat and also from outside the cockpit. Reasonable provision must be provided to prevent jamming by fuselage deformation.

## **APPENDIX D            ADAMS AND FIGURE HUMAN MODELLER**

### **ADAMS**

According to Mechanical Dynamics Inc. ADAMS stands for Automatic Dynamic Analysis of Mechanical Systems and is the world's most widely used mechanical system simulation software. With ADAMS you can build "virtual prototypes" on the computer and run realistic visual and mathematical simulations of complex mechanical system. ADAMS enables one to quickly implement multiple design variations until an optimal design is achieved. This reduces the number of costly physical prototypes, improves design quality, and dramatically reduces product development time.

In ADAMS, models are constructed with rigid body solids that are connected to each other with different type of joints. Forces, motions and constraints could be applied to the joints to simulate the full motional behaviour of the model. The rigid body construction of the ADAMS models imply that impact events can not be simulated to a level of micro structural crushing as in some finite element packages. ADAMS together with the FIGURE human modeller is, however, the perfect tool for investigating occupant response and the performance of energy absorbing mechanisms during high impact events.

With ADAMS a complete parameterised model of the mechanical system could be created in no time by building it from scratch in the pre-processing environment called ADAMS/View or by importing an existing CAD model into ADAMS/View. The model could then be subjected to a full 3D physical simulation by applying the appropriate constraints, motions and forces on the model. As a result a complete virtual simulation of any complex mechanical system in operation is obtained without manufacturing a single part.

ADAMS has its own build-in solver that checks the model and automatically formulates and solves the equations of motions for kinematic, static, quasistatic and dynamic simulations. Designers are normally interested in the peak accelerations during high impact events. The ADAMS SI2 solver differs from the default solver in that it not only converges on the displacements but also on both velocity and acceleration. The SI2 solver was therefore also used in the impact simulations of this project. Animations and plots could be viewed while the simulation is running, thereby saving valuable time not having to wait for the completion of the computations.



Because of the fact that impact events in ADAMS are modelled as contact between different bodies, it seemed reasonable to highlight some of the contact modelling capabilities of this program. ADAMS/Solver models contacts between two bodies as a force with a value of zero if no penetration exists between the two specified geometry's and as a force with a positive value when penetration exists. ADAMS has two types of contacts that could be specified and they are:

- Restitution based contact
- Impact function based contact

### Restitution Based Contact

In this method, ADAMS/Solver computes the contact force from a penalty parameter and a coefficient of restitution. The penalty parameter enforces the unilateral constraint and the restitution coefficient controls the dissipation of energy at the contact. If the energy of the two bodies is written as:

$$(E_{\text{Total}})_{\text{before}} = r * (E_{\text{Total}})_{\text{after}}$$

with  $(E_{\text{total}})_{\text{before}}$  denoting the total amount of energy before the impact and  $(E_{\text{total}})_{\text{after}}$  the total amount of energy after impact, and if the range of the restitution coefficient  $r$  is specified as  $0 \leq r \leq 1$ , it would imply that a value of zero would specify a perfectly plastic contact between two bodies and a value of one would specify a perfect elastic contact.

### Impact Function Based Contact

In this method, ADAMS/Solver computes the contact force from the IMPACT function available in the ADAMS function library. The force is essentially modelled as the output of a non-linear spring-damper. When using the IMPACT statement, the following parameters must be specified:

#### Impact Stiffness (K)

Specifies a material stiffness that can be used to calculate the normal force for the impact model. In general, the higher the stiffness, the more rigid the bodies in contact are.

#### Force Exponent (e)

ADAMS/Solver models the normal contact force as a non-linear spring-damper. The force exponent is used to specify the shape of the spring's stiffness curve. In general a force exponent of  $e = 1$  indicates a linear spring stiffness,  $e < 1$  indicates a softening spring and  $e > 1$  indicates a hardening spring as indicated by Figure D1.

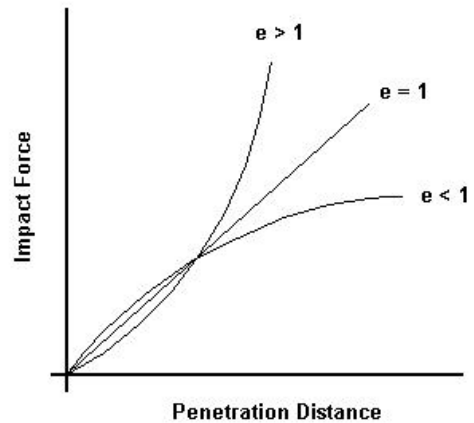


**Figure D1: ADAMS Impact function force exponent ranges**

#### Damping (C)

Damping specifies the damping properties of the contacting materials and therefore controls the energy dissipation of the contact.

#### Penetration Depth (d)

ADAMS/Solver uses a cubic step function to increase the damping coefficient from zero to full damping. The penetration depth coefficient  $d$  defines the penetration at which ADAMS turns on full damping (see Figure D2). The range of penetration depth is  $d \geq 0$ .

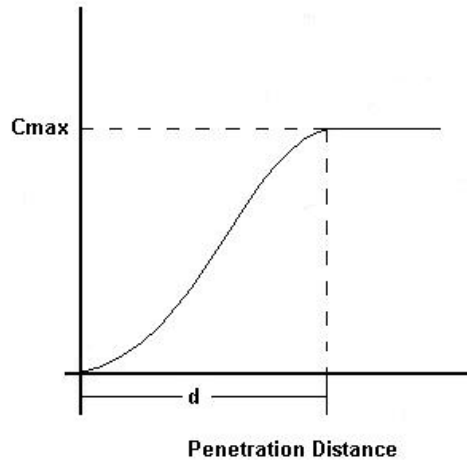


**Figure D2: ADAMS Impact function penetration depth and damping step function**

### **FIGURE Human Modeller**

According to Mechanical Dynamics Inc. (2002) research into the biomechanics field over the last 15 years has led to the development of FIGURE human modeller. FIGURE is an add-on to ADAMS/View and is used by over 30 major sports equipment manufacturers, orthopaedics companies, universities and government agencies. The intent of the product was to provide a tool to easily create human models with a sophistication level ranging from very simple to complex. These human models would be used to study the complex dynamic interaction between human bodies and mechanical systems without risking the comfort or safety of human beings and to address applications ranging from sports performance to gait simulations, injury evaluation to vehicle ride comfort. FIGURE not only allows the modelling of humans but is also capable of modelling virtually any biological subject created by the user.

#### **The Human Models**

The base level human model in FIGURE is the 15 segment 16 joint type model which consist of a head, neck, upper torso, middle torso, lower torso, upper and lower arms, upper and lower legs and feet. The high level model includes all the bones of the human body with the ability to manipulate each individual bone separately for more detailed modelling. At any given time the human model could be displayed as ellipsoids, skeletal or as a skin clothed model as indicated by Figure D3.

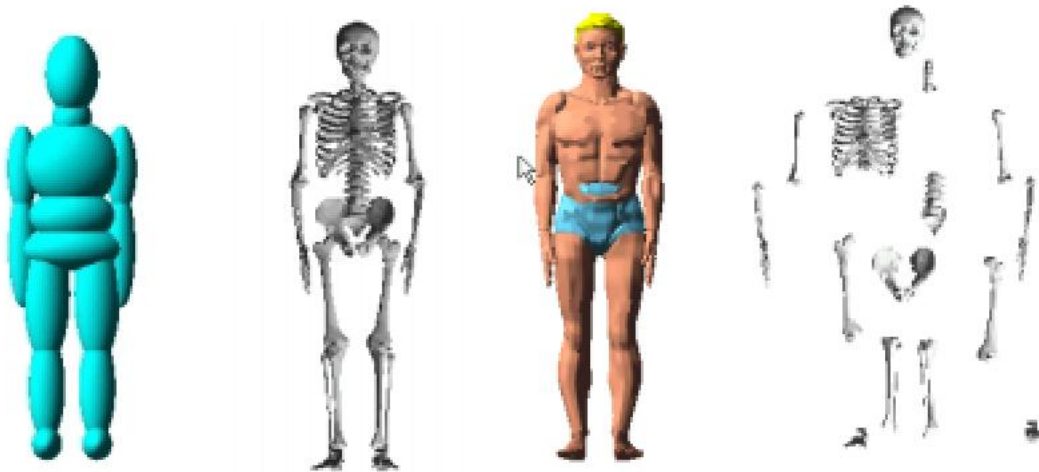


**Figure D3: Human models displayed as ellipsoids, skeletal or a skin clothed model (Mechanical Dynamics Inc. 2002)**

### Passive simulation

The joints of the model are tri-axes hinge joints located at anatomical locations, which could be replaced with any other constraint arrangements by the user. The forces in the joints may be of the passive or active type. Passive simulations involve the response of the human body due to the physics of the environment and may include falls, crashes, impacts etc. The human model used for passive simulation has the same segment mass properties and dimensions, joint stiffness, damping and friction, and joint limits as the Hybrid III Crash Test Dummy used by many automotive companies to evaluate safety systems (see Appendix A). Typical data received from such a simulation include segment contact force, displacement, velocity and acceleration, joint forces and torque's. These data could then be used to evaluate potential of injury with available injury criteria.

### Active Simulation

In an active simulation the human body becomes an active participant in the simulation therefore affecting the physics of the environment. This could be achieved by imposing motions, torque's or muscle forces onto the joints. Figure D4 shows typical active simulations with a man swinging a golf club and a walking man.

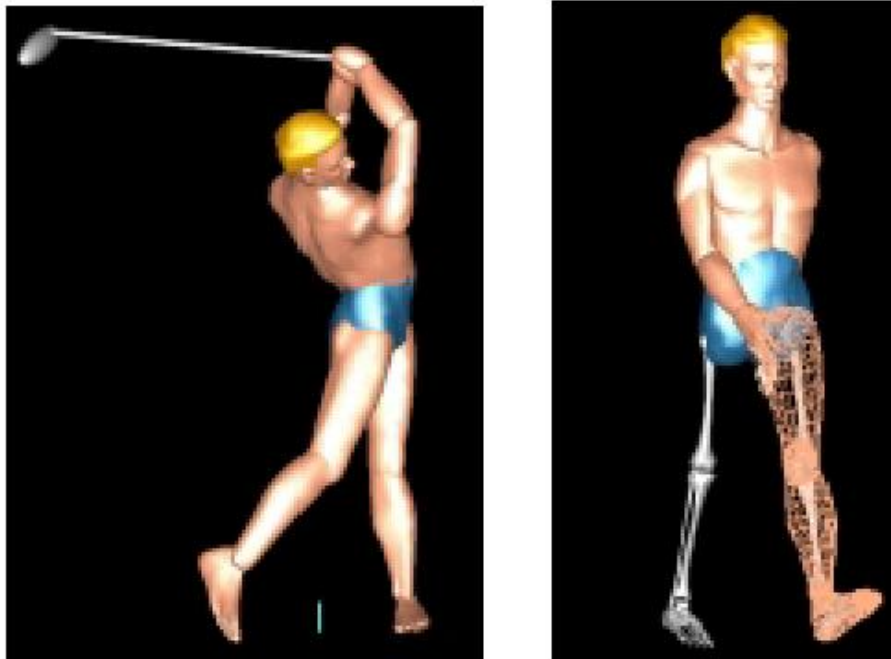


**Figure D4: Typical active simulation with FIGURE (Mechanical Dynamics Inc. 2002)**

## Features

Some of the important features of FIGURE are listed below:

- Three types of human body representation, ellipsoid, skeletal and skin
- Full human skeleton including all bone models
- Skeleton and skin models are scalable based on anthropometric input
- Capable of general biological modelling (animals and insects)
- Full anthropometric scaling representing male, female and child populations
- Capable of passive, inverse and active, forward dynamic simulations
- Passive joint properties of the Hybrid III Crash Dummy
- Capability to create muscle, tendon and ligament groups
- Soft tissue insertion points can be positioned with the cursor
- Powerful posture modelling capabilities including standard posture library
- Automatic PD controllers generated for each joint
- Motion import features
- Combination of human figures with any ADAMS models allows for full man-machine interaction
- Multiple figures interacting with each other's capability
- Easy to use
- Models may range in biofidelity from simple to very complex

## Applications

Applications for HUMAN FIGURE MODELLER

- Slips and falls
- Crash analysis
- Gait
- Prosthetics and joint replacement systems
- Sports performance and equipment
- Animal behaviour
- Man-machine effects
- Riding comfort
- Vibration
- General ergonomics
- Safety

**APPENDIX E      ADDITIONAL RESULTS**

***Validation and Verification Results***

Additional results of the validation process described in Chapter 4.4 that were not included in the main document are contained here.

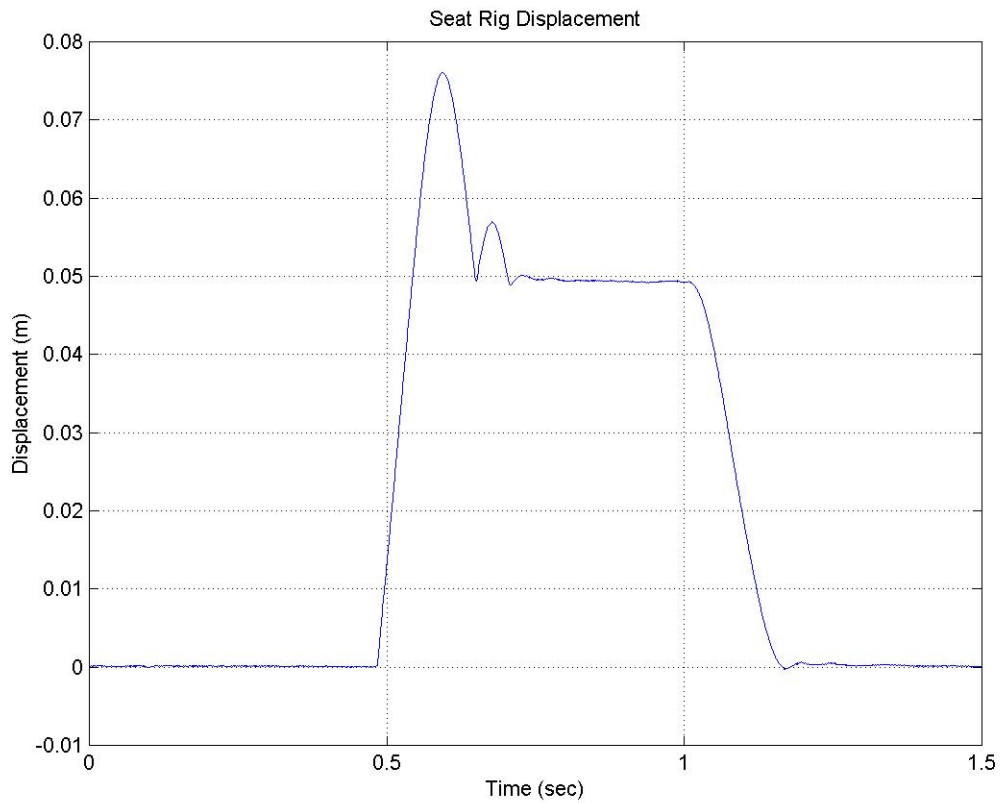


**Figure E1: Validation seat rig input displacement**

## Sled Impact Test Results

Additional results of the sled impact tests described in Chapter 4.5

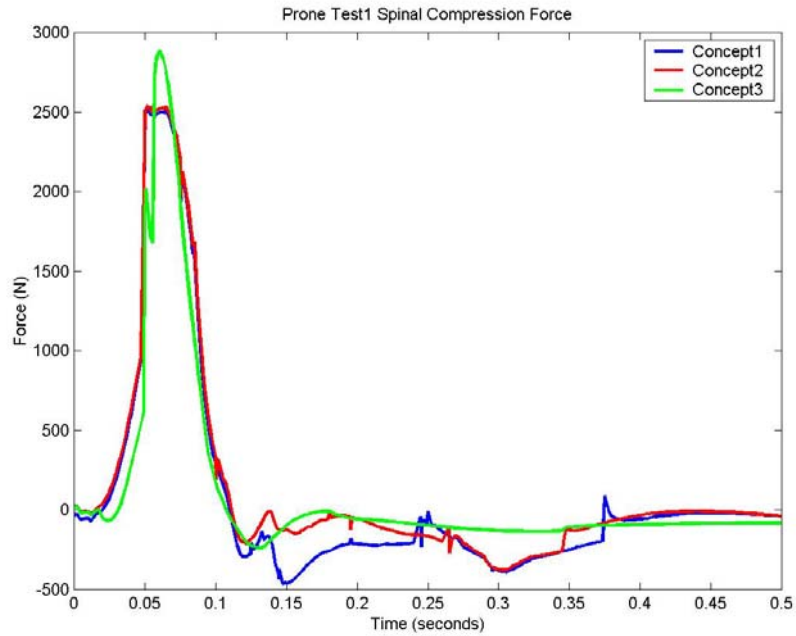


Figure E2: Test 1 prone concepts lumbar load comparison

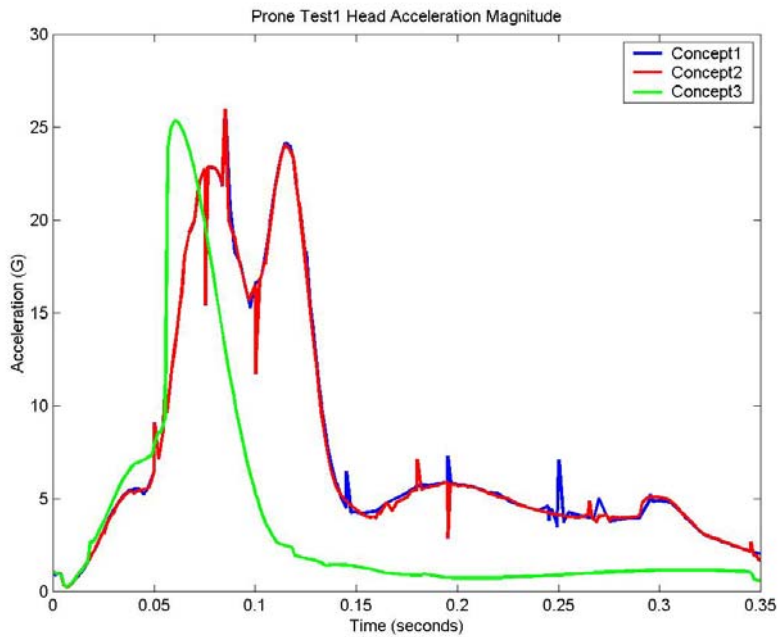


Figure E3: Test 1 prone concepts head acceleration comparison

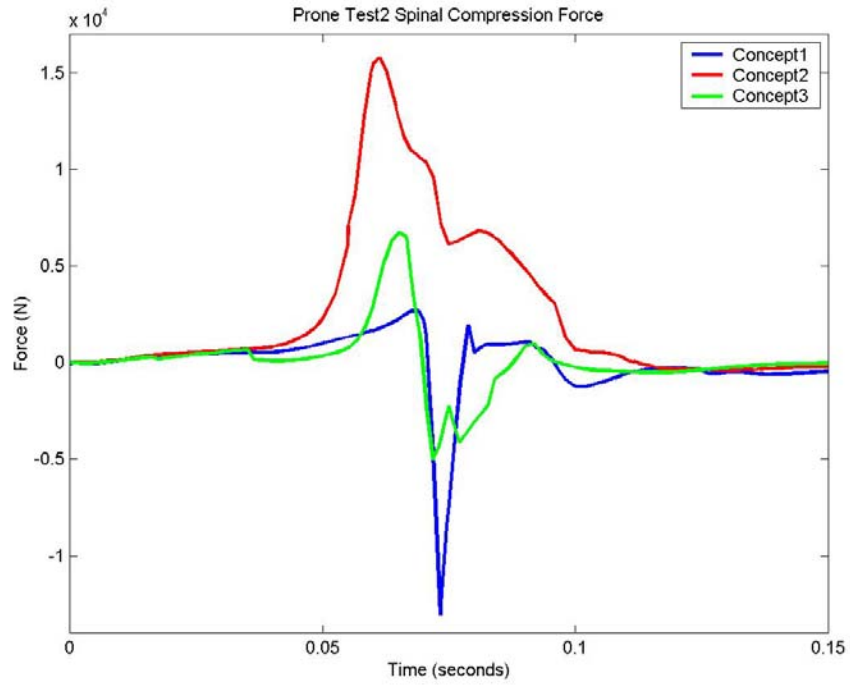


Figure E4: Test 2 prone concepts lumbar load comparison

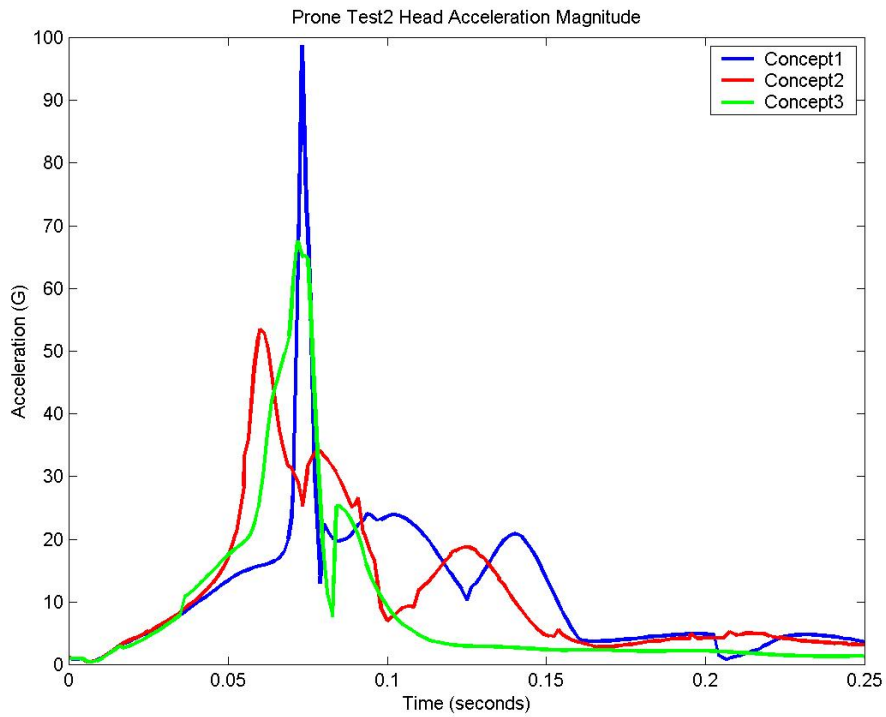


Figure E5: Test 2 prone concepts head acceleration comparison



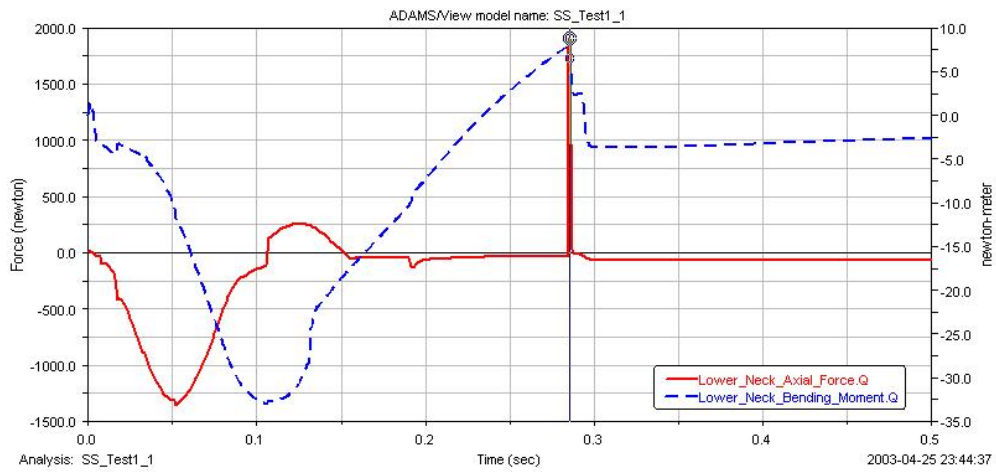
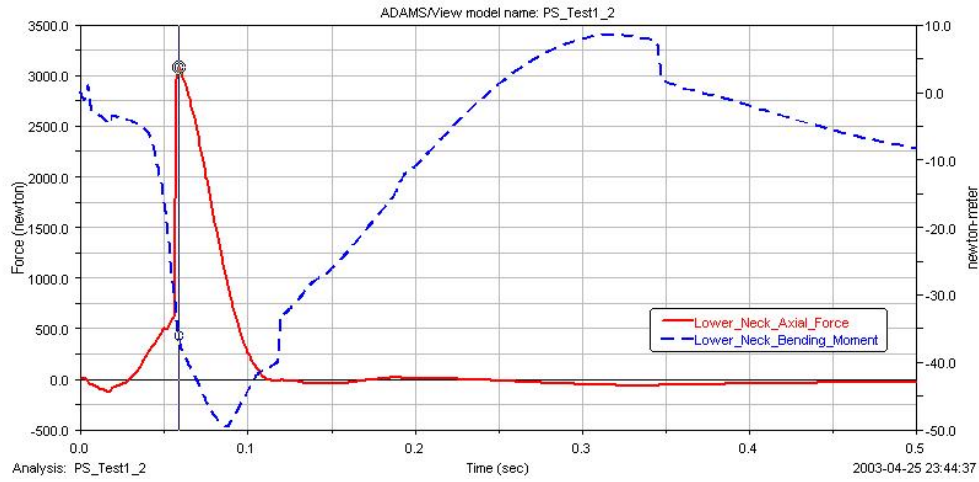
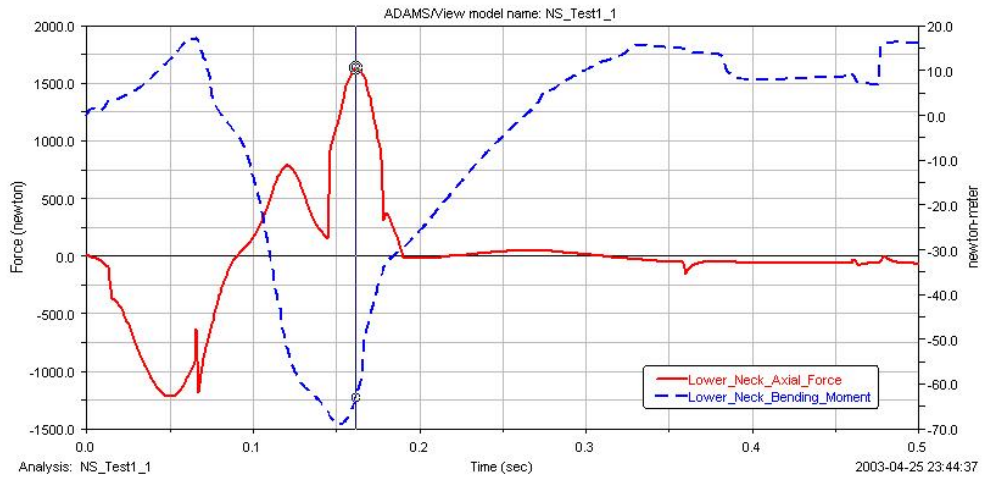


Figure E6: Test 1 neck axial loads and bending moments

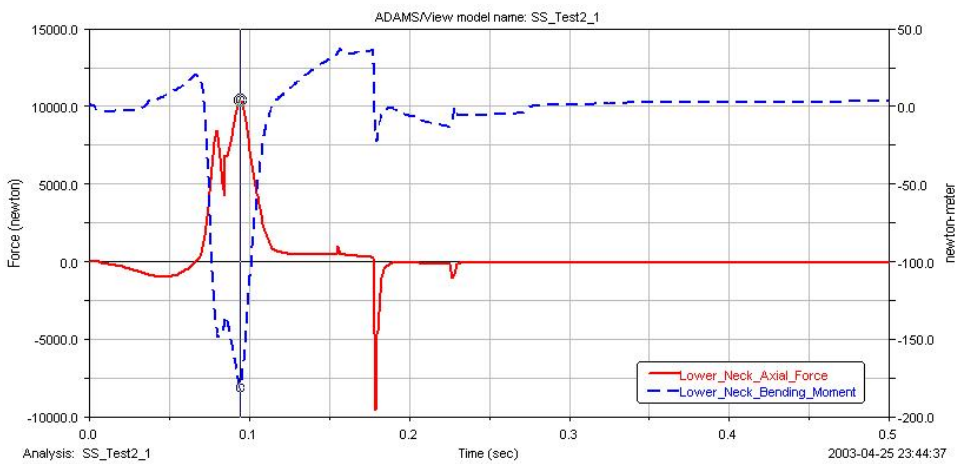
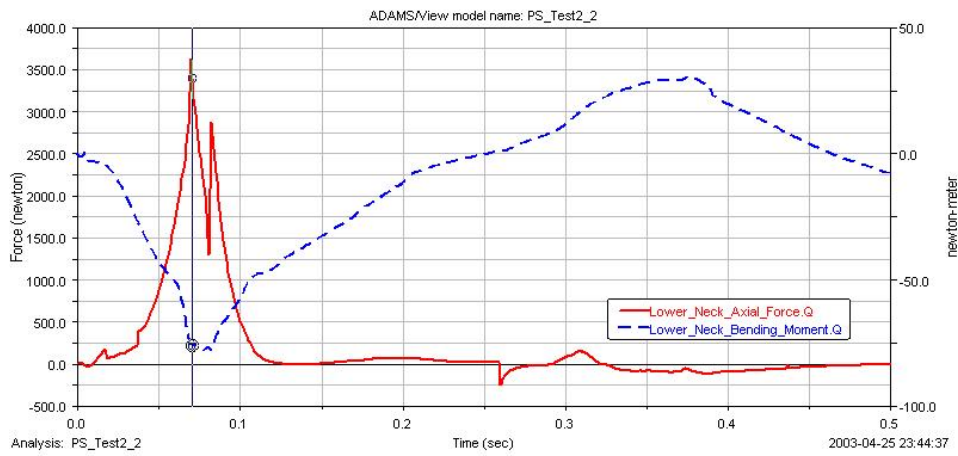
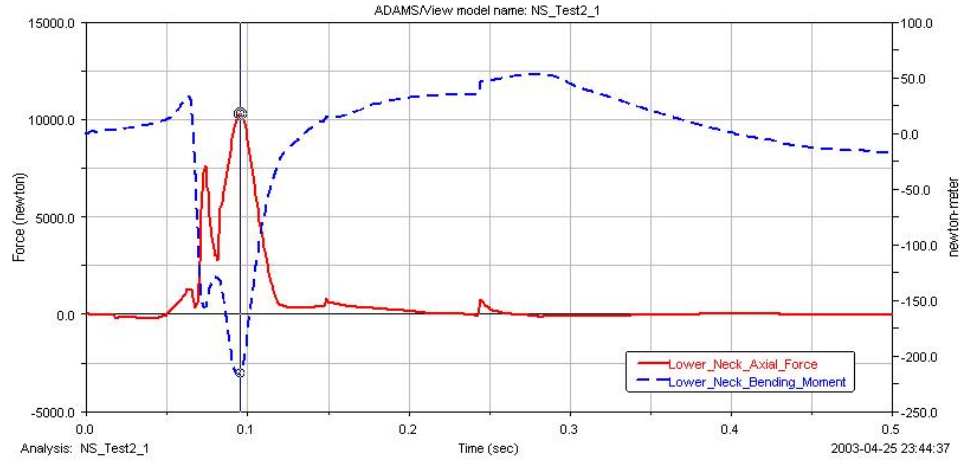


Figure E7: Test 2 neck axial loads and bending moments

### Fuselage Crash Test Results

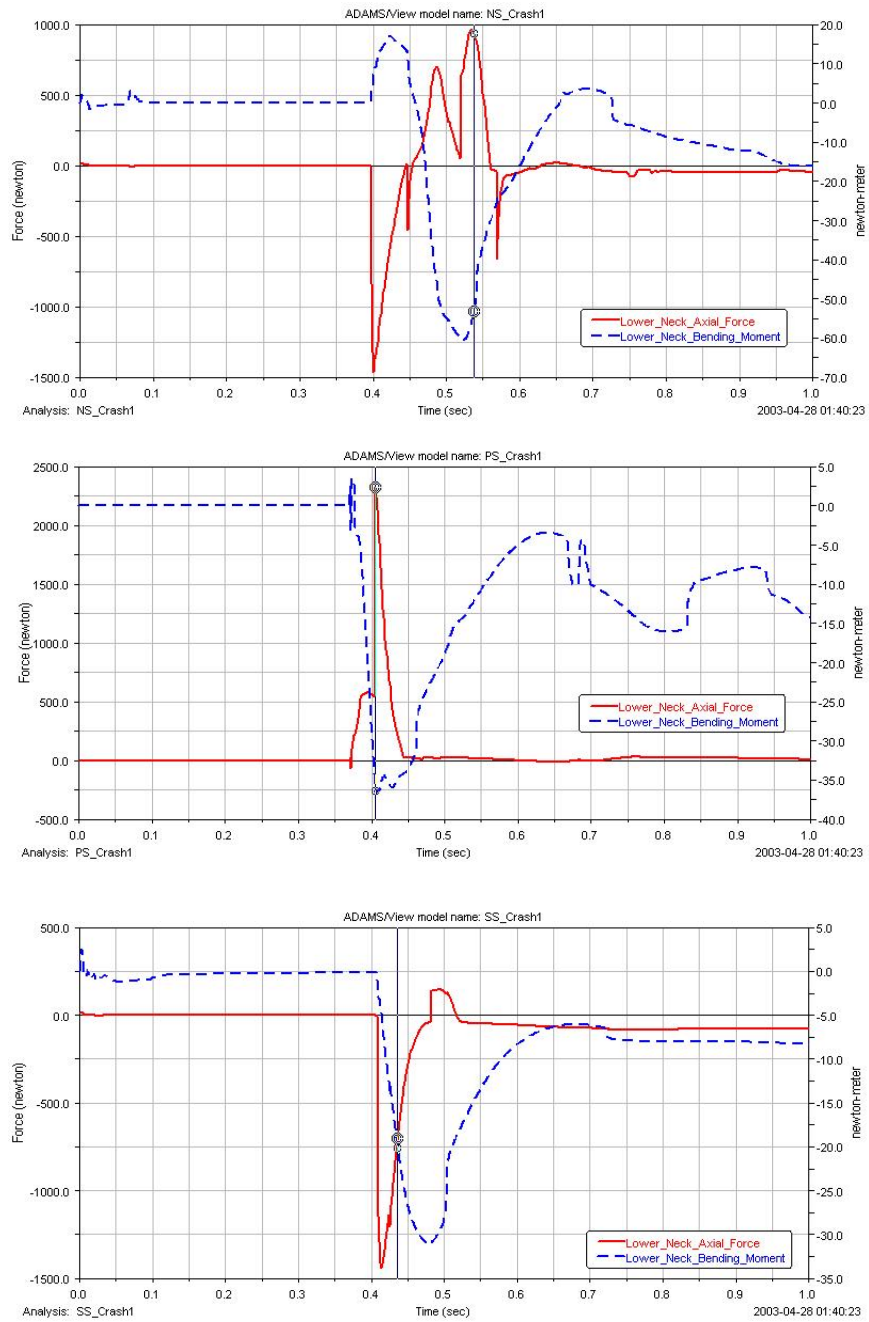


Figure E8: Crash 1 neck axial loads and bending moments

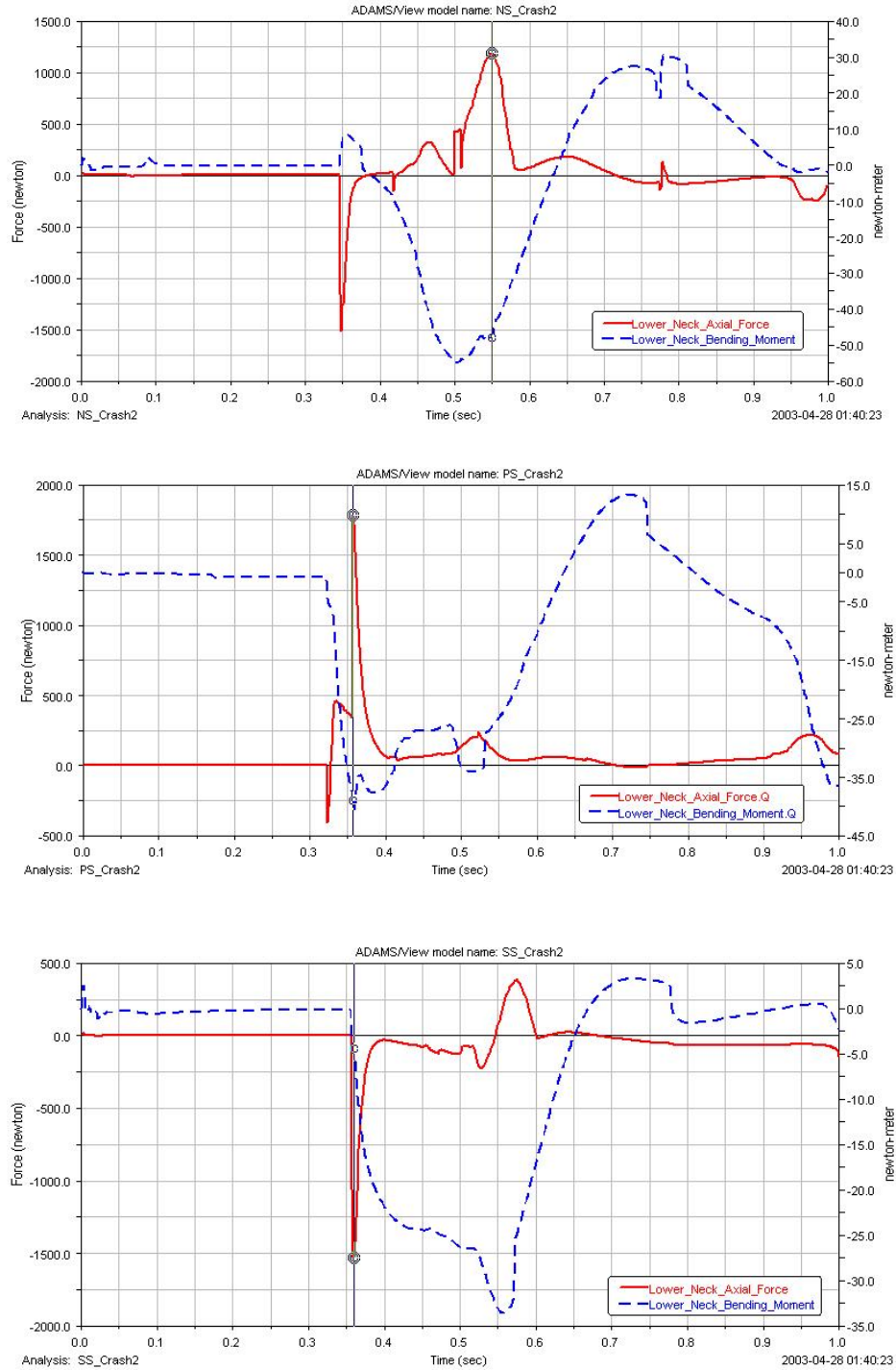


Figure E9: Crash 2 neck axial loads and bending moments

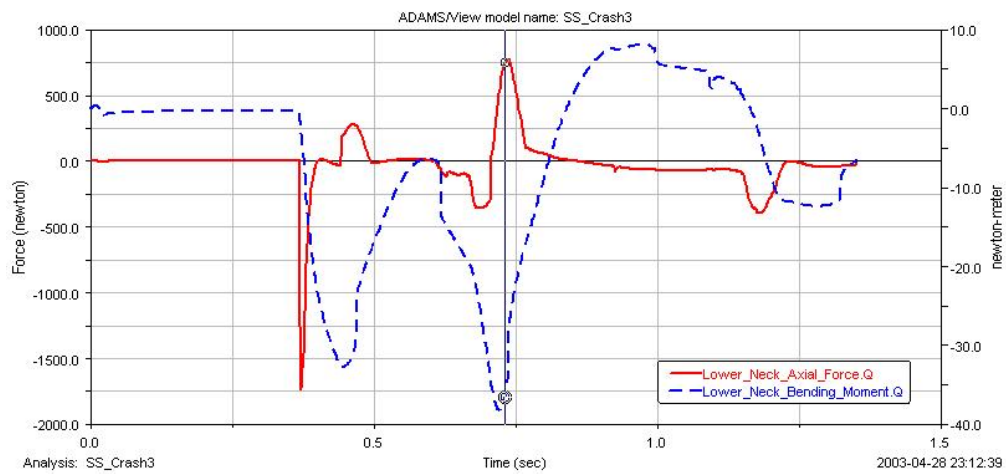
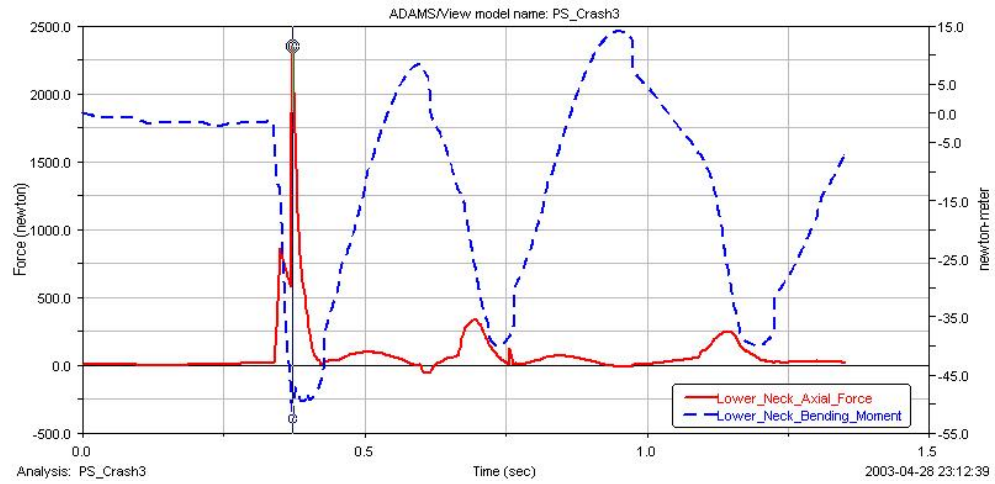
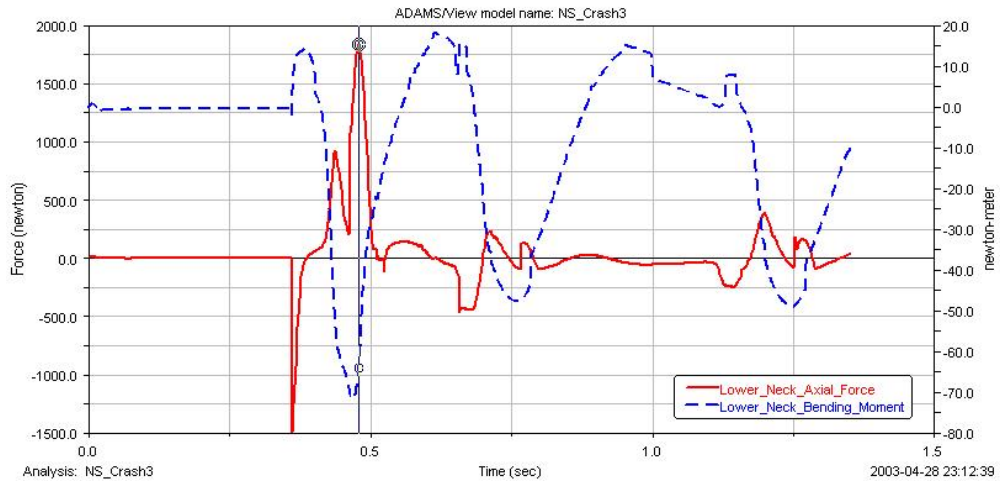


Figure E10: Crash 3 neck axial loads and bending moments

Values for  $N_{ij}$  were calculated as follow:

As an example, from Figure E6 for the normal seated position the worst case combination for neck force  $F_Z$  and neck bending moment  $M_Y$  are indicated by the rings on the black vertical line at approximately 0.16 seconds. The values at this point in time are:

$$F_Z = +1594\text{N}$$

$$M_Y = -65.94\text{Nm}$$

$$F_{INT} = 4500\text{N} \quad \text{from Table 2.2 for a tension force}$$

$$M_{INT} = 125\text{Nm} \quad \text{from Table 2.2 for extension (negative) moment}$$

$$\begin{aligned} N_{ij} &= F_Z/F_{INT} + M_Y/M_{INT} \\ &= 1594/4500 + 65.94/125 \\ &= 0.354 + 0.528 \\ &= 0.882 \end{aligned}$$

**Table E1: Calculation of neck injury criteria**

| Analysis    | Position | time (s) | Fz (N) | My (Nm) | Fint | Mint | Nij   |
|-------------|----------|----------|--------|---------|------|------|-------|
| Sled Test 1 | Normal   | 0.159    | 1594   | 65.94   | 4500 | 125  | 0.882 |
|             | Prone    | 0.059    | 3045   | 37.8    | 4500 | 125  | 0.979 |
|             | Supine   | 0.286    | 1912   | 6.52    | 4500 | 310  | 0.446 |
| Sled Test 2 | Normal   | 0.095    | 10282  | 215.76  | 4500 | 125  | 4.011 |
|             | Prone    | 0.07     | 3621   | 76.4    | 4500 | 125  | 1.416 |
|             | Supine   | 0.094    | 10378  | 181.1   | 4500 | 125  | 3.755 |
| Scenario 1  | Normal   | 0.531    | 926    | 58.39   | 4500 | 125  | 0.673 |
|             | Prone    | 0.405    | 2324   | 36.5    | 4500 | 125  | 0.808 |
|             | Supine   | 0.425    | 1207   | 13.55   | 4500 | 125  | 0.377 |
| Scenario 2  | Normal   | 0.546    | 1182   | 48.62   | 4500 | 125  | 0.652 |
|             | Prone    | 0.357    | 1784   | 38.97   | 4500 | 125  | 0.708 |
|             | Supine   | 0.36     | 1553   | 4.15    | 4500 | 125  | 0.378 |
| Scenario 3  | Normal   | 0.475    | 1758   | 68.71   | 4500 | 125  | 0.940 |
|             | Prone    | 0.372    | 2351   | 52.58   | 4500 | 125  | 0.943 |
|             | Supine   | 0.73     | 749    | 36.55   | 4500 | 125  | 0.459 |

Table E2: Injury Criteria Results

| Analysis    | Pilot Position | Injury Criteria (IC) |          |         | IC exceeded | Best Performance |        |        |
|-------------|----------------|----------------------|----------|---------|-------------|------------------|--------|--------|
|             |                | LLC<6700             | HIC<1000 | Nij<1.0 |             | LLC              | HIC    | Nij    |
| Sled Test 1 | Normal Seated  | 7599                 | 31.49    | 0.882   | 1           |                  | Normal |        |
|             | Prone Seated   | 240                  | 57.97    | 0.979   | 0           | Prone            |        |        |
|             | Supine Seated  | 7045                 | 39.19    | 0.446   | 1           |                  |        | Supine |
| Sled Test 2 | Normal Seated  | 4527                 | 1905     | 4.011   | 2           | Normal           |        |        |
|             | Prone Seated   | 5017                 | 270      | 1.416   | 1           |                  | Prone  | Prone  |
|             | Supine Seated  | 5335                 | 2432     | 3.755   | 2           |                  |        |        |
| Scenario 1  | Normal Seated  | 7619                 | 18.12    | 0.673   | 1           |                  |        |        |
|             | Prone Seated   | 673                  | 12.37    | 0.808   | 0           | Prone            | Prone  |        |
|             | Supine Seated  | 8783                 | 25.03    | 0.377   | 1           |                  |        | Supine |
| Scenario 2  | Normal Seated  | 7921                 | 2.78     | 0.652   | 1           |                  | Normal |        |
|             | Prone Seated   | 3549                 | 5.93     | 0.708   | 0           | Prone            |        |        |
|             | Supine Seated  | 9490                 | 4.77     | 0.378   | 1           |                  |        | Supine |
| Scenario 3  | Normal Seated  | 7754                 | 4.52     | 0.940   | 1           |                  | Normal |        |
|             | Prone Seated   | 2203                 | 14.64    | 0.943   | 0           | Prone            |        |        |
|             | Supine Seated  | 10305                | 8.47     | 0.459   | 1           |                  |        | Supine |

Table E3: Impact force on mandible of prone positioned pilot

| Analysis            | Position | Impact Force (N) | Head CG Acceleration (g) |
|---------------------|----------|------------------|--------------------------|
| Dynamic Sled Test 1 | Prone    | 2493.7           | 25.3                     |
| Dynamic Sled Test 2 | Prone    | 2478.2           | 57.7                     |
| Fuselage Crash 1    | Prone    | 1929.9           | 17.8                     |
| Fuselage Crash 2    | Prone    | 1661.3           | 15.4                     |
| Fuselage Crash 3    | Prone    | 2035.1           | 17.5                     |

## **APPENDIX F            COMPACT DISC**

For future reference and as back-up purpose, this document together with other relevant data used to complete the study was saved on a compact disc (cd) which is included at the end of this document. This appendix will serve as a layout of the cd and will describe some of the content. The main thesis word document and the following folders can be found on the cd:

- Pictures
- Result Files
- Videos

### ***Pictures***

This folder contains all the *jpeg* images used in the main document. The files are named according to the numbering system of the main document as indicated the list of figures and list of tables.

### ***Result Files***

The analysis results obtained from ADAMS were saved in text format.

### ***Videos***

To visualize the animations without the ADAMS post-processing program, video clips of all the simulation animations were created. This folder contains all the video clips, which can be viewed with a standard Windows Media Player.